ROBUST METHODS OF FINITE ELEMENT ANALYSIS: EVALUATION OF NON-LINEAR, LOWER BOUND LIMIT LOADS OF PLATED STRUCTURES AND STIFFENING MEMBERS

FREEMAN E. RALPH

National Library of Canada
Acquisitions and Bibliographic Services
395 Wellington Street
Ottawa ON K1A 0N4
Canada

Bibliothèque nationale du Canada
Acquisitions et services bibliographiques
395, rue Wellington
Ottawa ON K1A 0N4
Canada

Your file Votre référence

Our file Notre référence

0-612-54953-4

Canada

Robust Methods of Finite Element Analysis:

Evaluation of non-linear, lower bound limit loads of plated structures and stiffening members

By

Freeman E. Ralph

A Thesis

Submitted to the School of Graduate Studies

in Fulfilment of the Requirements for the Degree of

Master of Engineering

Faculty of Engineering and Applied Science

Memorial University of Newfoundland

St. John's, NF, Canada

May, 2000

Abstract

The scope of this thesis is to investigate robust methods of FEA to evaluate non-linear lower bound limit load estimates of ship type structures. The robust methods used in this thesis include the r-node method, Progressive Modulus Reduction (PMR) method, and the $m_\alpha$method. The results of each technique are compared to the results of full non-linear finite element analysis, analytical solutions and lab test data where available. The structures modelled in this thesis included a rectangular indeterminate beam, three types of mainframe stiffeners (flat bar, angle and tee), a flat bar stiffened panel and an Arctic icebreaker grillage.

Robust methods make use of a modulus reduction scheme to redistribute and relax peak stresses in the structure. By iterating and selectively correcting the local modulus in finite element models, the form of a limit state stress distribution can be evaluated. In order for the limit loads evaluated based on this limit state stress distribution to be lower bound, the conditions of the stress field in the structure must be "statically admissible."

The basis of the r-node method is the identification of redistribution nodes or r-nodes within a structure, which are essentially load-controlled locations. Identification of exact r-node locations may be difficult to achieve with finite mesh densities particularly in complex structures. As well, complicated structures pose added difficulties in achieving a progressive r-node stress relaxation with increased iterations. This may be partly attributed to the difficulty in locating exact r-node locations.

The m_α method was developed in an attempt to improve lower bound estimates of limit loads, making use of just two linear elastic analyses. The notion of a "reference volume" is used in conjunction with the "theorem of nesting surfaces" and the concept of leap-frogging to a near limit state to evaluate lower and upper bounds on the limit load. The results of this thesis indicate that for complicated structures, improved limit load estimates can be obtained if four or more iterations of moduli are carried out. Reducing the rate of relaxation (reducing modulus adjustment index q) may enhance convergence characteristics, but results in a higher state of limit stress evaluated.

The Progressive Modulus Reduction (PMR) method, which is an extension of the elastic compensation method, systematically adjusts or reduces the moduli of the pseudo-elastic stressed elements of a structure to synthesise the growth of the yield zone. The PMR method is used to evaluate the non-linear deflection of the structure for applied loads up to the limit load.

In general the robust methods are an attractive alternative for evaluating limit loads of ship type structures. Results are a significant improvement over classical methods and are either close for simple structures or sufficiently conservative when compared to full non-linear FEA results. Each robust method models material non-linearities and hence evaluates good estimates of a non-linear limit load. Also, because the solution process is stable, convergence difficulties, encountered with full non-linear analysis, are avoided. Limit loads can be evaluated in a cost effective manner, which is particularly attractive at the initial stages of design.

Acknowledgements

The author wishes to thank his supervisor, Dr. Claude Daley, for his financial, technical support and motivation throughout the course of this masters program. Thanks is directed to Dr. R. Seshadri for his generous contribution of technical guidance despite his heavy, time demanding responsibilities as the Dean of the Faculty of Engineering and Applied Sciences. The author would like to thank James Bond, American Bureau of Shipping, for providing the ANSYS model for the Arctic ice breaker grillage used in this work. The author would also like to acknowledge the Department of Education and Governments of Canada and Newfoundland and Labrador, and the Atlantic Accord Career Development Awards Board for the awarding of the *Atlantic Accord Career Development Award* as partial funding of this work. Finally, the author acknowledges the inspiration and support provided by his wife, Tina, parents, William and Dorothy Ralph and parents-in-law, Roderick and Lavinia Jeans.

Table of Contents

List of Tables

List of Figures

Nomenclature

B, n	creep parameters for second stage power law creep
E_o	original elastic modulus of a mechanical component or structure
E_M, E_R, E_s,	modified value of elastic modulus of a mechanical component or structure
$f(s_{ij}), f(s_{ij}^o)$	Von Mises yield function
$F(s_{ij}^o, \sigma^o, m^o, \mu^o, \phi^o)$	functional associated with Mura's formulation
h	height or depth of a beam
i	iteration number corresponding to a set of linear elastic finite element analyses
I	moments of inertia of a two-layered beam
k	yield stress of a material in pure shear
L	length of a beam--flat bar, angle, tee, or indeterminate beam
m	safety factor corresponding to an applied load P
m^o	a multiplier based on the average surface of dissipation corresponding to an applied load P
m_R^o	m^o based on the reference volume
m'	lower bound multiplier corresponding to an applied load P
m_α	proposed lower bound multiplier corresponding to an applied load P
M	applied external bending moment in a beam
M_e	elastic bending moment in a beam
M_p	plastic moment in a beam
N	number of plastic hinges or plastic hinge contours in a mechanical component or a structure at collapse; total number of finite elements

P	applied external load
P_L	proposed limit load ($= m_\alpha P$)
P_{LC}	classical lower bound limit load
P_{LM}	lower bound limit load based on extended variational method
$(P_L)_{r\text{-}node}$	limit load determined using the r-node method
P_{UC}	classical upper bound limit load
q	elastic modulus adjustment index
$Q_1, Q_2, \ldots$	generalized loads applied to a mechanical component or structure
Q_e	effective generalized stress
$\tilde{s}_{ij}^o$	statically admissible deviatoric stress field corresponding to the traction P
s_{ij}^o	statically admissible deviatoric stress field corresponding to the traction $m^o P$
S_m	code allowable stress
S_T	surface area of a structure over which traction is prescribed
SI	Von Mises equivalent stress in an element of a discretised structure
V	volume of a component or a structure
V_R	reference volume of a component or a structure
V_T	total volume of a component or a structure
V_β	partial volume of a component or a structure
β	geometric scaling factor that depends on the structure and boundary conditions
γ_1, γ_2	scaling parameters
δ	deflection
δ_{ij}	Kronecker delta

ΔV_i	volume of *i*th element
ε	elastic strain
ε_A	effective strain at highly loaded locations (element A) within a structure
ε_p	inelastic strain
ε_R	reference strain for reference stress
ζ	linear elastic iteration variable; ratio of the yield stresses in a two-layered beam
ζ_1, ζ_2	interpolation errors pertaining to r-node locations
θ	follow-up angle on the GLOSS diagram
μ^ρ	plastic flow parameter
ν	Poisson's ratio
ϕ^ρ	a point function defined in conjunction with yield criterion
σ	hydrostatic stress for an actual stress distribution
σ_A	effective stress at high loaded locations (element A) within a structure
σ_{arb}	arbitrary stress in the modulus of elasticity softening process
σ_e	equivalent element stress
$(\sigma_e)_{r\text{-}node}$	r-node equivalent stress
σ_M	maximum stress intensity in a component
$(\sigma_e^o)_M, (\sigma_e)_M$	maximum Von Mises equivalent stress in a structure for any arbitrary load P for an elastic stress distribution
$\overline{\sigma}_n$	combined r-node stress
σ_{nj}	r-node peak stress
σ_{ref}	reference stress based on the theorem of nesting surfaces

σ_R	reference stress
σ_Y	yield stress

Subscripts

arb	arbitrary
e	Von Mises equivalent
i,j	tensorial indices
L	limit
R	reference
Y	yield
I, II, ...	linear elastic analyses

Superscript

o	assumed quantities, upper bound designation

Acronyms and Abbreviations

FEA	Finite Element Analysis
GLOSS	Generalised Local Stress Strain
r-node	Redistribution Node
IB	Indeterminate Beam
FB	Flat Bar stiffener
L	Angle stiffener
T	Tee stiffener
FBSP	Flat Bar Stiffened Panel
AIG	Arctic Ice Breaker Grillage

BKIN	Binary Kinematic hardening
MISO	Multilinear Isotropic hardening

Chapter 1

Introduction

Stiffened panel structures are used extensively in structural design, particularly in the shipbuilding and offshore industry. A stiffened panel consists of a set of frames attached to a shell plate as shown in Figure 1.1. This is a typical example of a ship's structural grillage, and consists of three main classes of stiffening: main frame stiffeners, stringers, and transverse web frames. The main frame stiffeners make up the primary stiffening of the structure, the stringers the secondary stiffening and the transverse web frames the tertiary stiffening.

1.1 Background

Traditionally, frames have been designed elastically against first yield and checked for elastic buckling. Concern for the ultimate strength of structures has led to interest in the post-yield behaviour, which examines the collapse of structures due to the occurrence of large plastic deformations (Huges, 1988). Designers are therefore faced with the challenge of selecting the appropriate design and analysis tools to enable them to design a

safe and cost effective structure. Many tools are available to design and analyse structures and/or supporting members, but each tool has its own limitations. Simple analytical tools usually lead to over conservative designs, whereas more detailed numerical analysis tools which minimise the levels of conservatism generally have complex formulations and require huge amounts computer processing time.

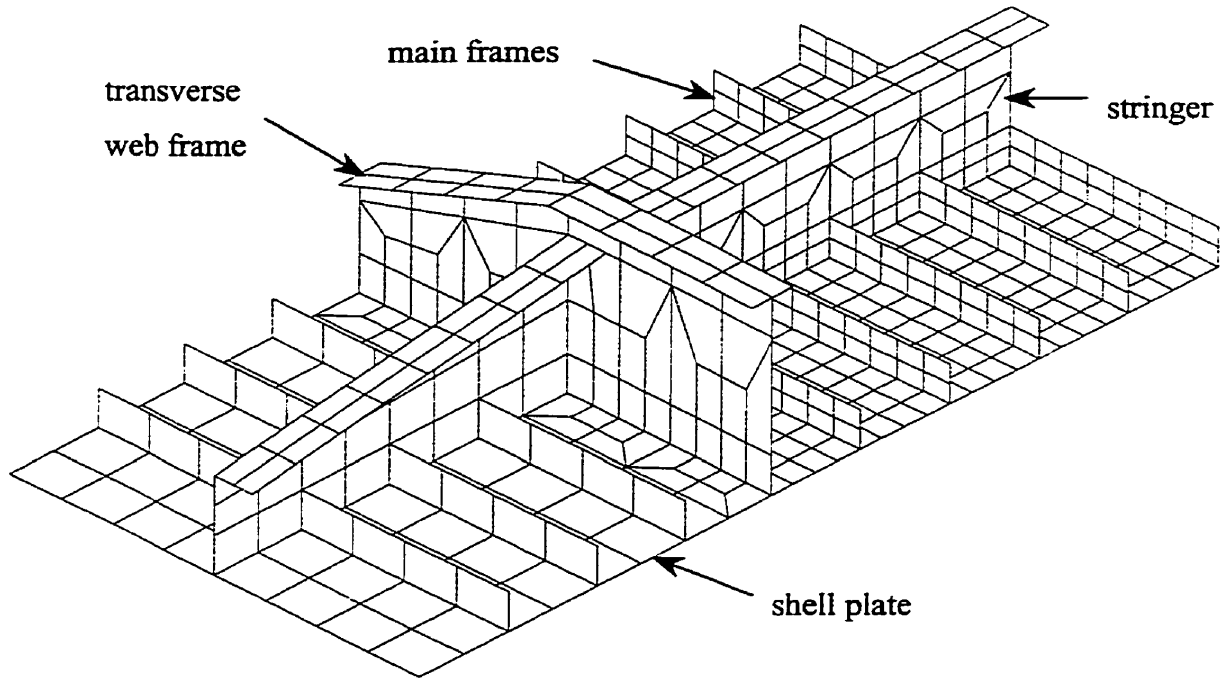

Figure 1.1: Ship's Grillage

Analytical solutions, which are theoretical solutions to a simplified structural geometry and loading conditions, are quite attractive to designers. Designers or analysts can quickly and easily quantify a particular structural behaviour with a few simple calculations and design against failure. However, analytical solutions require "idealised conditions" or details, which render them impractical for complex structures. In practice,

the structure (or problem) could be analysed in terms of the individual components. A disadvantage of this approach is that the boundary conditions are difficult to quantify and usually lead to extreme assumptions or idealised conditions. This results in designs that are often overly conservative depending on the overall complexity of the problem. For example, a main frame stiffener between two stringers on a ship's hull structure (grillage) could be analysed as a single beam with fixed or pinned end conditions where analytical solutions are readily available in literature. This suggests that the main frame stiffener running through a stringer is either rigidly attached or just simply supported at the stringer, both of which are incorrect from a practical point of view. The same conditions apply to a stringer supporting shell plate and main frame stiffeners between two transverse web frames. The assumed boundary conditions may render the design overly conservative.

Sometimes structural geometry and interaction effects are too complex to warrant the formulation of a simple analytical solution and hence empirical solutions are developed. In such cases, test data results describing a particular behavioural phenomenon are described in terms of best-fit equations, which are a composition of the underlying parameters defining the phenomenon and appropriate scaling factors. However, such solutions are often specific to a range of behavioural characteristics and have limitations for general design purposes.

Model tests are often carried out on structures to analyse performance characteristics. Using appropriate scaling laws, the analyst can model and test a structure to examine the

elastic behaviour effects up to first yield as well as the inelastic effects up to the point of total collapse. The inelastic effects include the formulation of plastic hinges, membrane effects and the ultimate load capacity of the structure at collapse. Although model tests are necessary for the purposes of research and the development of new or improved analytical solutions, the cost and time requirements rule them impractical as a design tool particularly at the initial stages of design.

With the development of computers came the development of Finite Element Analysis (FEA) tools. Using a discritised modelling scheme, complete structures (including components) could be modelled as a geometric mesh of elements, interconnected, so as to synthesise the actual structure. Complex structural analysis, including interaction effects between the supporting members as illustrated in Figure 1.1, could be easily carried out.

A classical approach to design using FEA is based on idealised linear elastic theory. Based on the maximum stress evaluated in a structure and the yield stress of the material, the load capacity of the structure up to first yield can be easily evaluated. This approach can be used to evaluate a lower bound limit load for a structure in a timely, cost effective manner. However, structures designed according to idealised elastic failure criteria (failure at first yield) are generally over designed. Since structures have significant load bearing capabilities beyond first yield, it is useful to design for inelastic behavioural characteristics.

Many finite element analysis packages have non-linear modelling capabilities making it possible to synthesise inelastic or post yield behaviour of a structure. Using appropriate mesh densities, boundary and loading conditions, and taking into account non-linearities associated with out of straightness, loss of stiffness due to yielding, etc., an FEA model can predict the behaviour of a complex structure with remarkable accuracy. However, carrying out a detailed non-linear analysis can prove to be very complex and time consuming. Depending on the geometric complexity of the model and the loading conditions, a full non-linear analysis may take days to complete. This is not attractive particularly at the initial stages of design.

The focus of this thesis, is to "investigate robust techniques of finite element analysis to evaluate non-linear lower bound limit loads of plated structures and stiffening members." These robust techniques are attractive because they form a hybrid of both classical finite element and analytical solutions, and conform to the non-linear behaviour of a material. They have the advantage of classical solutions in that they are simple, reliable, repeatable, and time efficient. They also have the advantage of full non-linear solutions in that they account for material non-linearity in their approach.

1.2 Ship Structural Design

As previously mentioned, ship structures have been traditionally designed elastically on the assumption that once a portion of the structure has yielded, any further increases in the load will result in pure plasticity or total collapse. However, it has been proven that these structures can sustain substantial structural damage and still operate safely. The

structures have significant amounts of plastic reserve capacity although they may have yielded in a localised zone.

This extra capacity is of great interest in the design of ship shaped offshore structures that operate in iceberg infested waters. An iceberg collision may undoubtedly cause damage to an offshore structure, but not necessarily in a global catastrophic sense. Small icebergs may collide and cause local damage or permanent set but not to the extent that the structure is deemed inoperable. Thus, ship structures can be designed plastically, accounting for inelastic effects, thereby reducing the level of conservatism in the design.

The object of this thesis is to introduce new improved methods of assessing the load capacity of a structure, accounting for inelastic or plastic effects in the material, for any given load configuration. For example, given an iceberg collision with a ship shaped offshore structure for a given contact configuration (i.e., size and shape of the contact zone assuming uniform pressure), robust methods of FEA can be used to predict the non-linear estimate of the load capacity of the structure. It should be noted, however, that the technique is not a design tool, but rather an analysis tool.

1.3 Scope of Work

The scope of this work is to investigate various robust methods of finite element analysis to evaluate non-linear lower bound limit load estimates of stiffened plated structures. These robust methods include the r-node method, Progressive Modulus Reduction (PMR)

method, and the m_α method. The results of each method are compared to the results of full non-linear finite element analysis, analytical solutions and lab test data where available.

Chapter 2

Theoretical Background

Structural analysis and design is generally carried out on the basis to two theoretical behaviour assumptions: the structure behaves either elastically or plastically. If the response of a structure without incurring any structural damage is of interest, then elastic theory is appropriate. However, if the ultimate capacity of a structure is of interest, then it would be necessary to use plasticity theory.

Although both types of analysis are necessary in structural design, depending on the application, neither of these types reflects the actual behaviour of a structure but rather upper and lower limits on its true behaviour. Also, many of the parameters that influence the behaviour of the structure (i.e., strength and/or applied load) may not be constants but may vary from one event to another. In such cases, a statistical method is appropriate that addresses the randomness of these parameters and the structure is designed to have a "probability of failure."

It is therefore necessary to improve the methods of limit analysis such that structural and material non-linearities are accounted for in the design. This will alleviate some of the uncertainty associated with design, thereby reflecting safer designs and improved design efficiency.

2.1 Elastic and Plastic Design and Analysis

The ideal elastic and elastic-perfectly plastic stress-strain behaviour of a beam subject to pure bending is illustrated in Figure 2.1. The elasticity curve illustrates a linear stress distribution through the section of the beam. Once the load level reaches the structure's elastic limit, the section starts to yield at the extreme fibres that are the greatest distance from the neutral axis. The plastic growth continues until the whole section of the beam has yielded.

Based on the geometry, and assumed ideal conditions, one can determine the relationship between the elastic and elastic-perfectly plastic bending moment capacities of the beam. The elastic bending moment capacity of the beam, assuming a uniform cross-section of thickness t and depth h, can be written as

$$M_e = 2*\left(\frac{1}{2}*\frac{th}{2}*\sigma_y\right)*\frac{2}{3}\frac{h}{2} = \frac{th^2\sigma_y}{6} \qquad (2.1)$$

where h is the through depth of the beam and σ_y is the yield stress of the material.

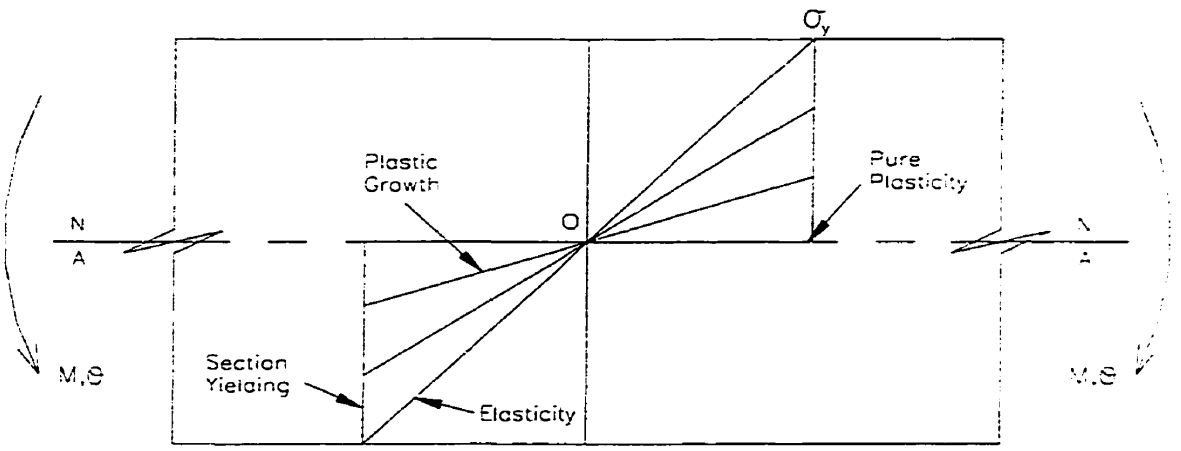

Figure 2.1: Stress and yielding of a beam section subject to pure bending

The plastic bending moment capacity of the beam can be written as

$$M_p = 2*\left(\frac{h}{2}*\sigma_y\right)*\frac{1}{2}\frac{th}{2} = \frac{th^2\sigma_y}{4} \qquad (2.2)$$

From equations (2.1) and (2.2)

$$M_p = 1.5*M_e \qquad (2.3)$$

2.1.1 Plastic Hinge Formation and Membrane Effects

Ship structures generally have significant load bearing capacities beyond their material yielding limits. The structures exhibit what is commonly known as "structural plasticity." The extent of structural plasticity can be categorised according to two behavioural characteristics, namely "plastic hinge formation" and "membrane action."

Rigid plastic hinge formation theory states that the collapse of a structure can be categorised by the formation of plastic hinges at particular locations within the structure, depending on the geometry and loading conditions. The location of plastic hinges for a fixed ended beam subject to uniform pressure is illustrated in Figure 2.2 (a). In practice, the collapse is not as sudden as idealised plastic hinge theory predicts because the theory ignores the elasto-plastic transition phase of the moment-curvature relationship (Huges, 1988).

Once the applied load reaches the yield capacity, permanent set will occur at the ends of the beam marking the beginning of inelasticity. Further increases in the loading will cause yielding to penetrate through the thickness of the beam until two plastic hinges or edge hinges form at the ends. The loss of stiffness is indicated by the reduction in the slope of the load deflection curve once the edge hinges have formed. Further increases in the load would result in the formation of a third plastic hinge at the midspan, representing a state of total collapse of the section.

For many structures, particularly plated structures, the formation of three hinges does not physically mean the section has totally collapsed. A structure considered collapsed according to plastic hinge theory may continue to have load-bearing capacity because of a phenomenon known as "membrane action." A structure that has fully yielded and experiences membrane behaviour has little or no reserve bending capacity but has added load bearing capacity because of tension in the material fibres. The structure continues to stretch having increased load bearing capacity until the material reaches it tensile fracture point as shown in Figure 2.2 (b).

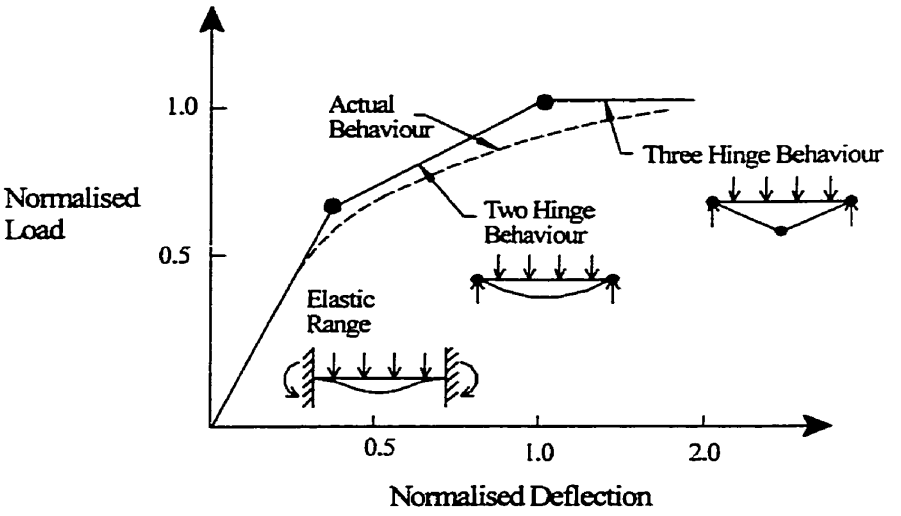

(a) Development of a Plastic Mechanism

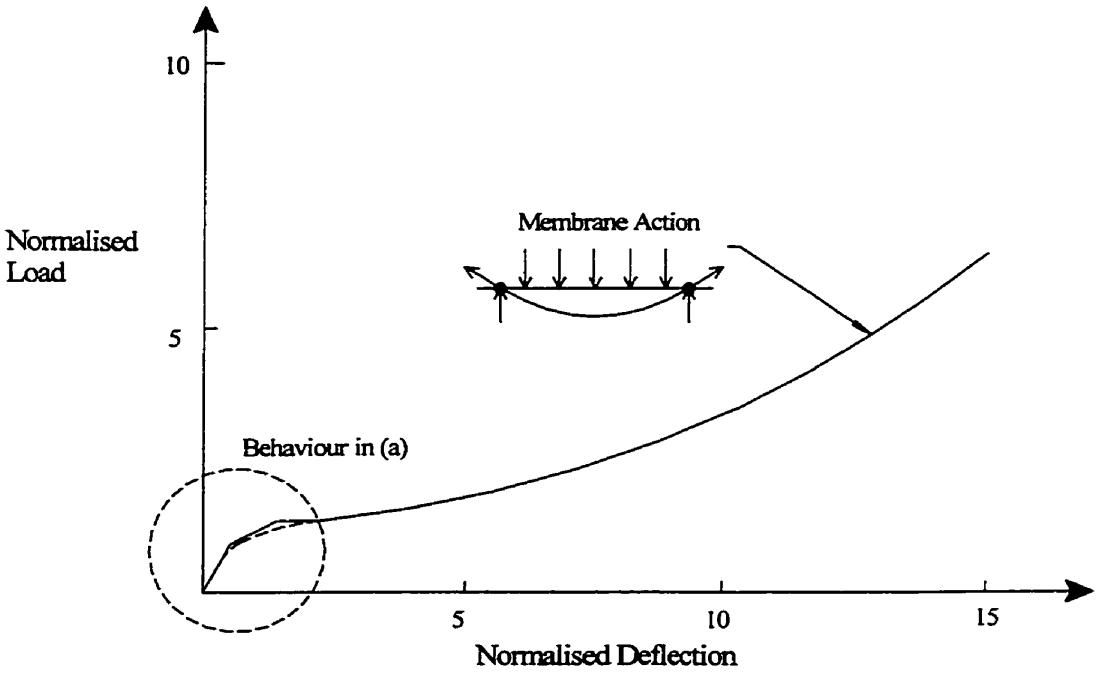

(b) Membrane Action

Figure 2.2: Plate failure by rigid plastic hinge formation and membrane action

Membrane effects become evident in flanged structures such as I beam, tee or angle sections but most significantly in plated structures such as a ship's hull structure. The structural members that form the support for the shell plate will exhibit a much higher load bearing capacity than predicted by elastic limits or plastic hinge formation theory.

Once the structure has lost its bending and shear capacity, membrane action in the shell plate (and regions of tension in the stiffeners) will allow the structure to have increased load-bearing capacity until the frames or stiffeners puncture the shell plating or tensile fracture occurs. An example of a ship's grillage including shell plate and the supporting members is illustrated in Figure 1.1.

2.2 Bounding Theorems

Limit states design is essentially the application of bounding theorems on the performance of a structure. The basis for design is that the structure is expected to behave within a set of bounding limits or it has a probability that it will fail under certain conditions. Generally, these limiting conditions are referred to as "ultimate limit states" and "serviceability limit states". The ultimate limit state criterion requires that a structure be designed to ensure that its factored strength is greater than the factored loads that will be imposed on the structure. The serviceability limit states criterion requires that the structure will function satisfactorily when subject to service loads (Adams *et al.*, 1979).

2.2.1 Statistical Analysis

Limit states design is often carried out using statistical methods of analysis where the design carries with it a "probability of failure," as demonstrated in Figure 2.3. Here, both the structural resistance and the applied loads acting are represented as probability or frequency distributions. The structural resistance distribution is a function of many distributions such as material strength, structural dimensions, etc., and the applied load is comprised of variable parameters such as wind, wave, current, water density, etc. Ideally, a safe design is one where the structural resistance always exceeds the applied load. However, statistically the two curves overlap (shaded region) such that the effect of the load may exceed the resistance of the structure, indicating failure. In these cases designers proportion the structure such that the overlap is minimal and the probability of failure is at an acceptable minimum.

Statistical analysis provides a safe, effective means of evaluating the integrity of structural design. However, the structural reliability is only as good as the availability and quality of the variational data for the parameters that define applied loads (wind, current, ice, temperature, etc.) and the resistive strength of the structural material.

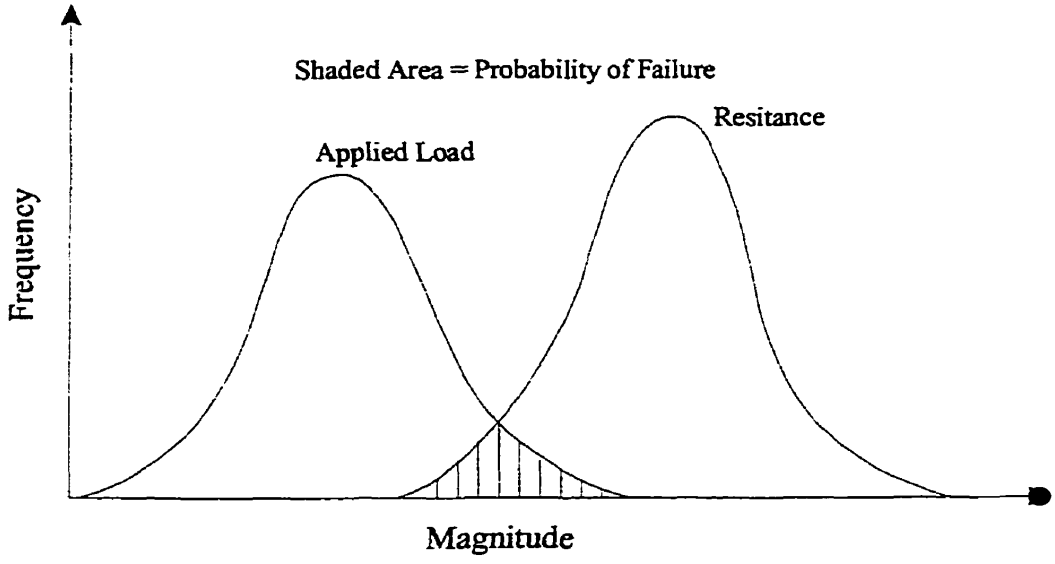

Figure 2.3: Frequency distribution curves (Sanderson, 1988)

2.2.2 Classical Lower and Upper Bound Theorems

The classical theorems of limit analysis are based on the upper and lower bound theorems. These theorems are based on the conditions of the stress fields and the strain fields respectively within a structure that has been subject to some externally applied load.

The *Classical Lower Bound Limit Theorem* is based on a concept of "static admissibility" of stress fields within a structure. A statically admissible stress field is one where the stress field throughout a structure for a given load application represents a state of equilibrium, in addition to satisfying the yield conditions. A safe field is one with all stresses inside the yield surface (Mangalaramanan, 1997). Thus the lower bound theorem can be stated as; "if a stress distribution can be found which satisfies equilibrium everywhere internally and balances the applied load, and is everywhere below yield, then

the structure is safe and will not collapse" (Calladine, 1969). In other words, a design is safe if the internal loads within a structure balance the externally applied loads and the stresses everywhere are below yield. This theorem gives lower safe bounds, and the maximum lower bound is the limit load.

The *Classical Upper Bound Limit Theorem* is based on the concept of "kinematic admissibility" of strain fields within a structure. A strain rate field defined throughout a structure is referred to as kinematically admissible for the given conditions of support if it is derived from a resultant strain field that is compatible with the conditions of support and certain continuity conditions (Mangalaramanan, 1997). Such a strain field is safe if and only if the rate at which the external loads do work (on the structure) is less than or equal to the rate at which energy is dissipated internally (Prager and Hodge, 1951). Applied loads that satisfy such conditions are considered upper bound. Thus the upper bound theorem can be stated as; "a structure experiencing plastic deformation will collapse if the rate of internal energy dissipation is equal to or less than the rate at which the external forces do work on that structure." An estimate of the plastic collapse by equating the rate of internal energy dissipation to the rate of work done in any deformation mechanism of the body will either be correct or high (Calladine, 1969). The theorem essentially says that if a failure path exists, the structure will take it. Thus this load is an upper bound and the minimum upper bound is the limit load (Seshadri and Fernando, 1992).

2.2.3 Extended Variational Theorems of Limit Analysis

In the past, researchers have used variational principles to derive statically admissable stress fields in limit analysis for perfectly plastic structures. It was Mura and Lee (1993) who demonstrated that variational principles can be used to evaluate a statically admissible multiplier, or safety factor, for a structure made of a perfectly plastic material subject to a given surface traction (Mangalaramanan, 1997).

It was previously understood that in limit analysis a statically admissible stress field couldn't exist outside the yield criterion defining the hypersurface (Prager, 1959). However, Mura *et al.* (1965) introduced a new concept, namely the "integral mean of the yield" criterion, which suggests that this requirement can be eliminated. They proposed that a stress distribution satisfying equilibrium and traction boundary condition, but violating yield, can still give a lower bound limit load provided the stress field does not violate the "integral mean of the yield" which is expressed as

$$\int_V \mu^0 [f(s_{ij}^0) + (\phi^0)^2] dV = 0 \qquad (2.4)$$

Based on the integral mean of the yield, where the yield criterion is given as

$$f(s_{ij}^o) = \frac{1}{2} s_{ij}^o s_{ij}^o - k^2 \qquad (2.5)$$

A new lower bound safety factor or multiplier m' can be evaluated and expressed as

$$m' = \frac{m^0}{1 + \max\{f(s_{ij}^0) + (\phi^0)^2\}/2k^2} \leq m \qquad (2.6)$$

which is valid for any set of $v_i^0, s_{ij}^0, \sigma^0, m^0, \mu^0, \phi^0$ satisfying

$$(s_{ij}^0 + \delta_{ij}\sigma^0)_{,i} = 0 \quad \text{in V} \qquad (2.7)$$

$$(s_{ij}^0 + \delta_{ij}\sigma^0)n_i = m^0 T_i \quad \text{on } S_T \qquad (2.8)$$

$$\int_V \mu^0 [f(s_{ij}^0) + (\phi^0)^2] dV = 0 \qquad (2.9)$$

$$\mu^0 \geq 0 \qquad (2.10)$$

A detailed formulation of the above lower bound multiplier m' is given in Appendix A (Mura *et al.*, 1965; Mangalaramanan, 1997). The application of the above formulation used with finite element analysis is given in section 3.5. This forms the basis for formulation of the m_α method of robust analysis given in section 3.6.

2.2.4 Theorem of Nesting Surfaces

The "theorem of nesting surfaces" was introduced by Calladine and Drucker (1962) and used to determine simple approximate solutions to the combined loading problems of power law creep. The theorem was developed based on elastic and plastic limit analysis results together with special solutions for single loads. Boyle (1982) later restated the theorem and used it to construct generalised models to simplify stress analysis of

complex structures under multiple loading. In essence, the theorem defines an "effective generalised stress," or "reference stress" stated in terms of energy dissipation rates within a structure under a system of loads.

The average energy dissipation rate for a structure subject to an applied load is given as

$$\sigma_R \varepsilon_R V = \int_V \sigma_{ij} \varepsilon_{ij} dV \qquad (2.11)$$

For a material behaviour expressed by the constitutive equation

$$\varepsilon = B\sigma^n \qquad (2.12)$$

Using equivalent stresses and strains, equation (2.11) can be written as

$$\sigma_R^{n+1} V = \int_V \sigma_e^{n+1} dV \qquad (2.13)$$

Further manipulation yields the reference stress (or "effective generalised stress") or the functional that forms the basis of the theorem of nesting surfaces (Calladine and Drucker, 1963; Boyle, 1982) and is given as

$$\sigma_R = Q_e(\sigma_{ij}) = F(\sigma_{ij}) = \left[\frac{1}{V_T} \int_{V_T} \sigma_e^{n+1} dV \right]^{\frac{1}{n+1}} \qquad (2.14)$$

The theorem essentially states that the functional is strictly monotonically increasing with the exponent n. Generally, if for a given stress space having hypersurfaces $Q_e(\sigma_{ij})$ = constant, then for increasing n they must 'nest' inside each other as

$$Q_e\big|_{n=1} \leq Q_e \leq \lim_{n\to\infty} Q_e \qquad (2.15)$$

In other words, the envelope defining this stress space has two surfaces. It is bound on the outside by surface, $n = 1$, which is analogous to linear elasticity and on the inside by surface $n = \infty$, which is the yield surface, assuming plasticity occurs at Q_e = constant.

For a linear elastic material, $n = 1$ and the effective generalised stress is given as

$$Q_e = \left[\frac{1}{V_T}\int_{V_T} \sigma_e^2 dV\right]^{\frac{1}{2}} \qquad (2.16)$$

To illustrate the notion of bounding surfaces that correspond to linear elasticity and perfect plasticity, consider the statically determinate structure shown in Figure 2.4. The two bars are of equal length with each pin-jointed to a rigid foundation. The loads Q_1 and Q_2 are applied at the central pin. The stress in each bar, assuming the cross-sectional areas are the same is given as

$$\sigma_1 = \frac{Q_1 + Q_2}{\sqrt{2}A} \qquad \sigma_2 = \frac{Q_1 - Q_2}{\sqrt{2}A} \qquad (2.17)$$

Thus, we can write the generalised effective stress as

$$\sigma_R = Q_e(\sigma_1,\sigma_2) = F(\sigma_1,\sigma_2) = \left[\frac{1}{V_T}\int_{V_T}\sigma_e^{n+1}dV\right]^{\frac{1}{n+1}}$$
$$= \left[\frac{1}{2}\left(\frac{Q_1+Q_2}{\sqrt{2}A}\right)^{n+1} + \frac{1}{2}\left(\frac{Q_1-Q_2}{\sqrt{2}A}\right)^{n+1}\right]^{\frac{1}{n+1}} \qquad (2.18)$$

where $V = 2LA$.

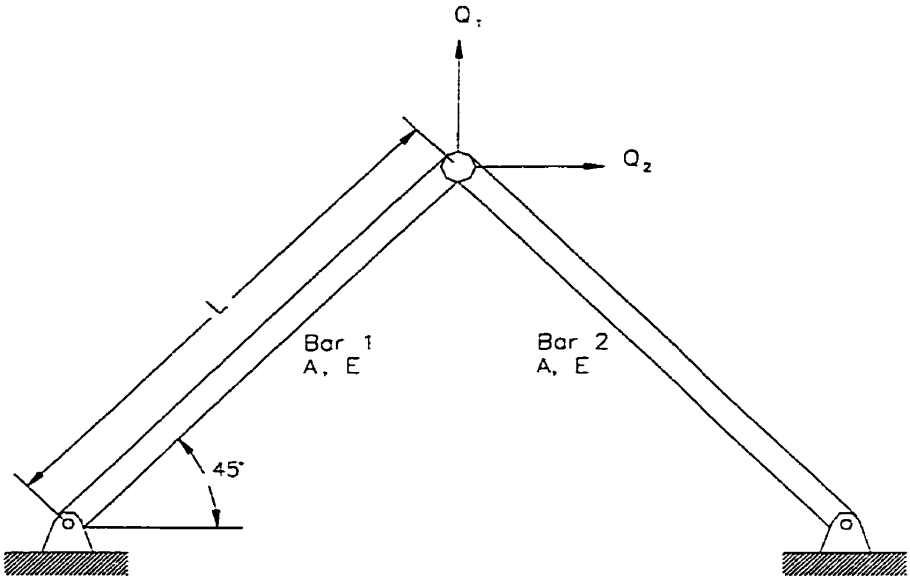

Figure 2.4: A two bar structure with pinned joints

For a linear elastic material $n = 1$,

$$Q_e = \sqrt{\left(\frac{Q_1}{\sqrt{2}A}\right)^2 + \left(\frac{Q_2}{\sqrt{2}A}\right)^2} \qquad (2.19)$$

For a plastic material $n = \infty$

$$Q_e \to \frac{Q_1}{\sqrt{2}A} + \frac{Q_2}{\sqrt{2}A} \qquad (2.20)$$

where $Q_1, Q_2 \geq 0$

If the effective stress is assumed to be unity ($Q_e = 1$), then the bounding surfaces $n = 1$, $n = \infty$ and also, $n = 3$ can be defined to demonstrate the nesting effect as shown in Figure 2.5. Also,the equation $Q_e|_{n=1} \leq Q_e \leq \lim_{n\to\infty} Q_e$ is verified.

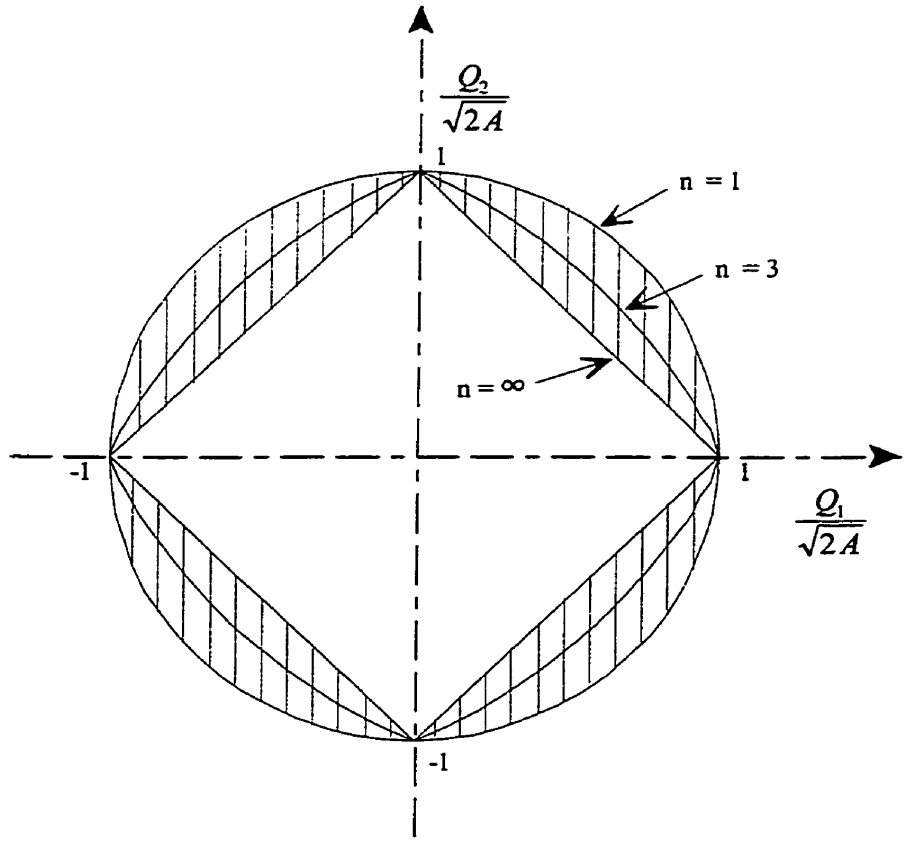

Figure 2.5: Nesting surfaces in a two bar structure for generalised loading

Chapter 3

Robust Techniques in Limit Load Determination

Robust methods of evaluating limit loads are highly attractive when compared with the alternative analytical or non-linear finite element methods for complex problems. The robust methods are relatively simple to implement and evaluate limit loads that account for material non-linearities such as structural plasticity. The solution process is carried out as a set of static analyses, which ensures a stable process without convergence difficulties. Hence, solutions to complex problems can be obtained quickly and easily.

Robust techniques used in the present thesis have been explored mainly for application to pressure vessel design. The objective of this thesis is to explore the effectiveness of using these robust methods to evaluate limit loads for ship structures.

3.1 Reduced Modulus Techniques

The use of robust methods in limit design began in 1981 with the development of a reduced modulus technique to categorise stresses in pressure vessels (Jones and Dhalla, 1981). A technique was developed to classify local clamp induced stresses in piping used in Liquid Metal Fast Breeder Reactors. It was found that clamp induced stresses redistribute due to material or geometric non-linearity and are therefore categorised as secondary. More importantly, however, it was found that the inelastic response of a structure could be investigated by systematically weakening the elastic modulus in the highly loaded regions of the structure. Comparisons with inelastic analysis indicated that this technique accurately simulated the inelastic behaviour of the clamped pipe for the purposes of design (Mackenzie and Boyle, 1993).

This procedure was extended to analyse the inelastic response and follow up characteristics of piping systems. The analysis involved progressively modifying the elastic modulus at each stage by performing repeated linear elastic analyses (Dhalla, 1984, and Severud, 1984). Dhalla later directed his efforts toward developing a simple procedure for classifying stresses at elevated temperatures using linear elastic analysis (Dhalla, 1987). The procedure was to carry out an initial elastic analysis and to identify the effective stress σ_A and strain ε_A at the highly loaded locations. The inelastic strain ε_P was then estimated based on the calculated elastic stress. This strain may be a maximum strain for the assumed load control behaviour or a specific limit such as a 1% membrane strain defined in the code. The minimum secant modulus was then calculated as

$$E_M^S = \frac{\sigma_A}{\varepsilon_P} \qquad (3.1)$$

where σ_A is the element stress and ε_P is the estimated inelastic strain. At least three new values of reduced moduli were then defined between this minimum secant modulus and the original Young's modulus, and applied to the highest stressed regions of the structure. This procedure establishes a relaxation trend with repeated iterations.

Marriott (1988) proposed a reduced modulus method for determining primary stresses in pressure vessel components and highlighted the possibility of determining limit loads. The analysis involved performing an initial elastic analysis and identifying all elements having stresses above the code allowable. The elastic modulus of these elements would be reduced on an element by element basis using the equation

$$E_R = E_o \frac{S_m}{SI} \qquad (3.2)$$

where E_o is the previous value of the modulus, S_m is the code allowable stress, and SI is the element stress intensity. A second analysis would be carried out, evaluating a new stress distribution followed by a readjustment of the elastic moduli of critically stressed elements. This procedure would be iterated until the maximum stress intensity was less than S_m or some other convergence criteria. Reducing stresses in the structure so that the stresses are everywhere below the allowable or yield stress of the material suggests that a statically admissible stress field exists. Thus, the procedure of modulus reduction is one that yields a lower bound limit load, provided all stresses are everywhere below yield.

3.2 *Generalised Local Stress Strain (GLOSS)*

Several papers by Seshadri *et al.* have applied the reduced modulus procedure in a number of areas. Elastic modulus adjustment techniques were developed with the introduction of a method of analysis called the Generalised Local Stress Strain (GLOSS) Analysis (Seshadri and Kizhatil 1990; Kizhatil and Seshadri 1991; Seshadri 1990). The typical GLOSS diagram is shown in Figure 3.1.

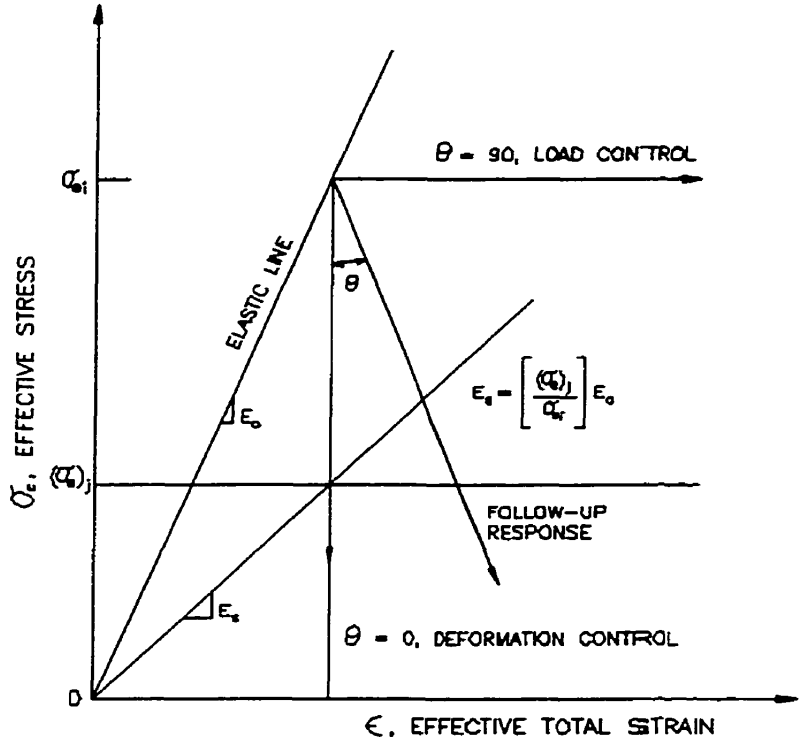

Figure 3.1: GLOSS diagram illustrating follow-up angle

The understanding behind the method is that inelastic stresses at given locations in a structure redistribute following a uniaxial stress relaxation process. Assuming an elastic perfectly plastic material and pure deformation control, inelasticity would cause stresses to relax to $(\sigma_e)_j$ while maintaining strain at the original level. The method suggests that

this inelastic effect can be incorporated in an elastic analysis by modifying the elastic modulus of a pseudo-elastically stressed element using the scheme

$$E_s = E_o \frac{(\sigma_e)_j}{\sigma_{ei}} \qquad (3.3)$$

where $(\sigma_e)_j$ is an arbitrarily chosen stress to modify the elastic modulus, σ_{ei} is the equivalent element stresses, and E_o is the previous value of the Young's modulus for an element. It was demonstrated that reduced modulus methods predict inelastic effects with sufficient accuracy in pressure component design. Stress categorisation procedures were also proposed.

3.3 Elastic Compensation Method

Mackenzie and Boyle used a reduced modulus technique to develop a method of estimating limit loads using a sequence of elastic finite element analyses (Mackenzie and Boyle, 1993). The method, termed elastic compensation, aims to evaluate a lower bound limit load that satisfies the lower bound theorem, producing a statically admissible stress field. The analysis aims at selectively reducing (or iterating) the elastic modulus of local pseudo-elastic stressed elements to redistribute the stresses in the structure and to synthesise the formation of a limit state stress distribution. Iteration zero would be the first of a series of linear elastic analyses. The modulus adjustment or modification is carried out as

$$E_i = E_{(i-1)} \frac{\sigma_{arb}}{\sigma_{e(i-1)}} \qquad (3.4)$$

where $\sigma_{e(i-1)}$ is the stress corresponding to the previous modulus $E_{(i-1)}$ and σ_{arb} is a stress level chosen to redistribute or reduce the stress. Provided σ_{arb} is carefully selected, consecutive iterations should result in a net decrease in the maximum stress in the structure. Several iterations are carried out until the lowest value of the maximum stress in the structure is evaluated (peak stresses no longer reduce with increased iterations). Since the analysis giving σ_{max} is an elastic analysis, the resultant stress is proportional to the applied load P, given as

$$\sigma_{\max} = \beta P \qquad (3.5)$$

where β is the proportionality constant based on geometry and loading conditions for the final analysis. To ensure a statically admissible stress field, the stresses in the structure must be everywhere equal to or less than yield. Therefore, an applied load satisfying this condition is a limit load given as

$$\sigma_Y = \beta P_L \qquad (3.6)$$

Thus from equations (3.5) and (3.6) the expression for the limit load is

$$P_L = P \frac{\sigma_Y}{\sigma_{\max}} \qquad (3.7)$$

Mackenzie and Boyle demonstrated that the use of the elastic compensation method with the lower bound limit load theorem was very effective. The solutions were exact for simple components and sufficiently accurate for more complex structures analysed using FEA. However, an analyst must use caution in selecting a load or a limiting stress in defining the modulus modification function.

3.4 GLOSS R-Node Method

Seshadri (1991) proposed a reduced modulus method called the GLOSS r-node method to give approximate estimates of a limit load. The r-nodes are identified as load controlled locations within a structure, and the growth of an r-node peak (and the associated equivalent stress value) can characterise the nature of a plastic collapse mechanism. The locations of the r-node peaks indicate the precise positions of plastic hinges that would form in the structure.

3.4.1 Redistribution Nodes and Load Control

The basis for this work (Seshadri and Mangalaramanan, 1997) began in 1961 when Schulte recognised that in the solution of a creep analysis of beams, certain points in the cross section maintained the same stress level as the solution progressed from the initial elastic solution to the final stationary solution (Schulte, 1961). These points were later labelled "skeletal points" and were defined as locations within a structure where little or no change in stress levels occurred at intermediate states between the initial elastic and

final fully plastic (Marriott and Keckie, 1964). Seshadri and Marriott (1993), despite the belief that there was no significance attached to skeletal points, studied the notion of reference stress (or r-node stress) and limit loads, and demonstrated a unifying relationship based on the load-controlled nature of the r-nodes.

Two types of controlled stresses within a structure are load-controlled and deformation controlled. Load-controlled stresses are induced stresses, which preserve equilibrium with externally applied forces and moment and are statically determinate. Deformation controlled stresses result from statically indeterminate actions. Once plasticity occurs, the statically indeterminate stresses redistribute themselves throughout the component or structure, except at the r-nodes which are statically determinate. On the GLOSS diagram in Figure 3.1, the r-nodes are positions where the follow up angle θ would be 90 degrees indicating locations where stress levels remained unchanged from one iteration to the next (Managalaramanan and Seshadri, 1997).

3.4.2 Plastic Collapse of Structures

To illustrate the concept of plastic collapse and its relationship with r-nodes, and hence limit loads, consider a rectangular beam cross-section subject to pure bending. The material constitutive relationship is given by

$$\varepsilon = B\sigma^n \qquad (3.8)$$

where B and n are material parameters. If it is assumed that the structure behaves elastically, then $n = 1$, but if perfect plasticity is assumed then $n = \infty$. The variations of the stress distributions for the beam are given in Figure 3.2. The intersection of the stress distributions for $n = 1$ and $n = \infty$ is the location of the redistribution or r-node, and all other stress distributions corresponding to all other n's are assumed to passed through the same node (Mangalaramanan and Seshadri, 1997).

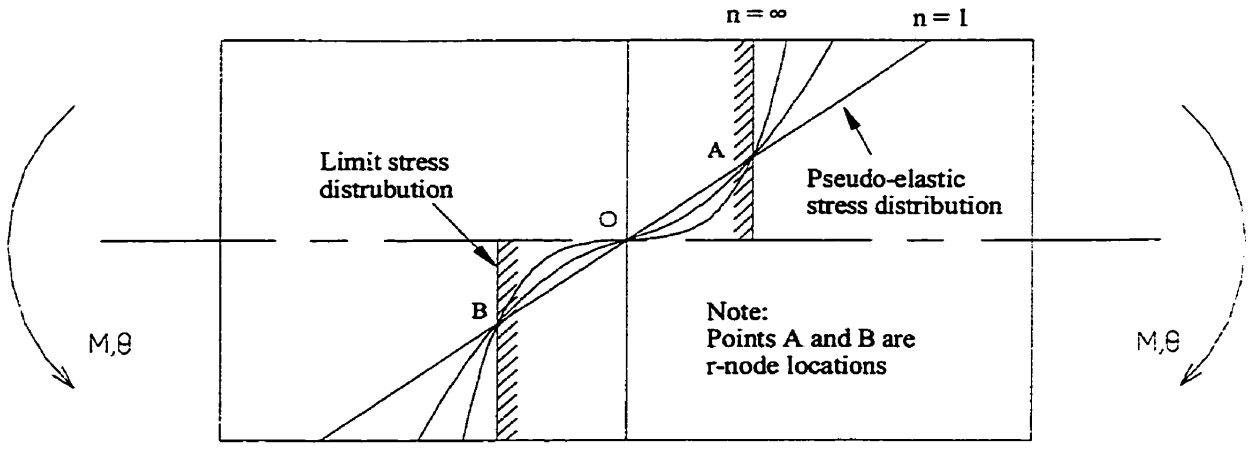

Figure 3.2: R-node locations in a beam subject to bending

The method suggests that when inelasticity occurs, the inelastic stress will redistribute throughout the component or structure, except at specific locations where the stress is essentially statically determinate. These locations are called redistribution nodes or r-nodes and represent load-controlled locations within the structure. The reference stress, or effective stress, at the r-node is related to the yield stress of an elastic perfectly plastic material by the expression

$$(\sigma_e)_{r-node} = \mu\sigma_Y \qquad (3.9)$$

where $\mu < 1$ prior to the formation of a plastic hinge, and $\mu = 1$ when a plastic hinge forms. Since the r-nodes are load-controlled locations within a structure, the induced effective stresses are proportional to the applied load(s) given as

$$\begin{aligned} (\sigma_e)_{r-node} &= \gamma_1 P \\ (\sigma_e)_{r-node} &= \gamma_2 \{P, M\} \end{aligned} \qquad (3.10)$$

where γ_1 and γ_2 are scaling parameters dependent on the loading, geometric configurations and material behaviour (Seshadri and Fernando, 1992). For an elastic perfectly plastic material, when the Von Mises equivalent r-node stress reaches yield stress, the externally applied load will correspond to a limit load given as

$$\begin{aligned} \sigma_Y &= \gamma_1 P_L \\ \sigma_Y &= \gamma_2 \{P_L, M_L\} \end{aligned} \qquad (3.11)$$

Therefore from the r-node stress evaluated for a given load P, the limit load P_L for a statically determinate structure is given as

$$\begin{aligned} P_L &= \left[\frac{\sigma_Y}{(\sigma_e)_{r-node}}\right] P \\ \{P, M\}_L &= \left[\frac{\sigma_Y}{(\sigma_e)_{r-node}}\right] \{P, M\} \end{aligned} \qquad (3.12)$$

If there are N r-node peaks or plastic hinge locations within a structure, the formation of a plastic collapse mechanism can be tracked by rearranging the peak equivalent reference

stresses in descending order. The equivalent reference stress used to evaluate the limit load can then be evaluated as the average of the r-node peaks in the structure and given as

$$\overline{\sigma_n} = \frac{\Sigma_{j=1}^{N} \sigma_{nj}}{N} \qquad (3.13)$$

The limit load is therefore evaluated as

$$\overline{P_L} = \left[\frac{\sigma_Y}{\overline{\sigma_n}}\right] P \qquad (3.14)$$

Non-peak r-node stresses will also exist in a structure and may represent a large portion or volume of the structure. However, while these nodes are also load-controlled locations, they may not lead to cross-sectional plasticity (Managalaramanan and Seshadri, 1997).

3.4.3 Location of the R-Nodes

The r-node method provides a simple and systematic means of carrying out inelastic analyses of mechanical components and structures based on just two linear elastic finite element analyses. The first linear elastic analysis is carried out and a pseudo-elastic stress distribution[1] evaluated. The elastic modulus of each element within the model is modified according to the equation

[1] The elastic stress distribution for a structure evaluated numerically can be termed pseudo-elastic since it does not identify yielding limits and is hence not representative of the true stress-strain relationship for a structure. The stress-strain relationship for the structure is elastic for any level of applied load.

$$E_M = E_o \frac{\sigma_{arb}}{\sigma_e} \qquad (3.15)$$

where E_o is the original elastic modulus, σ_e is the element stress and σ_{arb} is an arbitrarily chosen stress to redistribute the pseudo-elastic stresses in the structure.

A second analysis is performed evaluating a new stress distribution, which is compared to the stress distribution from the first analysis. Based on two consecutive linear elastic analyses, locations where stresses of the same element do not change ($\Delta\sigma = 0$) are identified as r-nodes. In other words, the follow-up angle θ on the GLOSS diagram (Figure 3.1) is determined for each element and elements having $\theta = 90^\circ$ are be identified as r-nodes. Seshadri later studied the locations of r-nodes within a structure, and provided guidance on the location of true r-nodes within any structure (Seshadri, 1997). The GLOSS r-node method has been used to evaluate limit loads for various pressure vessel components, (Seshadri, 1991; Seshadri and Fernando, 1992; Seshadri and Marriott, 1993), framed structures and arches (Fernando and Seshadri, 1993), and symmetric and non-symmetric plate structures (Mangalaramanan and Seshadri, 1995). An r-node procedure has also been developed to perform a minimum weight design of mechanical components and structures using r-nodes (Mangalaramanan and Seshadri, 1997).

3.5 Extended Lower Bound Theorem

Mura and Lee (1965) proposed a method of determining limit loads using an extended lower bound theorem derived based on variational principles. They used this theorem to

evaluate the limit load of a structure subject to tension and obtained good limit load estimates. However, for more complicated structures, a procedure more generic in nature was necessary. Seshadri and Managalaramanan (1997) adopted the elastic modulus modification procedures in conjunction with the extended lower bound theorem and evaluated limit loads directly based on linear elastic stress distributions. The use of elastic modulus modification procedures ensured static admissibility in the evaluated stress distributions.

Mura *et al.,* (1965), demonstrated that the factors m^o, μ^o and ϕ^o in the functional

$$F = m^0 - \int_{V_T} \mu^0 [f(s_{ij}^o) + (\phi^0)^2] dV \qquad (3.16)$$

can be determined by rendering the function stationary, where $f(s_{ij}^0) = \frac{1}{2} s_{ij}^o s_{ij}^o + k^2$ and $k^2 = \sigma_y^2/3$. The formulation of the function F is given in Appendix A.

In these equations, s_{ij}^0 is the linear elastic stress distribution, which corresponds to an applied traction $m^0 P$. If $\tilde{s}_{ij}^0$ is a statically admissible stress distribution corresponding to an applied traction P, then $m^0 P$ would correspond to $m^0 \tilde{s}_{ij}^0$, making it clear that

$$s_{ij}^0 = m^0 \tilde{s}_{ij}^0 \qquad (3.17)$$

Therefore, equation (3.16) can be rewritten as

$$F = m^0 - \int_{V_T} \mu^0 [\tfrac{1}{2}(m^0)^2 \tilde{s}_{ij}^0 \tilde{s}_{ij}^0 - k^2 + (\phi^0)^2] dV \qquad (3.18)$$

The Von Mises equivalent for uniaxial state of stress yields the equations

$$\tfrac{1}{2}\tilde{s}_{ij}^{0}\tilde{s}_{ij}^{0} = \frac{(\sigma_e^0)^2}{3} \qquad (3.19)$$

$$k^2 = \frac{\sigma_y^2}{3} \qquad (3.20)$$

Substituting equations (3.19) and (3.20) into equation (3.18) gives

$$F = m^0 - \int_{V_T} \frac{\mu^0}{3}\left[\left\{(m^0)^2(\sigma_e^0)^2 - \sigma_y^2\right\} + 3(\phi^0)^2\right] dV \qquad (3.21)$$

If the functional F is rendered stationary, the factors m^0, μ^0, and ϕ^0 can be evaluated using the equations

$$\frac{\partial F}{\partial m^0} = 0, \quad \frac{\partial F}{\partial \mu^0} = 0, \quad \frac{\partial F}{\partial \phi^0} = 0 \qquad (3.22)$$

Evaluating leads to

$$\phi^0 = 0 \qquad (3.23)$$

$$m^0 = \frac{\sigma_y \sqrt{V_T}}{\sqrt{\sum_{k=1}^{N} (\sigma_{ek}^0)^2 \Delta V_k}} \qquad (3.24)$$

where σ_{ek}^0 and ΔV_k are the Von Mises equivalent stresses and volumes of the respective elements in a given FEA discritised model (Seshadri and Mangalaramanan, 1997).

Comparing this formulation for m^0 with that obtained by Calladine and Drucker (1961) and Boyle (1982) using the theorem of nesting surfaces, equation (2.16), it is seen that

$$m^0 = \frac{\sigma_y}{\sigma_R} \tag{3.25}$$

This implies that a monotonic increase in the reference stress in a structure will result in a monotonic decrease in m^0 with increasing n. Since equation (2.14) gives a lower bound on the reference stress for $n = \infty$, then m^0 corresponding to $n = 1$ is an upper bound multiplier for limit loads.

The lower bound theorem according to Mura *et al.* (1965) is given as

$$m' = \frac{m^0}{1 + \max\{f(s_{ij}^0) + (\phi^0)^2\}/2k^2} \le m \tag{3.26}$$

Substitution of equations (2.5), (3.19) and (3.20) into equation (3.26) and simplifying gives

$$m' = \frac{2m^0\sigma_y^2}{\sigma_y^2 + (m^0)^2(\sigma_e^0)_M^2} \le m \tag{3.27}$$

where $(\sigma_e^0)_M$ is the maximum equivalent stress in a structure for a prescribed load P. The evaluation of equations (3.24) and (3.27) becomes trivial when evaluated using linear elastic FEA. The limit load can then be evaluated as

$$P_{LM} = m'P \tag{3.28}$$

It is also clear from the above formulation that the limit load is bound by

$$m' \leq m \leq m^0 \qquad (3.29)$$

3.6 m_α Method

In an attempt to improve lower bound estimates of limit loads, a method making use of just two linear elastic analyses was developed, designated as the m_α method (Seshadri and Managalaramanan, 1997). The notion of reference volume is used in conjunction with the theorem of nesting surfaces to evaluate improved lower and upper bounds on the limit load. Also, reference volume evaluated for two linear elastic analyses is used to account for localised collapse, along with the technique "leapfrogging" to a limit state. These concepts, in conjunction with the elastic modulus adjustment technique (Seshadri and Fernando, 1992) are used to obtain improved lower estimates of the limit load.

3.6.1 Theorem of Nesting Surfaces

The theorem of nesting surfaces formally discussed in the previous chapter is generally illustrated with the equation

$$Q_e = \left[\frac{1}{V_T} \int_{V_T} \sigma_e^{n+1} dV \right]^{\frac{1}{n+1}} \qquad (3.30)$$

where Q_e is the effective generalised stress which increases monotonically with the exponent n.

The theorem of nesting surfaces states that "if for a given stress space having a hypersurface $Q_e(\sigma_{ij})$ = constant, then for increasing n they must 'nest' inside each other as

$$Q_e\big|_{n=1} \leq Q_e \leq \lim_{n\to\infty} Q_e \qquad (3.31)$$

The stress space is bound on the outside surface $n = 1$, which is analogous to linear elasticity and on the inside surface $n = \infty$, which is the yield surface, assuming plasticity occurs at Q_e = constant. For a linear elastic material, $n = 1$ and the effective generalised stress is given as

$$Q_e = \left[\frac{1}{V_T}\int_{V_T} \sigma_e^2 dV\right]^{\frac{1}{2}} \qquad (3.32)$$

The same stress given as a FEA discretised scheme is given as

$$Q_e = \sqrt{\frac{\sum_{k=1}^{N} \sigma_{ek}^2 \Delta V_k}{V_T}} \qquad (3.33)$$

where N is the number of elements and V_T is the total volume of the component or structure.

3.6.2 Reference Volume and Local Plastic Collapse

Structures that collapse as a result of inelastic action do so because a significant portion or section of the structure has yielded. Although the whole structure is considered collapsed, only a local region has experienced inelasticity. Thus, the upper bound limit load multiplier m^o, evaluated on the basis of total volume (V_T), will be overestimated and the lower bound limit load multiplier m' will be underestimated.

The concept of reference volume is introduced to identify the 'kinematically active' portion of the structure that is influenced most by plastic action (Seshadri and Mangalaramanan, 1997). It basically confines the zones of plastic collapse to a local sub region of the structure as shown in Figure 3.3. Thus the magnitude of the upper bound multiplier would be based on the sub-volume given as

$$V_\beta = \sum_{k=1}^{\beta} (\Delta V_k) \tag{3.34}$$

To effectively carry out the various summations in identifying this region of plasticity, it is necessary to carry out the following sequence based on decreasing energy dissipation:

$$(\sigma_{e1}^0)^2 \Delta V_1 > (\sigma_{e2}^0)^2 \Delta V_2 > \ldots > (\sigma_{eN}^0)^2 \Delta V_N \tag{3.35}$$

where N represents the sequential ordering of the element energy levels in a decreasing manner and e is the element number.

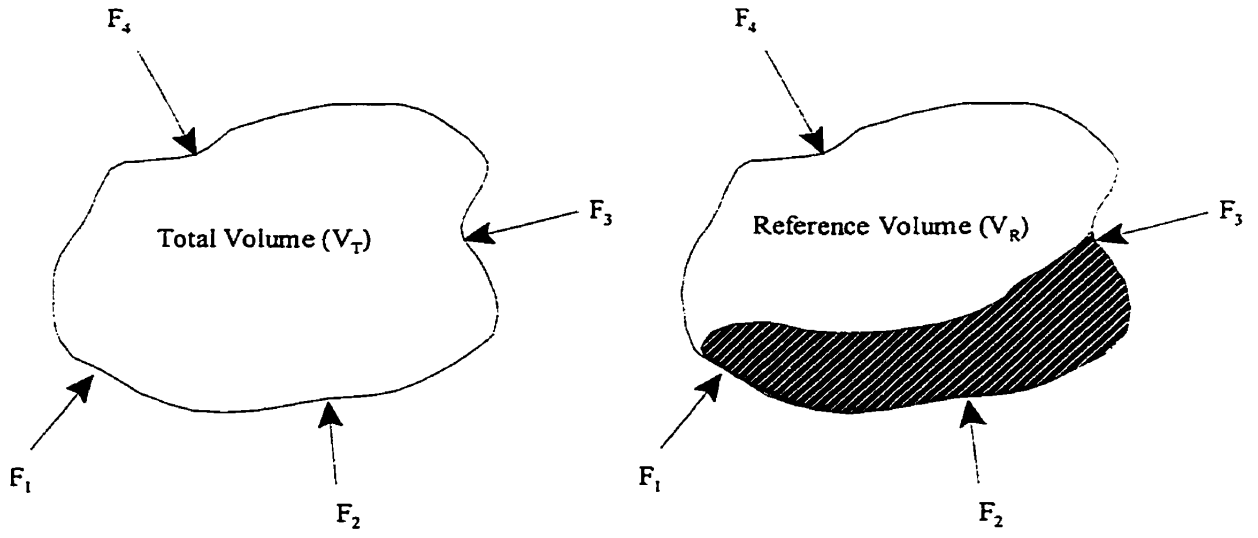

Figure 3.3: Total and reference volumes

If we assume only one element for the structure then β=1 and equation (3.24) evaluates a classical lower bound given as

$$m^0 = \frac{\sigma_y}{\sigma_{el}^0} \qquad (3.36)$$

3.6.3 Iteration Variable, ζ

It is necessary to define the iteration variable (ζ) such that infinitesimal changes to the elastic modulus of the various elements during subsequent linear elastic analyses (two, three, etc.) would induce a change in ζ or $\Delta\zeta$ (Seshadri and Mangalaramanan, 1997). The change in $\Delta\zeta$ would depend on the nature of the modulus adjustments.

It is understood that with iterations of the elastic modulus and consecutive linear elastic FEA that the peak stresses in the resultant stress distribution will decrease and level off. If this is true, then for the degenerate case[2] of equation (3.36), an increase in ζ would result in an increase in the upper bound multiplier m^0. However, based on total volume, m^0 decreases with increased ζ. Therefore, there must be some sub-volume, (V_R), such that $\Delta V_1 < V_R \leq V_T$ where the multiplier m^o is invariant for two consecutive linear elastic finite element analyses and the theorem of nesting surfaces is barely satisfied. The identification of the reference volume based on the upper bound multiplier m^o evaluated for two consecutive iterations is illustrated in Figure 3.4.

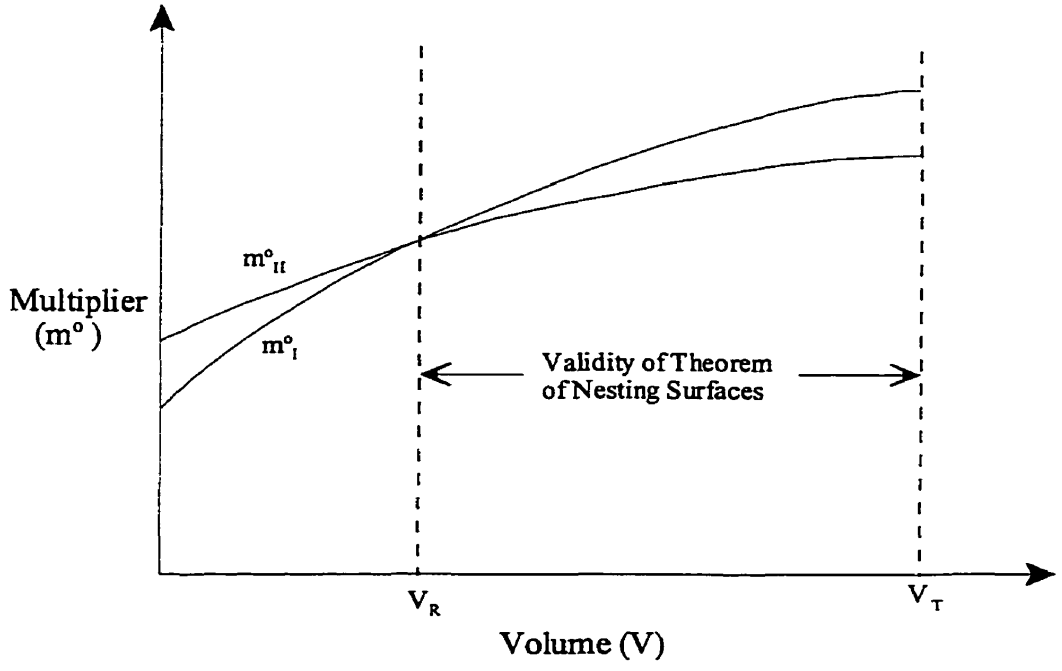

Figure 3.4: Determination of reference volume V_R and Mura's upper bound multiplier $m^o(V_R)$ on the basis of two consecutive linear elastic analyses such that the theorem of nesting surfaces is barely satisfied

[2] Degenerate case refers to the evaluating of limit loads or m^o based on the maximum stress in the structure.

3.6.4 Improved Lower Bound Limit Load – m_α Method

The m_α method is essentially an improved limit load formulation, which is extended from Mura's variational formulation. The m_α multiplier can be obtained by simply "leap-frogging" to the limit state on the basis of just two linear elastic finite element analysis (Seshadri and Mangalaramanan, 1997).

The elastic modulus of the elements are modified in the same manner as the GLOSS r-node method according to the equation

$$E_k = E_o\left[\frac{\sigma_j}{(\sigma_e)_k}\right]^q \qquad (3.37)$$

where σ_j is an arbitrarily chosen stress and q is a modulus adjustment index (nominally taken as 1). Elements are modified on an element by element basis (k = 1 to N for N elements). Seshadri and Mangalaramanan (1997) have shown that for q < 1, the behaviour of sensitive structures can be stabilised.

On the basis of two consecutive linear elastic finite element analyses, and the equation for the upper bound multiplier given as

$$m^0 = \frac{\sigma_y\sqrt{V}}{\sqrt{\sum_{k=1}^{N}(\sigma_{ek})^2\Delta V_k}} \qquad (3.38)$$

m^o_I and m^o_{II} can be obtained as

$$m_1^0 = c_1$$
$$m_2^0 = c_2 \qquad (3.39)$$

where c_1 and c_2 are constants. The theorem of nesting surfaces asserts that $m_1^0 \geq m_2^0 \geq m$, where m is the exact factor of safety.

The lower bound formula according to Mura, *et al.* (1965) as a function of the iteration variable (ζ) can be expressed as

$$m'(\zeta) = \frac{2m^0(\zeta)\sigma_y^2}{\sigma_y^2 + [m^0(\zeta)]^2[\sigma_M^0(\zeta)]^2} \qquad (3.40)$$

where $\sigma_M^0(\zeta) = (\sigma_e^0)_M$ is the maximum equivalent stress at iteration ζ_i. All quantities m', m^0, and σ_M are functions of ζ. Unlike the upper bound multiplier, the lower bound multiplier should increase with successive iterations where $m_1' \leq m_2' \leq m$.

With successive iterations (beyond two), m' and m^0 should converge to the exact safety factor or multiplier m for a given structural geometry and loading conditions as shown in Figure 3.5.

Differentiating both sides of equation (3.40) with respect to ζ will give

$$\frac{dm'}{d\zeta} = \frac{\partial m'}{\partial m^0}\frac{dm^0}{d\zeta} + \frac{\partial m'}{\partial \sigma_M^0}\frac{d\sigma_M^0}{d\zeta} \qquad (3.41)$$

This equation, written as finite differences, gives

$$\Delta m' = \left.\frac{\partial m'}{\partial m^0}\right|_{\zeta=\zeta_i} \Delta m^0 + \left.\frac{\partial m'}{\partial \sigma_M^0}\right|_{\zeta=\zeta_i} \Delta\sigma_M^0 \qquad (3.42)$$

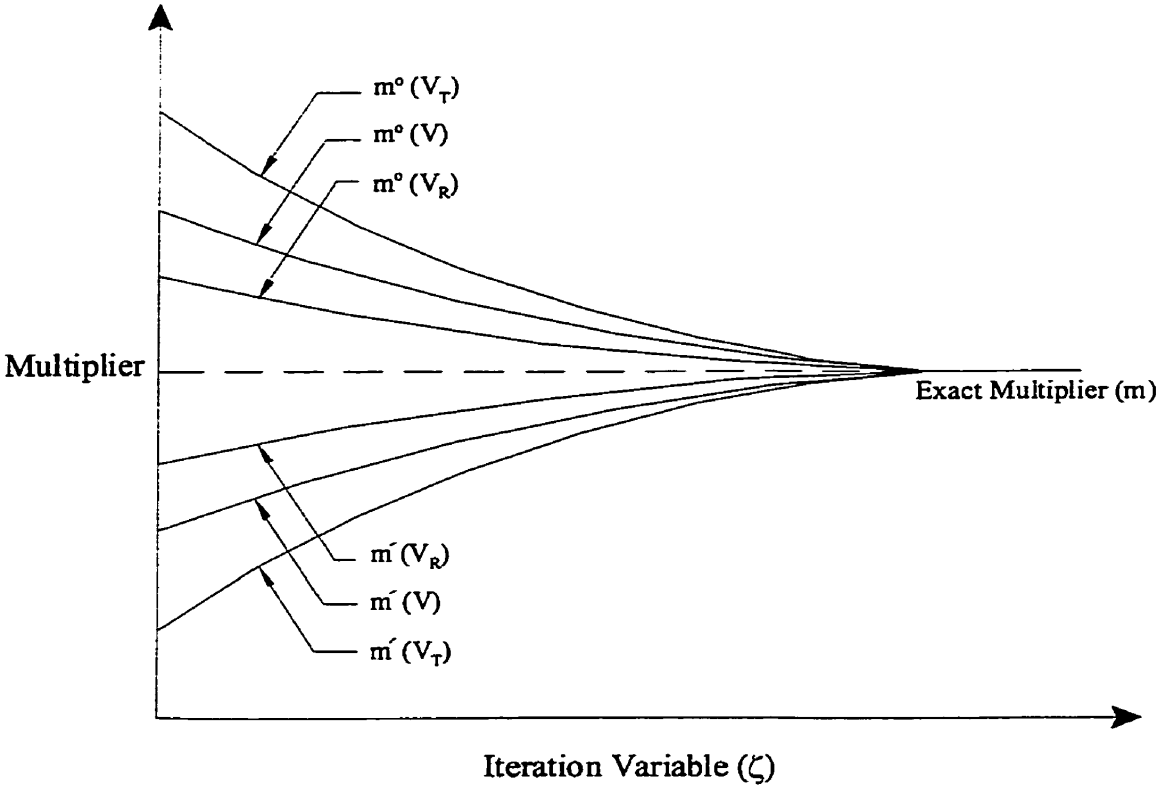

Figure 3.5: Variation of m' and m^0 with linear elastic FEA iterations

This equation is valid for any iteration. Next we define the following quantities in terms of m_α:

$$\begin{aligned} \Delta m' &= m_\alpha - m_i' \\ \Delta m^0 &= m_\alpha - m_i^0 \\ \Delta\sigma_M^0 &= \frac{\sigma_y}{m_\alpha} - \sigma_{Mi}^0 \end{aligned} \qquad (3.43)$$

where i subscript refers to the iterations number. It is clear from equation (3.27) that with increased iterations as $m_0 \to m_\alpha$ and $m' \to m_\alpha$, and insisting that $\sigma^0_{M\infty} \to \sigma_y / m_\alpha$, that m_α will be a lower bound.

Making use of equations (3.40), (3.42) and (3.43) and carrying out the necessary algebraic manipulations, the following quadratic equation can be obtained:

$$Am_\alpha^2 + Bm_\alpha + C = 0 \qquad (3.44)$$

where

$$A = (m_i^0)^4(\bar{\sigma}^0_{Mi})^4 + (m_i^0)^2(\bar{\sigma}^0_{Mi})^2 - 1$$
$$B = -8(m_i^0)^3(\bar{\sigma}^0_{Mi})^3$$
$$C = (m_i^0)^3(\bar{\sigma}^0_{Mi})$$

and $$\bar{\sigma}^0_{Mi} = \frac{\sigma^0_{Mi}}{\sigma_y}$$

The coefficients A, B, and C can be evaluated based on the results of any linear elastic FEA. To ensure real root, the discriminate must be greater than zero.

$$(m_i^0)(\bar{\sigma}^0_{Mi}) \le (1+\sqrt{2}) \qquad (3.45)$$

The notion of "leapfrogging" using two consecutive linear elastic FEA iterations is illustrated in Figure 3.6. It is possible to carry out this formulation on the basis of one linear elastic FEA, but results may be improved with the notion of reference volume determined on the basis of two consecutive analyses. Instead of evaluating the upper

bound multiplier on the basis of the total volume of the structure, a slightly more conservative estimate can be evaluated for some sub-volume of local plasticity involving α elements (a multiplier m based on α elements – m_α). It is worth noting that increased iterations of the elastic modulus (up to three or four) would result in a more relaxed structure and hence a further improved estimate of the m_α lower bound multiplier.

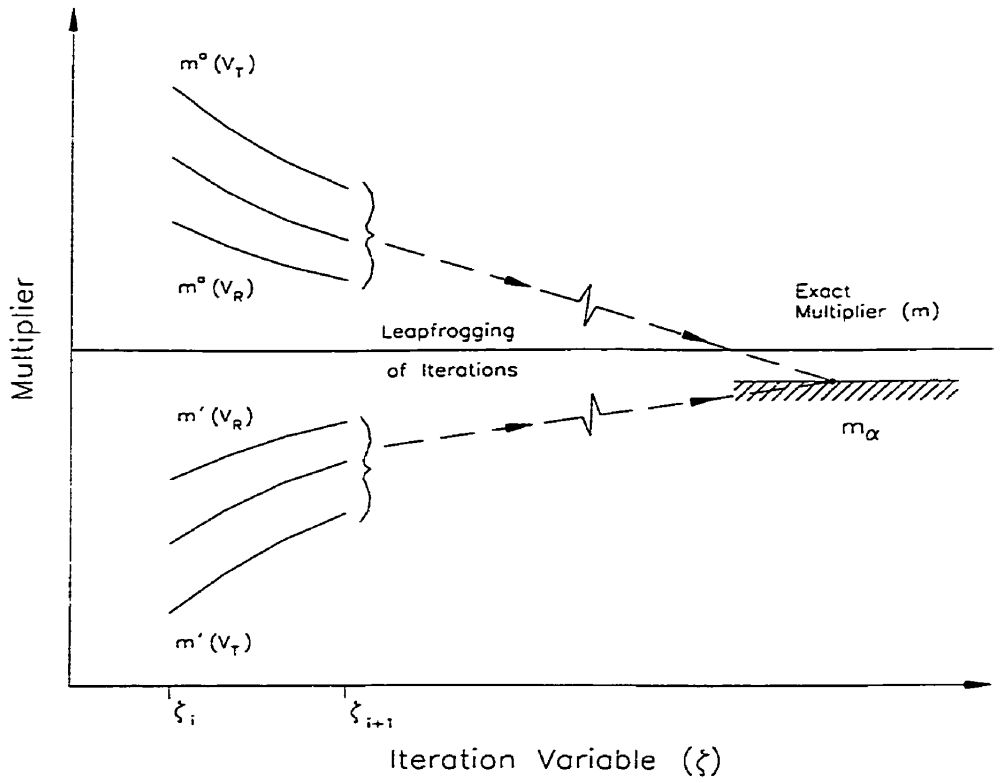

Figure 3.6: Leapfrogging to a near limit state using elastic FEA iterations

3.6.5 Classes of Components and Structures

It is useful to carry out a number of iterations of elastic finite element analysis to assess the behaviour of the structure both locally and globally (Seshadri, 1991; Seshadri and

Fernando, 1992). The analyst can observe the behaviour of the upper and lower limit load multipliers m^0, m' and the maximum equivalent stresses σ_M as a function of the iteration number (ζ) to ensure convergence criteria and the theorem of nesting surfaces are satisfied. Seshadri and Mangalaramanan (1997) suggest that a large number of iterations are not necessary because the behaviour is dependent on the geometry and loading configurations as well as the elastic modulus modification scheme. However, increased iterations do progressively relax the structure and hence enhance the accuracy of the limit load estimates. What is important for GLOSS r-node and m_α methods is that for any two consecutive iterations, proper convergence behaviour and the theorem of nesting surfaces are satisfied. The trend of convergence of any two consecutive linear elastic analyses is necessary for setting bounds on the structure. They suggest categorising the structure as demonstrating either a Class I, Class II or Class III type behaviour.

3.6.5.1 Class I

Class I type structures are categorised by monotonic convergence behaviour. Typically, m_α limit load estimates of structures having this classification are reliable. The convergence behaviour is based on the inequalities

$$\begin{aligned} \frac{dm^0}{d\zeta} &\leq 0 \\ \frac{dm'}{d\zeta} &\geq 0 \\ \frac{d\sigma_M^0}{d\zeta} &\leq 0 \end{aligned} \qquad (3.46)$$

3.6.5.2 Class II

Structures categorised as Class II type exhibit a behaviour where the maximum equivalent stress in the structure increases with an increase in the iteration number ζ or a further iteration of elastic moduli of the elements. The classification is based on the inequalities

$$\left.\begin{aligned} &\frac{dm^0}{d\zeta} \leq 0 \\ &\frac{dm'}{d\zeta} \\ &\frac{d\sigma_M^0}{d\zeta} \end{aligned}\right\} Fluctuate \qquad (3.47)$$

Should a structure be classified as a Class II type, reducing the elastic modulus adjustment index number (q) from 1 to 0.5 or 0.25 may result in the structure exhibiting a Class I type behaviour.

3.6.5.3 Class III

Class III type structures do not follow normal convergence criteria, thus violating the theorem of nesting surfaces. Results in such cases are invalid. These structures are categorised by the inequalities

$$\left.\begin{array}{l} \dfrac{dm^0}{d\zeta} > 0 \\ \dfrac{dm'}{d\zeta} \\ \dfrac{d\sigma_M^0}{d\zeta} \end{array}\right\} Fluctuate \qquad (3.48)$$

As with Class II type structures, changing or reducing the elastic modulus adjustment index number (q) from 1 to 0.5 or 0.25 may result in the structure exhibiting a Class I type behaviour.

3.7 Progressive Modulus Reduction (PMR) Method

Another method of modulus reduction used in limit load determination is the Progressive Modulus Reduction (PMR) which is an extension to the elastic compensation method (Mackenzie and Boyle, 1993; Marriott, 1988) and GLOSS r-node method (Seshadri, 1991 and Mangalaramanan and Seshadri, 1997). As previously stated, when a structure is loaded beyond its yield capacity, the stress redistribution that takes place because of inelastic effects should be accounted for in the analysis. This effect can be accounted for by systematically reducing the elastic modulus of elements having pseudo-elastic stresses (stress exceeding the yield stress of the material) with several iterations. This essentially mimics the form of a limit state stress distribution.

The main purpose of the PMR method was to use stress relaxation techniques to evaluate the load deflection curve for a structure. The growth of the yield zone up to the point of

plastic collapse was captured by progressively increasing the applied load and iterating the elastic modulus until static admissibility is achieved.

This method satisfies the lower bound static admissibility criteria which states that if the maximum Von Mises equivalent stresses are everywhere below yield, and equilibrium is attained between internal forces and external applied loads such that the stress distribution is statically admissible, the applied load is a lower bound.

The PMR method models the growth of the plasticity zone in an iterative fashion. An initial analysis is carried out for a given geometry and loading conditions and a stress distribution is evaluated. As with GLOSS and r-node methods, the elastic modulus of the elements having stresses above the yield stress σ_Y of the material are reduced according to $E_i = f(\sigma_e, \sigma_Y)$, normally given as

$$E_i = E_{i-1} \frac{\sigma_Y}{\sigma_e} \qquad (3.49)$$

A second analysis is carried out with the new stiffness distribution E_i (i.e., yield zone) and a new stress distribution is evaluated. The process is iterated until static admissibility is achieved (element stresses are in equilibrium with the external load and are everywhere below yield). In this way a growing yield or plasticity zone is synthesised in a nominally elastic model. This iteration process is illustrated in Figure 3.7. By choosing a reference stress σ_R that is slightly below yield (i.e., replacing σ_Y in equation (3.49) with $\sigma_R \sim 0.95\sigma_Y$), the iteration process can be optimised. This increases the extent of relaxation for

a given iteration and hence reduces the number of iterations required to achieve convergence or the reducing the pseudo-elastic stresses (i.e., $\sigma_e > \sigma_Y$) to the yield stress level.

The PMR technique is not subject to the possibility of local instabilities. It evaluates the limit load and the non-linear response of a structure by progressively increasing the applied load and iterating the elastic modulus at each stage until static admissibility is achieved.

The method at present does not account for large deformations, although this is an area for further development. The PMR method is another suitable way to compare the plastic hinge load values with a more precise estimate of the true load-deflection behaviour. The algorithmic approach to implementing the technique is discussed in the next chapter.

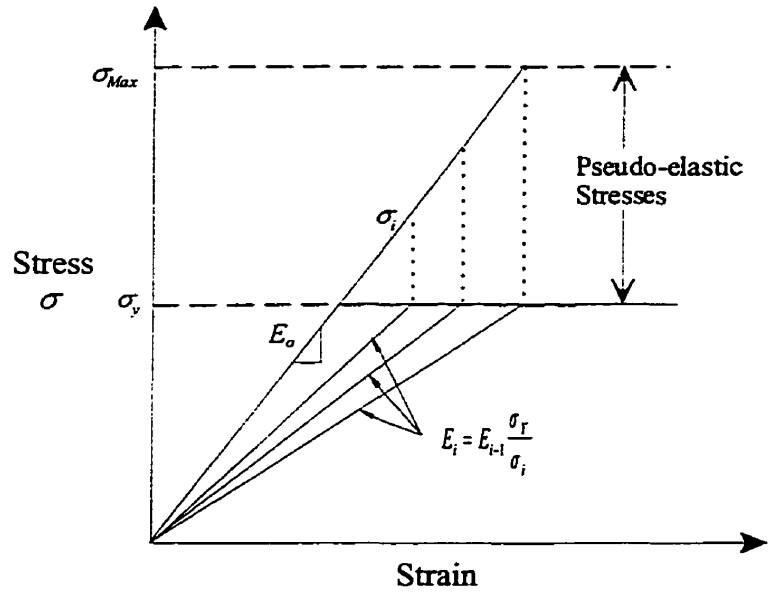

a) PMR Algorithm for Stress Relaxation

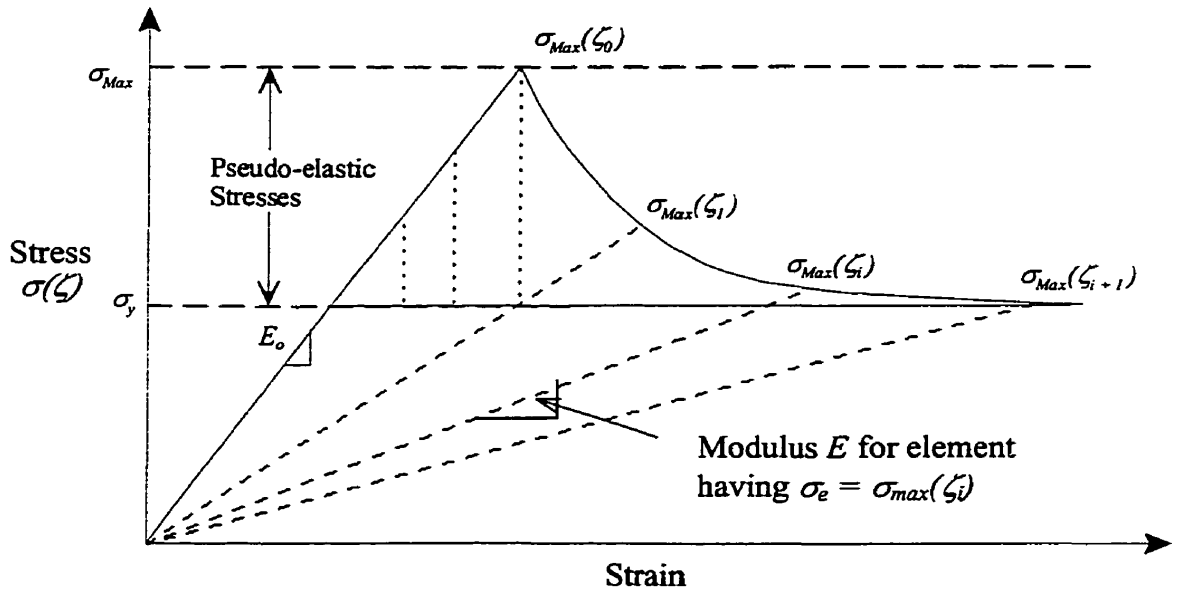

b) Stress relaxation with increased iterations (ζ)

Figure 3.7: Progressive Modulus Reduction (PMR) algorithm: a) Pseudo-elastic stress are reduced by adjusting the modulus of the pseudo-elastically stressed elements. b) Relaxation of pseudo-elastic stresses with iteration number (ζ)

Chapter 4

Structural Analysis Using Finite Element Analysis Tools

4.1 Elastic Finite Element Analysis

With the onset of finite element analysis (FEA), the classical approach to elastic design became more versatile. Where analytical solutions required structures to be grossly simplified into individual components for analysis, FEA made it possible to model and analyse complex structures accounting for interaction effects between the various components.

Conventional methods of ship design use a classical approach for evaluating limit loads. Once a component or element in the structural model has yielded, the structure is assumed to have failed. Based on the elastic modulus and the yield stress for the material, a static solution can be easily obtained. The analysis evaluates a stress strain distribution as a function of the geometry and loading conditions. Since the applied load is proportional to the stress distribution in the structure, the material yield stress is proportional to the limit load of the structure. Therefore, the stress field that corresponds

to the limit load is statically admissible (i.e., the stress everywhere in the structure is below yield, and equilibrium conditions between the applied load and internal stresses are satisfied). The limit load of a structure for a given geometry and applied load can be evaluated as

$$P_L = P\frac{\sigma_Y}{\sigma_{\max}} \qquad (4.1)$$

where P is the applied load, σ_Y is yield stress of the material and σ_{MAX} is the maximum evaluated stress in the structure. This is a very simple yet improved method of analysing ship structures. However, the results are often over conservative. The level of conservatism is influenced by the number of elements used in the model and the assumed boundary conditions. In the case of a ship's hull, ideally the analyst would model the complete hull structure with a large number of elements, but at the cost of enormous amount of processing time. In practice, the complete hull would be modelled with a moderate number of elements to quantify a global behaviour, and the results used to define bounding conditions for a more detailed model of a section of the hull.

A further cause of over-conservatism in using elastic FEA is ignoring the inelastic effects and structural plasticity. To account for material inelastic effects, full non-linear FEA can be used but at the expense of extended processing time.

4.2 Non-linear Finite Element Analysis

Full non-linear finite element analysis can be used to analyse ship structures. Detailed modelling with provision for inelastic effects makes it possible to simulate the behaviour of a structure having applied loads well in excess of the yielding limit. The ability to assess the added capacity of a structure beyond yield is important in reducing conservatism in the design. With appropriate models, the analyst can provide guidance on a structure's true behaviour at the initial design phase, at various construction phases and during deployment or operation.

In the present study, full non-linear finite element analysis was carried out using the finite element software ANSYS (1992). The ANSYS program performs non-linear analyses by solving a series of linear approximations (equations) to the non-linear problem, where each successive approximation is corrected based on the previous results.

According to the guidelines set out in the ANSYS user manual (ANSYS, 1992), an approach to non-linear solutions is to subdivide the applied load into a series of load increments. The load increments can then be applied over several load steps or several sub-steps within a load step. At the completion of each incremental solution, the program adjusts the stiffness matrix to reflect the non-linear changes in structural stiffness before proceeding to the next load increment. To minimise error that can accumulate with each load increment, causing the final result to be out of equilibrium, a Newton-Raphson method of iterations was used. This method drives the solution to an equilibrium convergence (or tolerance limit) at the end of each load step. Before each solution, the

Newton-Raphson method evaluates the out-of-balance load vector or the difference between the restoring forces (loads corresponding to the element stresses) and the applied loads. If the convergence criteria (limit on allowable difference) are not satisfied, the out-of-balance load vector is re-evaluated, the stiffness matrix is updated and a new solution is obtained. Iterations continue until convergence criteria is met. The load increases until convergence criteria cannot be satisfied for a given load step at which point the analysis terminates. The convergence can be enhanced using automatic time stepping, and bisection.

Material non-linearities were accounted for in this thesis by assuming the material of the structures to be elastic-perfectly plastic. An example of a run file for a full non-linear analysis is given Appendix C.

4.3 Robust Techniques: An Improved Lower Bound Approach

The previous chapter discussed the various robust methods that can be used in conjunction with linear elastic FEA to evaluate lower bound limit loads that account for inelasticity in the structure. Three of these techniques are implemented with linear elastic FEA. These include Progressive Modulus Reduction (PMR), GLOSS R-Node and the m_α-method. Each of these methods are essentially modulus reduction methods that satisfy the criteria identified for a lower bound limit load theorem and are therefore an improvement to the traditional classical approach to limit load analysis. The lower bound limit load theorem essentially states that for a limit load to be lower bound and valid, the

stress distribution evaluated for a given geometry and applied loading must be "statically admissible." This means that equilibrium is attained between the internal and external forces, and the stresses are everywhere below the yield stress of the structure's material.

4.3.1 Progressive Modulus Reduction (PMR) Method

One robust method of analysing ship structures is the Progressive Modulus Reduction (PMR) method, which is an extension of the elastic compensation method and GLOSS r-node methods. While robust methods, including PMR, use modulus reduction algorithms to mimic a limit state stress distribution (Marriott, 1988; Mackenzie and Boyle, 1993; Seshadri, 1991; Mangalaraman and Seshadri, 1997), the PMR method used in this thesis essentially models the growth of the yield or plastic zone in an iterative fashion up to plastic collapse.

The method evaluates the inelastic response of the structure to an applied load. The applied load is increased until a limit load is reached and static admissibility cannot be achieved (the maximum stress cannot be relaxed to the material yield level). The applied load corresponding to the last converging solution is the limit load for the structure. The ANSYS runfile used to implement the PMR algorithm for various structures is given in Appendix D1 and D1-1.

The algorithm for the PMR method is outlined below:

1. Carry out initial linear elastic analysis evaluating the stress distribution associated with the geometry and loading conditions. All pseudo-elastic element equivalent stresses (i.e., $\sigma_e > \sigma_Y$) are identified.

2. Adjust the modulus of all the pseudo-elastically stressed elements according to the equation (see Appendix C1-1)

$$E_M = E_o\left[\frac{\sigma_{arb}}{\sigma_e}\right]^q \qquad (4.2)$$

where E_o is the original elastic modulus, σ_e is the equivalent element stress, σ_{arb} is the arbitrary stress chosen to relax the elastic modulus of the pseudo-elastically stressed elements (nominally taken as the yield stress σ_Y) and q is the modulus adjustment index (nominally taken to be unity). A second analysis is carried out and a new stress distribution evaluated. As with step 1, the pseudo-elastic stresses are identified on an element by element basis and the elastic moduli are modified according to equation (4.2). Choosing σ_{arb} slightly below σ_Y (<5%) can reduce the number of iterations required to achieve convergence or static admissibility.

3. Iterations continue until static admissibility is achieved or all stresses in the structure are below the yield stress σ_Y for a given structural geometry and loading condition. The deflection of the structure can then be determined.

4. The applied load is increased in conjunction with steps 1 to 3 until further increases do not satisfy the conditions necessary to achieve static admissibility.

4.3.2 GLOSS R-Node Method

The GLOSS r-node method is essentially a modulus modification technique. However, with the r-node method, all element moduli are modified and not just pseudo-elastically stressed elements. This redistributes the stresses about specific load controlled locations within the structure. These load-controlled locations are identified as regions where the stress does not change with consecutive linear elastic finite element analyses and are called redistribution nodes or r-nodes. The ANSYS run file used to implement the r-node algorithm for various structures is given in Appendix D2 and D2-1. The algorithmic procedure for the GLOSS r-node method is outlined below (Mangalaramanan and Seshadri, 1997):

1. Carry out initial linear elastic analysis evaluating the stress distribution associated with the geometry and loading condition for the structure. Element stresses are stored in an output file for post-processing involving identification of r-node locations.
2. Adjust the modulus of each element on an element by element basis regardless of the magnitude of the stress according to the equation (see Appendix D2-1)

$$E_M = E_o\left[\frac{\sigma_{arb}}{\sigma_e}\right]^q \qquad (4.3)$$

where E_o is the original elastic modulus, σ_e is the element stress, σ_{arb} is an arbitrarily chosen stress to redistribute the stresses in the structure and q is the modulus adjustment index (nominally taken to be 1).

3. Carry out a second analysis to evaluate a new equivalent stress distribution. Since r-nodes are load-controlled locations within a structure, they can be isolated as elements where the follow up angle θ from one analysis to the next is 90° or where the stress does not change from one analysis to the next. For simple two-dimensional structures, only two linear elastic analyses are required, but for structures having more complex geometry in three dimensions, three or more analyses may be required (i.e., two or more iterations). Element stresses are again stored in an output file for post-processing involving identification of r-node locations.

4. Identify the peak r-node stress locations or locations where plastic hinges will potentially form by plotting r-node stresses on a section by section basis. The plot is trivial for two-dimensional analyses (i.e., beam bending for a flat bar) but for three-dimensional structures or models (i.e., beams with flanges or ship grillages) the plot becomes complex and difficult to represent.

5. Track the r-node stresses until a local or global collapse mechanism is detected. Depending on the structure and loading conditions, a mechanism may be defined by just one peak r-node stress (or plastic hinge) or by many peak r-node stresses in the model. If N hinges must form to define a collapse mechanism in a structure, the effective r-node stress can be evaluated as

$$\overline{\sigma}_n = \frac{\Sigma_{j=1}^{N} \sigma_{nj}}{N} \qquad (4.4)$$

4.3.3 m_α-Method

The m_α-method is essentially an improved limit load approach to Mura's limit load. It predicts limit loads by leapfrogging based on two consecutive linear elastic finite element analyses to a limit state from which the limit load multiplier can be evaluated. As with the r-node method, all elastic moduli are modified on an element by element basis such that the stresses are permitted to redistribute about specific load controlled locations within the structure. Also, on the basis of two consecutive linear elastic finite element analyses, the sub-region of a structure exhibiting the most inelastic action can be identified, from which an improved upper bound multiplier m^o can be evaluated where the theorem of nesting surfaces is barely satisfied (Mura *et al.*, 1965). Thus the m_α estimate evaluated on the basis of this new upper bound multiplier m^o is an improved, more conservative estimate over the same multiplier evaluated on the basis of the total volume of the structure. The ANSYS run file used to implement the r-node algorithm for various structures is given in Appendix D2 and D2-1. The algorithmic procedure to evaluate the m_α limit load multiplier is outlined as (Mangalaramanan and Seshadri, 1997):

1. Carry out initial linear elastic analysis evaluating the stress distribution associated with the geometry and applied loading. Element stresses are stored in an output file for post-processing.
2. As with the r-node method, adjust the modulus of all elements on an element by element basis regardless of the magnitude of the stress, according to the equation

$$E_M = E_o \left[\frac{\sigma_{arb}}{\sigma_e} \right]^q \qquad (4.5)$$

where E_o is the original elastic modulus, σ_e is the element stress, σ_{arb} is an arbitrarily chosen stress to redistribute the stresses in the structure and q is the modulus adjustment index (nominally taken to be 1).

3. Carry out a second linear analysis to evaluate a new equivalent stress distribution. Element stresses are again stored in an output file for post-processing.

4. For each linear elastic analysis, calculate energy dissipation $\sigma^2 \Delta V$ for each element in the structure and sort them in descending order. Evaluate the upper bound multiplier m^0 for each element for each of the two consecutive analyses and plot the variation of m^0_1 and m^0_2 against increasing volume $\Sigma \Delta V$ for both analyses. The volume identified at the intersection of the two curves is the reference volume where the theorem of nesting surfaces is barely satisfied and from which the reference volume upper bound multiplier m^o_R can be obtained.

5. The upper and lower bound multipliers m^0, m' and can then be evaluated for increasing volume. The trends must be checked to ensure compliance with the theorem of nesting surfaces.

$$\begin{aligned} \frac{dm^0}{d\zeta} &\leq 0 \\ \frac{dm'}{d\zeta} &\geq 0 \\ \frac{d\sigma^0_M}{d\zeta} &\leq 0 \end{aligned} \qquad (4.6)$$

6. The m_α multiplier can then be evaluated by solving the quadratic equation

$$Am_\alpha + Bm_\alpha + C = 0 \tag{4.7}$$

where

$$A = (m_i^0)^4(\bar{\sigma}_{Mi}^0)^4 + (m_i^0)^2(\bar{\sigma}_{Mi}^0)^2 - 1$$
$$B = -8(m_i^0)^3(\bar{\sigma}_{Mi}^0)^3$$
$$C = (m_i^0)^3(\bar{\sigma}_{Mi}^0)$$

and $$\bar{\sigma}_{Mi}^0 = \frac{\sigma_{Mi}^0}{\sigma_y}$$

The coefficients A, B, and C can be evaluated based on the results of any linear elastic finite element analysis. To ensure real root, the discriminant must be greater than zero.

$$(m_i^0)(\bar{\sigma}_{Mi}^0) \le (1+\sqrt{2}) \tag{4.8}$$

Should the structure fail to satisfy the theorem of nesting surfaces, yielding a Class II or Class III type of structure, the modulus adjustment index should be reduced from 1 to 0.5 or 0.25 and the preceding steps re-worked.

Chapter 5

FEA Models and Testing Program

5.1 Structural Models

To explore the effectiveness of using robust methods to evaluate lower bound limit loads, three types of structures were analysed. These include beam type structures or main-frame stiffeners including rectangular and flanged stiffeners, a flat bar stiffened panel, and an arctic icebreaker grillage. The stiffeners include a flat bar (FB) stiffener, an angle (L) stiffener and a tee (T) stiffener. The particulars of these are given in the following sections. The ANSYS input files used to generate these models are given in Appendix B.

5.1.1 Indeterminate Beam (model – IB)

A statically indeterminate rectangular beam was modelled for this work. The beam geometry and loading conditions are illustrated in Figure 5.1, (Seshadri and Mangalaramanan, 1997). A uniformly distributed load was applied over the top surface

of the beam. The shaded or hatched regions indicate zones of plasticity that would develop as the beam is loaded beyond its elastic yielding limit. According to plastic hinge theory, the beam is considered collapsed when the two zones of plasticity develop until through section yielding occurs or plastic hinges form. The particulars of the beam are given in Table 5.1.

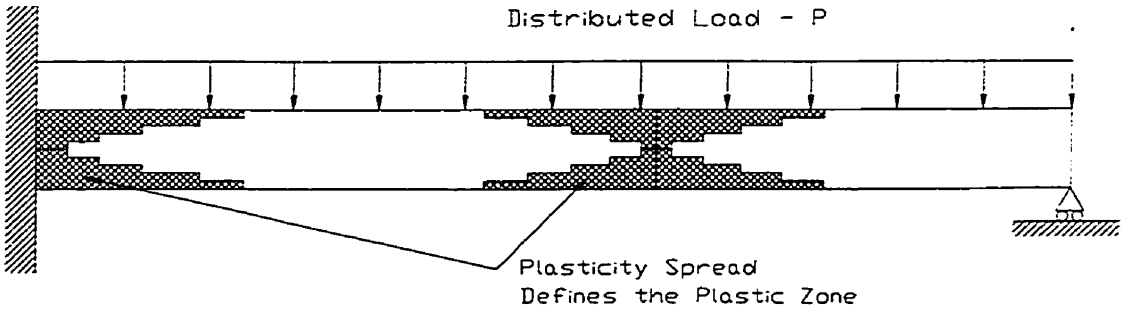

Figure 5.1: Indeterminate Beam (model - IB)

Table 5.1: Indeterminate Beam (model – IB) particulars

Length (mm)	50.8
Web Height (mm)	2.54
Thickness (mm)	1
Elastic Modulus (MPa)	206850
Yield Strength (MPa)	206.85
Applied Distributed load (N/mm)	0.1274

5.1.2 Mainframe Stiffeners

Three types main frame stiffeners were modelled and analysed including a flat bar (model - FB), an angle (model - L) and a tee (model - T) shown in Figure 5.2, Figure 5.3 and Figure 5.4 respectively. The mainframe stiffeners represent the structure of components that form the primary support on a ship's grillage as illustrated in Figure 1.1. The ends of the beams are assumed fixed on all six degrees of freedom indicating a rigid connection to the stringer. The restraining effect of the shell plate is modelled by restraining the nodes on the top edge of the stiffener from lateral displacement. A uniformly distributed load was applied over the full length of the stiffener. To break lateral symmetry in the flat bar and tee stiffeners, a small eccentric transverse load was applied at the free edge (less than 0.5% of the bending load). The particulars for the different stiffeners are listed in Table 5.2.

Table 5.2: Mainframe stiffener particulars

Particular	Flat Bar (model - FB)	Angle (model - L)	Tee (model - T)
Length (mm)	1200	1200	1200
Web Height (mm)	200	200	200
Web Thickness (mm)	15	15	15
Flange Width (mm)	-	60	120
Flange Thickness (mm)	-	15	15
Elastic Modulus (MPa)	207000	207000	207000
Yield Strength (MPa)	245	245	245

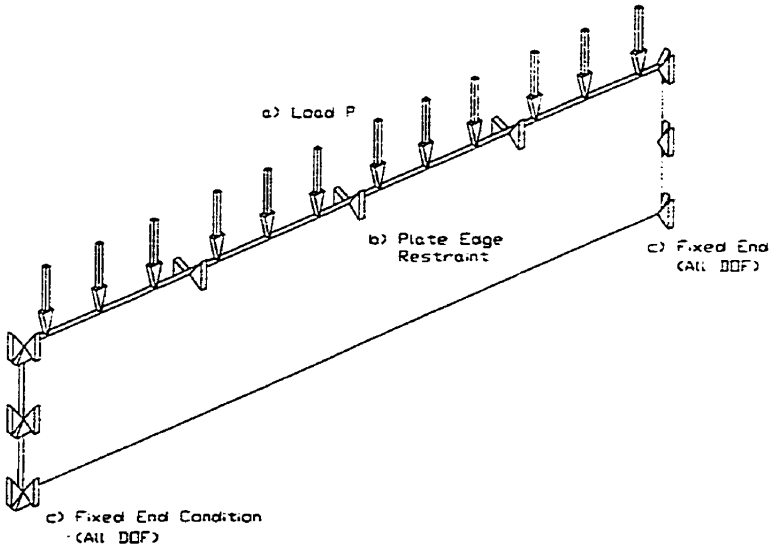

Figure 5.2: Flat bar (model - FB) stiffener

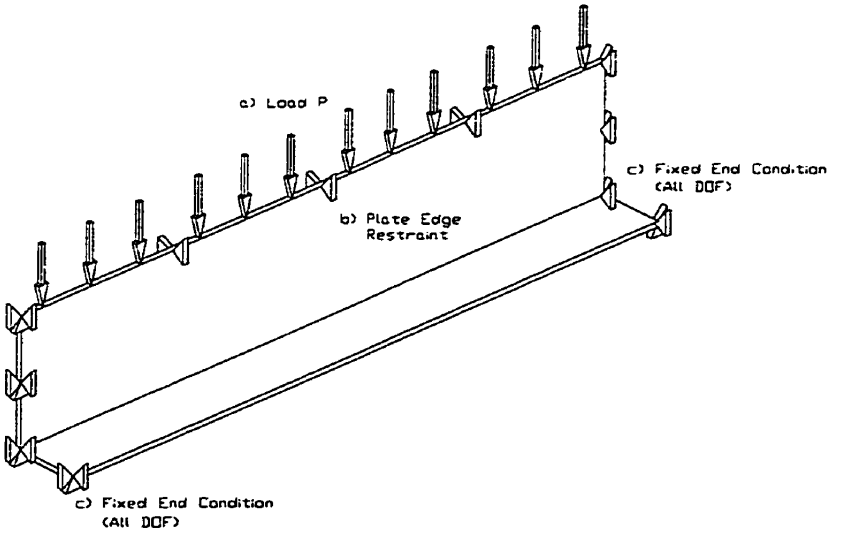

Figure 5.3: Angle (model – L) stiffener

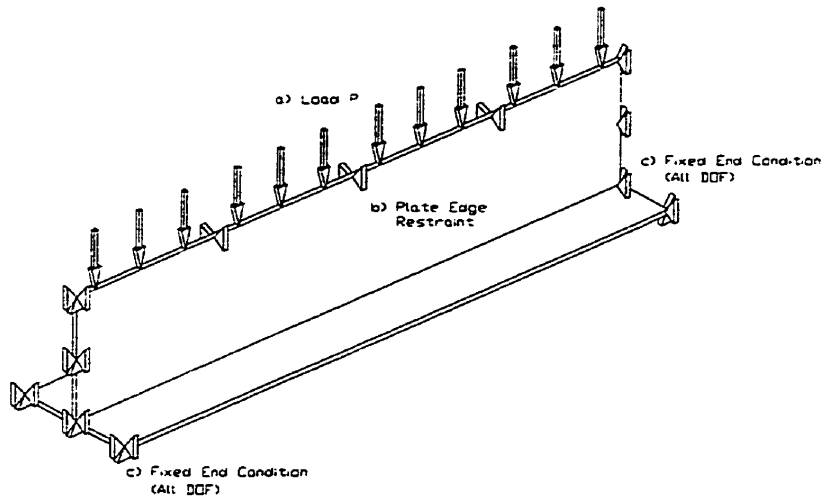

Figure 5.4: Tee (model – T) stiffener

5.1.3 Flat Bar Stiffened Panel (model - FBSP)

A flat bar stiffened panel was modelled and analysed as illustrated in Figure 5.5. The model resembles a structural assembly between two stringers and main transverse frames. The particulars of the panel are given in Table 5.3. The boundary conditions applied to the model include fixed conditions at both ends of the panel and restraining conditions preventing lateral displacement and axial rotation at the edges of the plate. A uniformly distributed load was applied over the shell plate surface. To break the lateral symmetry in the flat bar stiffeners, a small eccentric transverse load was applied at the free edges (less than 0.5% of the bending load).

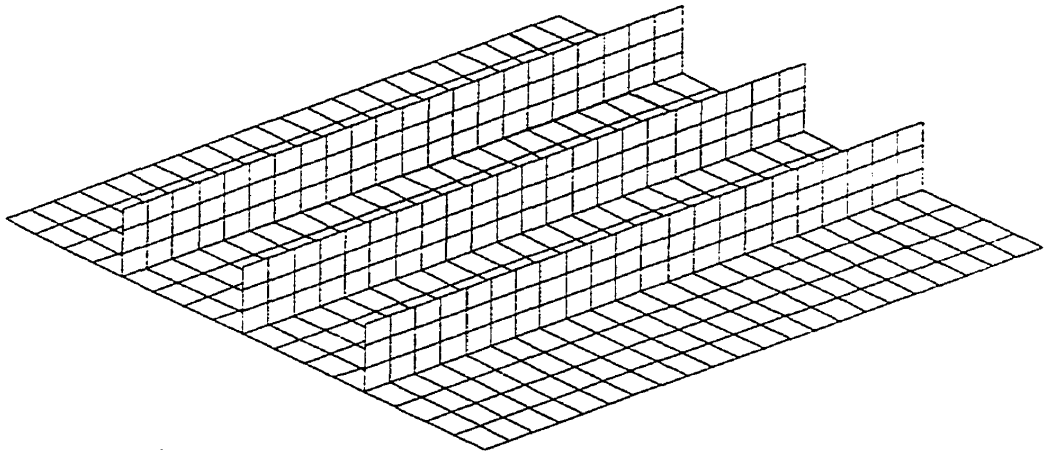

Figure 5.5: Flat Bar Stiffened Panel (model - FBSP)

Table 5.3: Flat bar stiffened panel (model - FBSP) particulars

Length (mm)		1200
Breadth (mm)		1600
Plate thickness (mm)		15
Stiffener :	Thickness (mm)	15
	Height (mm)	200
	Spacing (mm)	400
Young's Modulus (MPa)		207000
Yield Strength (MPa)		245

5.1.4 Arctic Icebreaker Grillage (model - AIG)

A model of an arctic icebreaker grillage as shown in Figure 5.6 was also analysed. This model was previously analysed by Mil Systems for Transport Canada in 1995 (Bond and Kennedy, 1998). Their objective was to test a physical model in the lab and attempt to correlate the results with full non-linear analysis.

The grillage was analysed using robust techniques to predict the lower bound limit load of the structure, accounting for non-linear effects. The results were then compared to a full non-linear analysis, as well as full-scale lab results (Bond and Kennedy, 1998).

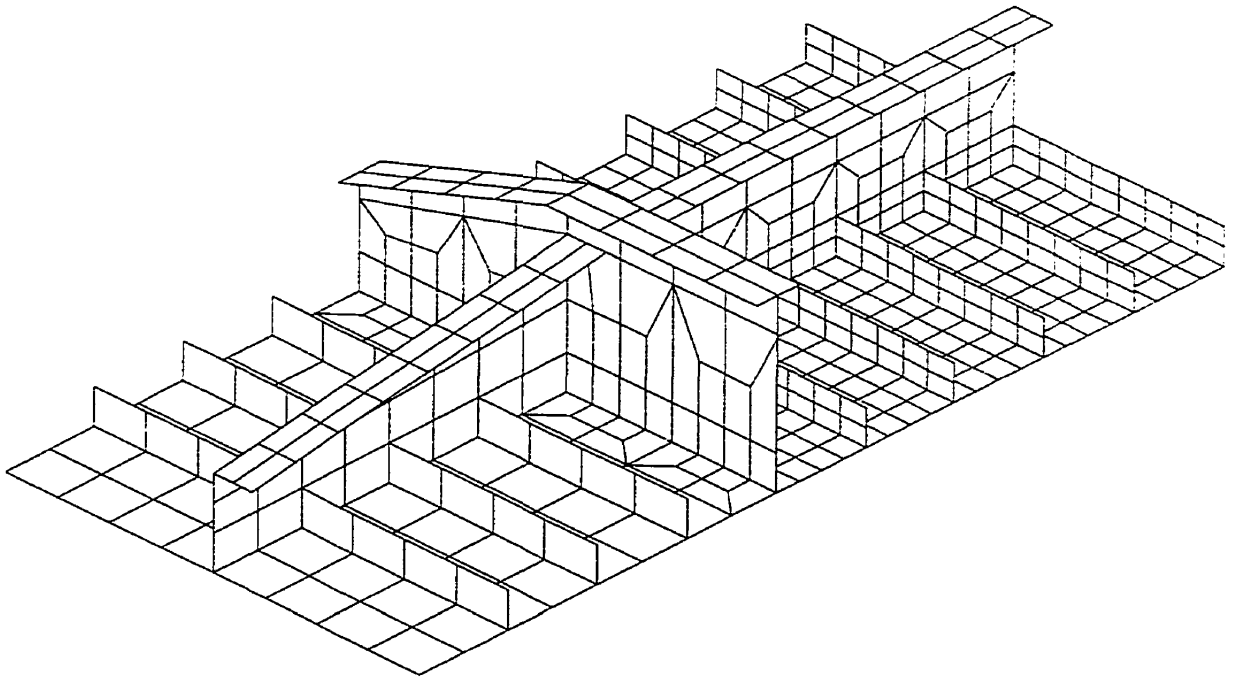

Figure 5.6: ¼ model of an arctic icebreaker grillage (model – AIG)

The grillage was modelled as a one quarter symmetrical panel in order to reduce the number of elements, nodes, and hence the total number of degrees of freedom, thereby reducing the computer processing time.

The main dimensions of the test panel were 2600 x 5000 mm. The grillage (AIG) particulars are listed in Table 5.4. A pressure load was applied to the structure in the lab spread out over 5 patches, each having an area of 60,000 mm^2 (200mm x 300mm), for a

total area of 300,000 mm^2. The finite element model was one quarter of this structure, modelling symmetry in two directions or planes. Load deflection plots were obtained where the method of analysis permitted.

Table 5.4: Grillage (model - AIG) particulars (actual structure values)

Particular		Thickness (mm)	Height (mm)
Main Frame	1	10.88	133
	2	10.88	133
	3	10.88	133
	4	5.965	190
	5	8.185	159
	6	9.805	144
	7	10.88	133
	8	6.33 *	124
Stringer	WEB	11.0125	-
	FLG.	11.0125	-
Transverse Web Frames	WEB	10.94	-
	FLG.	8.325	-
Shell Plate		10.98	
Young's Modulus, E (N/mm^2)		207000	-

* Center mainframe on line of symmetry. Frame thickness is halved.

5.2 Types of Analysis

Two types of analyses are used in this work, namely elastic analysis and non-linear analysis. Elastic analysis is basically the evaluation of a static solution on the basis of a

structure's stiffness, applied loading and bounding conditions. Evaluated limit loads are lower bound, satisfying the conditions of static admissibility. Non-linear analysis is a time history analysis that accounts for changes in the structural stiffness as a structure deforms over time or with increased loading. ANSYS performs a non-linear analysis by solving a series of linear approximations (equations) to the non-linear problem. Each successive approximation is corrected based on the previous result.

Full non-linear analyses were carried out by breaking the applied load into a series of load increments, which were applied over several sub-steps. At the completion of each increment, ANSYS readjusted the stiffness matrix to reflect the non-linear changes (material or geometric) in structural stiffness before proceeding to the next step.

To model the material non-linearity, such as structural plasticity, non-recoverable stress-strain relationships for the materials used in the model must be defined. The models used in this thesis assumed the stress-strain condition of the material to be elastic-perfectly plastic.

5.3 Imperfections

To effectively perform a full non-linear analysis and to predict the true behaviour of a structure, imperfections must be accounted for in the model, including material non-linearity and out of frame straightness in the structural component. However, for this study such detail was not necessary since the purpose was to compare robust techniques

with full non-linear analysis and generally, physical lab test data was not available. The main concern was that the same model was used for the robust and the non-linear analyses. Imperfections were introduced just to break numerical symmetry where necessary. This was achieved by applying a small lateral force on the free edge of stiffeners (< 0.5% of the applied load).

For Arctic ice breaker grillage, imperfections such as variations in the thickness and out of frame straightness were measured from the experimental model and incorporated into the numerical model as forced displacements (Bond and Kennedy, 1998). This ensured that the numerical model was a true representation of the structure tested in the lab.

5..4 Meshing

5.-4.1 Element Type

The element type chosen for the analysis was a plastic shell element called a shell-43. This element type represents a quasi-3D element in that it models in three dimensions, but the element itself is a 2-D element. It is well suited to model thin or moderately thick, non-linear, flat, or warped shell structures in three dimensions. The element is defined by four nodes, each having six degrees of freedom allowing translations and rotations in and about the nodal x, y and z directions respectively. The element also has plasticity, creep, stress stiffening, large deflection and large strain capabilities.

5.4.2 Meshing Densities

Models constructed in this study were meshed using a moderate mesh density. The meshing density was selected such that sufficient elements were used to allow adequate deformations in the model. Using a moderate number of elements gave satisfactory results for comparison and increased the run time efficiency.

The size of the mainframe stiffener elements was limited to 20 mm x 20 mm throughout the model. The number of elements along the length, height and flange widths was 60, 20, and 3 respectively. This applies to model – FB, model – L and model – T mainframe stiffeners.

For the flat bar stiffener panel (model – FBSP), the element size was selected as 50 mm x 50 mm. The number of elements along the length and width of the panel and the height of the main frames were 24, 32 and 4 respectively.

The mesh density varied in the arctic icebreaker grillage (model - AIG) model (Bond and Kennedy, 1998). A much finer mesh density was used to define the main frame stiffeners near the centre of the grillage, and at points of load application where deformations were critical. The length and height of main frame stiffeners was defined using 30 and 4 elements respectively. The mesh density was reduced (i.e., coarser elements were used) outside critical areas where deflection was less significant. For example, the height of the stiffeners outside of the critical areas where the load was applied was defined with a single element since lateral deflections would be insignificant.

Chapter 6

Results and Discussion

The results of the robust methods discussed in Chapter 4 are presented and discussed in this Chapter. Limit loads were evaluated for several types of structures described in Chapter 5 including:

i) indeterminate beam (model - IB);

ii) three mainframe stiffeners including flat bar (model - FB), angle (model - L) and tee (model - T) each modelled with a shell plate restraining boundary condition

iii) flat bar stiffened panel (model - FBSP); and

iv) one quarter symmetrical model of an arctic icebreaker grillage (model - AIG).

The m_α and the r-node methods are discussed in detail in terms of stress relaxation and numerical convergence of bounding limit loads toward the exact value of the collapse load of the structure. The evaluated limit loads for all robust methods, including m_α, r-node and Progressive Modulus Reduction (PMR) for the different models or structures

are presented and discussed in the last section of this chapter. Comparisons are made to full non-linear analysis results and lab test results where available.

6.1 R-Node Method

The results of the r-node method are formally presented in this section. Each of the models or structures listed above and described in Chapter 5 have been analysed to study the effect of progressive elastic modulus relaxation and the influence of the modulus adjustment index q on the maximum equivalent stresses and r-node stresses. As previously discussed, the stress relaxation process is synthesised by continuously adjusting the elastic modulus of each element in the structure based on newly evaluated stresses. For the robust methods of analysis to be valid, the convergence of the stresses must satisfy the theorem of nesting surfaces and the resultant stress distribution must be statically admissible. With increased iterations, there should be a progressive reduction in the maximum equivalent and maximum r-node stresses in the structure. This suggests that the r-node stress for the structure should converge toward the exact value of the limit stress of the structure's material. The limit load of the structure can be evaluated based on this level of limit stress.

6.1.1 Indeterminate Beam (model - IB)

The distribution of r-node stresses in the indeterminate beam is illustrated Figure 6.1. The figure identifies two well-defined r-node stress peaks. These are located near the

locations where plastic hinges would form should the structure be loaded to collapse; one at the fixed end of the beam and the other at the approximate mid-span of the beam.

The r-node stress for this structure is calculated as the average of the two r-node peaks (Seshadri, 1997). The limit load multiplier is then the ratio of yield stress of the material to the r-node stress. The estimate of the collapse load can be obtained as

$$\sigma_{r-node} = \frac{25.95 + 21.93}{2} = 23.94 MPa$$

$$P_L = \frac{\sigma_y}{\sigma_{r-node}} P = \frac{206.85}{23.94} x 0.1724 N/mm$$

$$P_L = 1490 \ kN/m$$

The r-node estimate of the collapse load is compared to other robust limit load estimates in Table 6.13. The variations of the r-node stresses and the influence of the modulus relaxation index for the first four iterations are given in Table 6.1.

With increased iterations (modifying the elastic modulus and reanalysing) the stresses in the structure redistribute causing the two r-node stress peaks to relax and also level off to some limiting level, as illustrated in Figure 6.2 (r-node stress curve corresponding to q = 0.5). The levelling off of the peak stresses is most evident in Table 6.1. The difference between the two peak stresses at iteration four (4.02 MPa) is much less than the difference evaluated for iteration one (8.32 MPa). The result is a lower estimate of the r-node stress, corresponding to an improved estimate of the limit load of the structure that more closely reflects the exact limit load.

Also illustrated in Figure 6.2 is the influence of the modulus adjustment index q. At iteration 7 the r-node stress for modulus reduction using the nominal value of the modulus adjustment index, $q = 1$, dropped considerably. This resembles a numerical instability that results from an excessive rate of modulus reduction (i.e., the modification factor σ_R / σ_{ei} is too large). Reducing the modulus adjustment index q, and hence the modification factor, can alleviate this problem. The result is a smoother relaxation process and decrease in the average r-node stress with increased iterations as shown in the r-node stress vs. iteration number curve for $q = 0.5$.

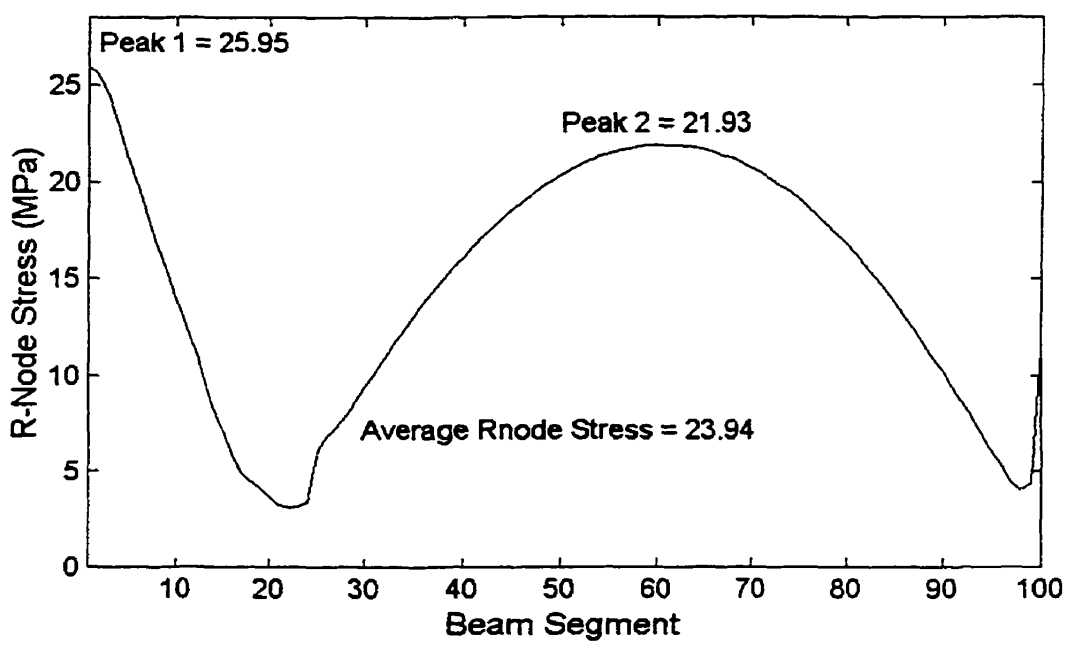

Figure 6.1: R-node stress distribution along the length of the indeterminate beam (model - IB) for iteration $\zeta = 4$; $q = 0.5$

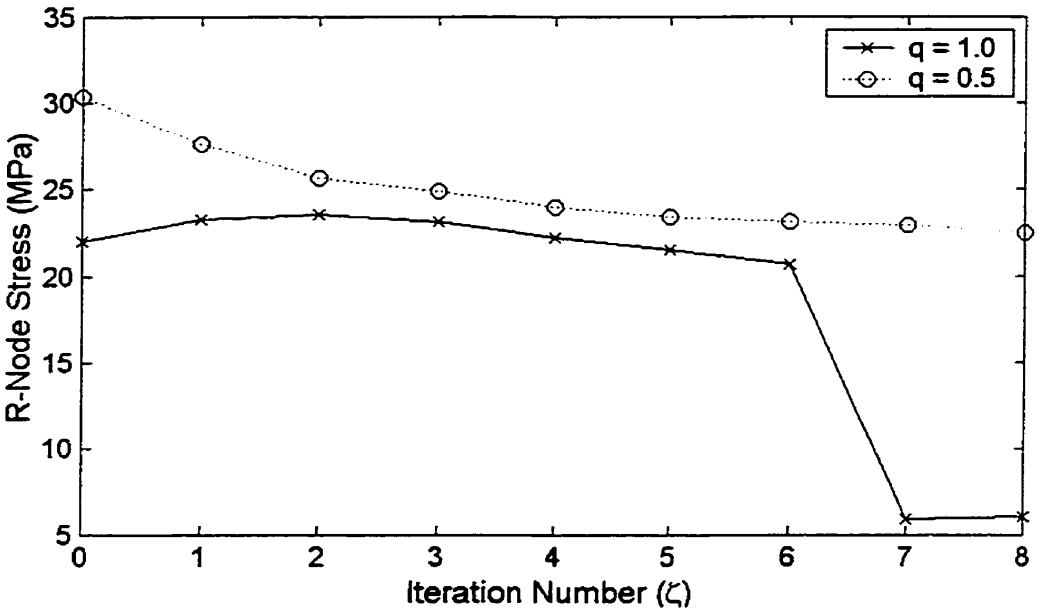

Figure 6.2: Variation of average r-node stresses for increasing ζ and influence of modulus adjustment index q for indeterminate beam (model - IB)

Table 6.1: Variations of r-node stresses and maximum equivalent stresses for increasing ζ for indeterminate beam (model - IB)

Iteration number ζ	Peak r-node stresses (MPa) $q = 0.5$		Average r-node stress $\frac{\sigma_1 + \sigma_2}{2}$	Maximum equivalent stress σ_{max} (MPa)
	σ_1	σ_2		
0	34.54	26.22	30.38	44.99
1	31.47	23.81	27.64	35.68
2	28.74	22.62	25.68	30.51
3	27.62	22.10	24.86	27.23
4	25.95	21.93	23.94	25.35

6.1.2 Mainframe Stiffeners

Three types of mainframe stiffeners were analysed using the r-node method, including a flat bar (model - FB), angle (model - L) and tee (model - T). The distribution of r-node stresses in the mainframe stiffeners, modelled with fixed end conditions and uniformly distributed load, is illustrated in Figure 6.3. The figure identifies three r-node stress peaks positioned at the precise locations of the plastic hinges that would form should the structure be loaded to collapse.

The estimate of the r-node limit load evaluated as the average of three r-node peaks for the flat bar (FB) $\zeta = 4, q = 0.5$ is calculated as

$$\sigma_{r-node} = \frac{54.32 + 43.92 + 54.32}{3} = 50.85MPa$$

$$P_L = \frac{\sigma_y}{\sigma_{r-node}} P = \frac{245}{50.85} x100kN$$

$$P_L = 482 \ kN$$

The influence of the iteration number ζ on the r-node stresses of the ship type stiffeners is illustrated in Figure 6.4, Figure 6.5 and Figure 6.6. In general, as the iteration number increases, the maximum stresses in the structure redistribute and progressively relax, resulting in a progressive decrease in the average r-node stresses in each structure. This results in a lower estimate of the r-node stress that corresponds to an improved estimate of the limit load of the structure, more closely reflecting the exact limit load.

However, increased iterations do not always result in a progressive decrease in the r-node stress as illustrated in Figure 6.6. As noted for iteration four, unexpected jumps or increases in the r-node stress curves may occur. This may be a result of numerical instabilities induced if the modulus of certain elements is over relaxed from one iteration to the next. Another cause is linked to the numerical limitations surrounding proper identification the exact locations of the r-node stresses. Previous authors utilising the r-node method state that r-node locations have the same stress for any two consecutive linear elastic analyses. Theoretically, this is true but realistically the locations may vary slightly. Direct locations of r-nodes may be difficult to identify since the stresses are only relatively the same for two consecutive linear elastic analyses. Using a finer element mesh density may alleviate the problem, but at the expense of increased CPU time.

Reducing the value of the modulus adjustment index q can help alleviate the problem. Reducing q slows down the rate of relaxation resulting in a progressive reduction in r-node stress with increased iterations. The notion of relaxation behaviour is discussed later in section 6.2 for the m_α method analysis.

However, reducing the modulus adjustment index q may increase the r-node stress for a given iteration (i.e., $\sigma_{\text{r-node } (q = 1;\ \zeta = 1)} < \sigma_{\text{r-node } (q = 0.5;\ \zeta = 1)}$). This is because reducing the modulus modification index q reduces the magnitude of the modulus adjustment factor $(\sigma_Y/\sigma_i)^q$. Thus, for a given iteration (particularly iterations one or two) the evaluated r-node stress, based on reduced q, may be considerably higher. The margin, however, is

most significant for the first one to four iterations and reduces with further iterations as shown in Figure 6.4.

The r-node stresses and maximum equivalent stresses for the flat bar (model - FB), angle (model - L) and tee (model - T) stiffeners for the first four iterations are listed in Table 6.2, Table 6.3 and Table 6.4 respectively. It is clear from these tables that r-node stresses are considerably lower than the maximum equivalent stresses, particularly the equivalent stresses evaluated at first yield (iteration 0), which is the stress generally used in classical design of ship structures. The r-node stresses are based on the average of peak r-node stresses in the structure.

The analyst may also use the maximum r-node peak stress as the scaling stress, ensuring that the limit load estimate for the structure is more conservative. As with the averaged r-node stress calculations, increasing the number of iterations progressively relaxes the structure, thereby lowering the maximum equivalent stresses and giving an improved estimate of a limit load. It is recommended that a minimum of three or four iterations be carried out to ensure the peak stresses are sufficiently relaxed and the stresses are converging properly. The added CPU time is not significant.

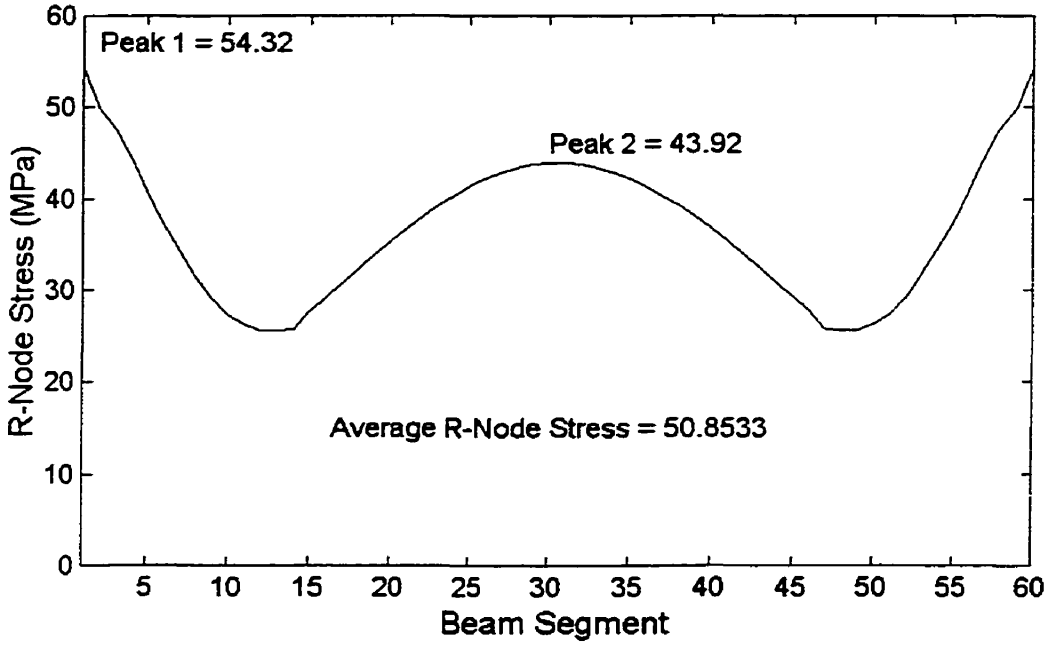

Figure 6.3: Typical r-node stress distribution for main frame stiffeners having fixed end conditions and uniformly applied load for $\zeta = 4$; $q = 0.5$ for model - FB

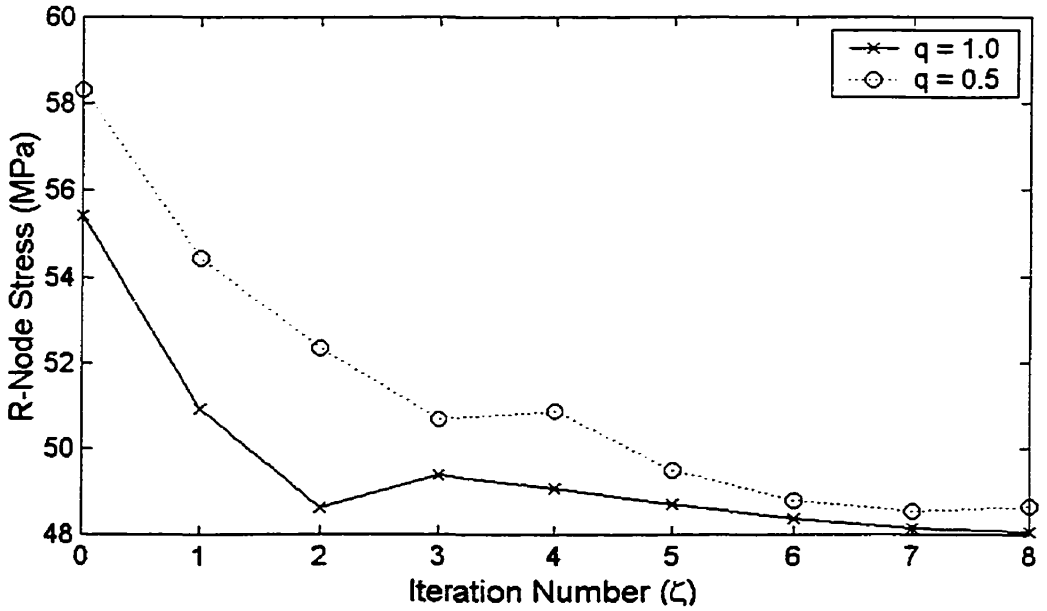

Figure 6.4: Variation of average r-node stresses for increasing ζ and the influence of the modulus adjustment index q for the flat bar stiffener (model - FB)

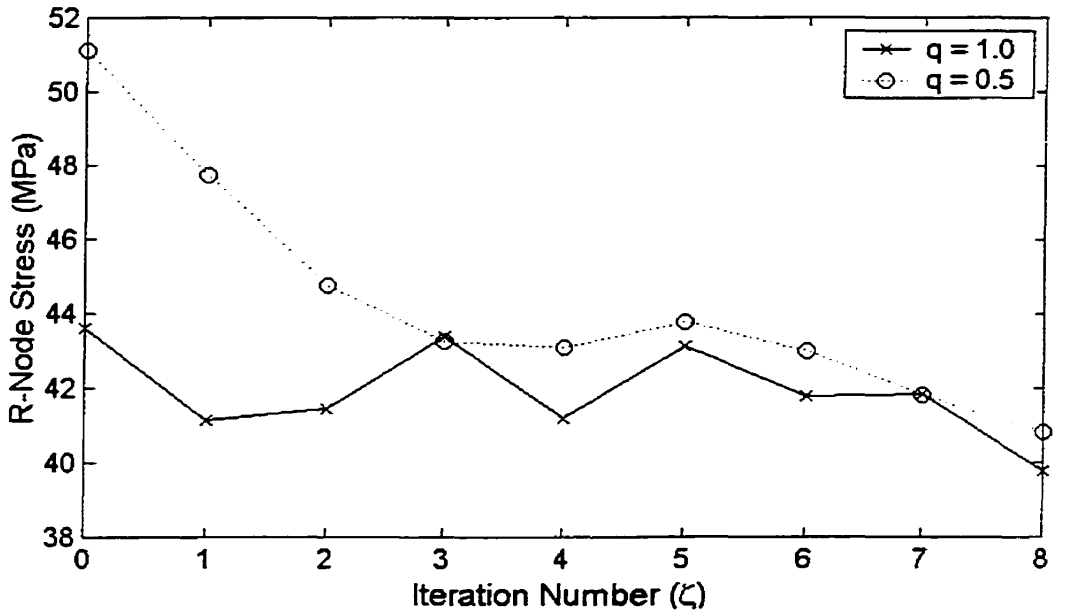

Figure 6.5: Variation of average r-node stresses and influence of modulus adjustment index q for the angle stiffener (model - L) for increased iterations ζ

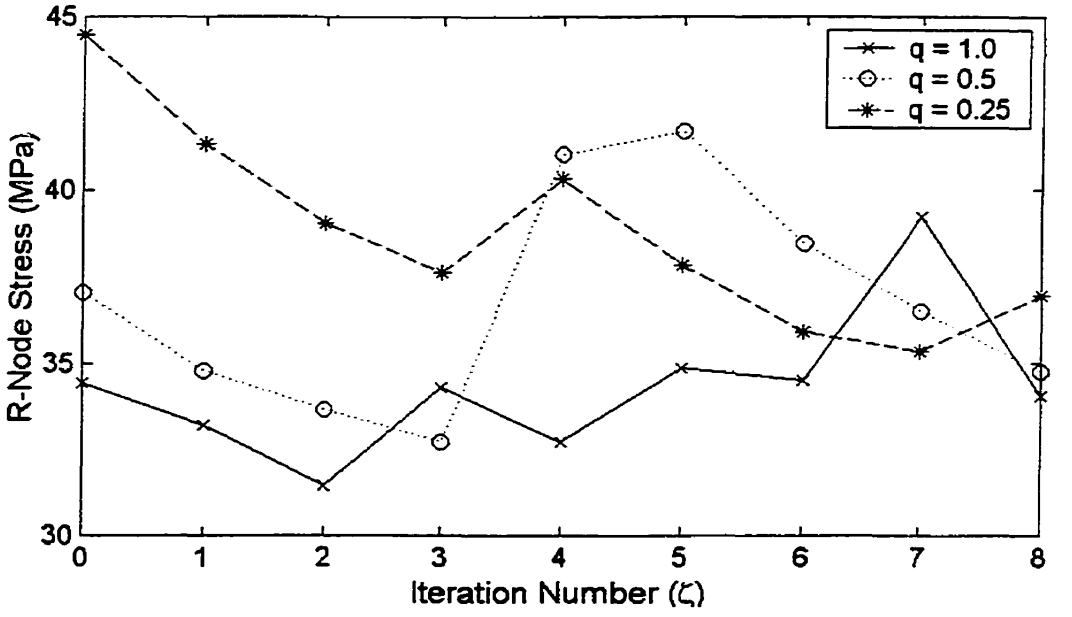

Figure 6.6: Variation of average r-node stresses for increasing ζ, and influence of modulus adjustment index q for the tee stiffener (model - T)

Table 6.2: Variations of r-node stresses and maximum equivalent stresses for increasing ζ for the flat bar stiffener (model - FB)

Iteration number ζ	Peak r-node stresses (MPa) $q = 0.5$			Average r-node Stress $\frac{\sigma_1 + \sigma_2 + \sigma_3}{3}$	Maximum equivalent stress σ_{max} (Mpa)
	σ_1	σ_2	σ_3		
0	65.43	44.08	65.43	58.31	96.70
1	60.39	42.55	60.39	54.44	76.83
2	57.27	42.47	57.27	52.34	65.22
3	54.45	43.07	54.45	50.66	58.39
4	54.32	43.92	54.32	50.85	54.32

Table 6.3: Variations of r-node stresses and maximum equivalent stresses for increasing ζ for the angle stiffener (model - L)

Iteration Number ζ	Peak r-node stresses (MPa) $q = 0.5$			Average r-node stress $\frac{\sigma_1 + \sigma_2 + \sigma_3}{3}$	Maximum equivalent stress σ_{max} (MPa)
	σ_1	σ_2	σ_3		
0	57.57	38.21	57.57	51.12	88.07
1	53.99	35.26	53.99	47.75	68.40
2	50.05	34.20	50.05	44.77	57.15
3	47.87	34.03	47.87	43.26	50.55
4	47.44	34.33	47.44	43.07	47.44

Table 6.4: Variations of r-node stresses and maximum equivalent stresses for increasing ζ for the tee stiffener (model - T)

Iteration Number ζ	Peak r-node stresses (MPa) $q = 0.25$			Average r-node stress $\frac{\sigma_1 + \sigma_2 + \sigma_3}{3}$	Maximum equivalent stress σ_{max} (MPa)
	σ_1	σ_2	σ_3		
0	51.77	29.86	51.77	44.47	75.48
1	47.88	28.30	47.88	41.35	65.72
2	45.00	27.22	45.00	39.07	58.09
3	43.21	26.49	43.21	37.64	52.10
4	47.48	26.02	47.48	40.33	47.48

6.1.3 Flat Bar Stiffened Panel (model - FBSP)

The variations of the average r-node stresses and the influence of the iteration number for increased iterations for the flat bar stiffened panel (model - FBSP) is illustrated in Figure 6.7. The calculated values for the average r-node stresses and maximum equivalent stresses for the first 4 iterations are given Table 6.5. The average r-node stresses are calculated as the average of the peak stress in each shell plate panel (between stiffeners) and the peak stresses in each stiffener. As mentioned in the previous section, if and when convergence difficulties occurred, the elastic modulus adjustment index q was reduced to stabilise the relaxation process. It is again demonstrated that with increased iterations, the r-node stress and the maximum equivalent stress in the structure converge to some limiting value. This is because the redistribution of stresses in the structure results in a relaxation of the maximum stresses.

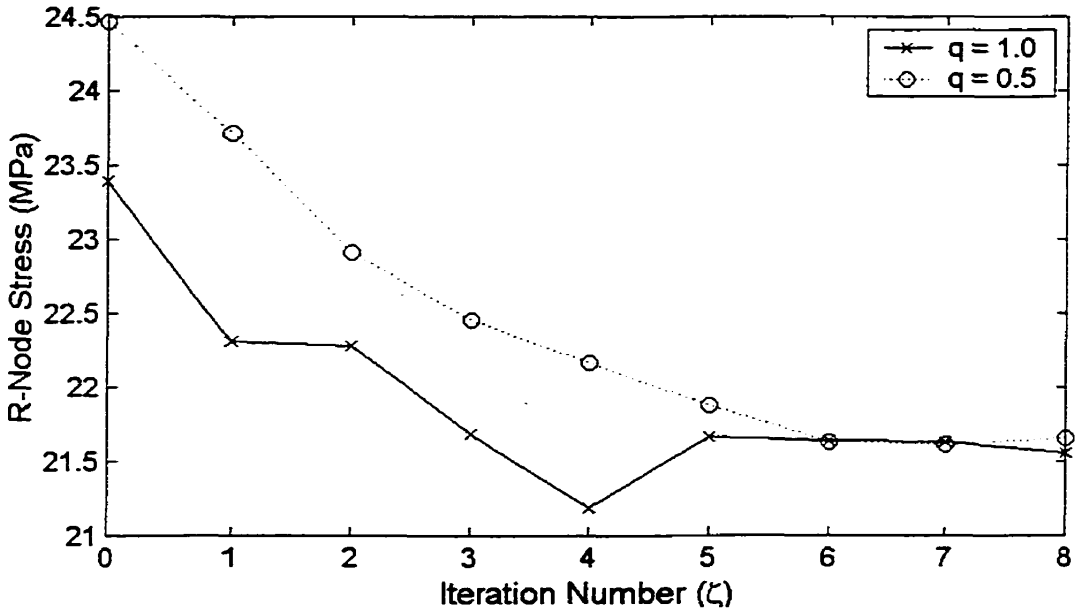

Figure 6.7: Variation of average r-node stresses for increasing ζ and influence of modulus adjustment index *q* for the flat bar stiffened panel (model - FBSP)

Table 6.5: Variation of average r-node stresses and maximum equivalent stresses for increasing ζ for the flat bar stiffened panel (model - FBSP)

Iteration Number (ζ)	Average r-node stress $\sigma_{r\text{-}node}$		Maximum equivalent stress σ_{MAX} (MPa)	
	$q = 1$	$q = 0.5$	$q = 1$	$q = 0.5$
0	23.39	24.47	35.70	35.70
1	22.31	23.71	25.32	30.87
2	22.28	22.91	24.63	26.86
3	21.68	22.45	24.00	24.50
4	21.19	22.16	23.06	24.45

6.1.4 Arctic Icebreaker Grillage (model - AIG)

The variations of the maximum r-node stresses and the influence of the iteration number for increased iterations for the arctic icebreaker grillage (model - AIG) is illustrated in Figure 6.8. The values of the maximum r-node stresses and maximum equivalent stresses for the first four iterations are listed Table 6.6. Because of the level of complexity associated with the structure and the variation in the mesh density, it was difficult to identify precise locations of all r-node peaks. Thus, the limit loads were evaluated on the basis of the maximum r-node stress in the structure.

The plot of r-node stress and iteration number ζ in Figure 6.8 shows that the structure is not relaxing with increased iterations. Reducing the value of the modulus adjustment index q smoothes the curve, but does not initiate a monotonic decrease in the r-node stresses in the structure. As with the angle and tee stiffeners, this is attributed to numerical instabilities induced from over relaxation from one iteration to the next, as well as the numerical limitations surrounding proper identification of the exact locations of the r-nodes. Variations in the size and shape of elements used to construct the grillage model make even the selection of relative r-node locations difficult to identify for two consecutive iterations. The use of finer, uniformly shaped element meshing might help alleviate the problem, but again, at the expense of increased CPU time.

Even though the r-node stresses encounter numerical relaxation difficulties, the values of the maximum equivalent stresses do progressively reduce, as illustrated in Table 6.6.

Given that the applied load (pressure) to the structure is 1.8 N/mm^2 over an area of 300,000 mm^2, with a yield stress of 345 MPa, the resulting estimates of load capacities for each iteration can be evaluated. The results for iteration four are presented later in section 6.3, Table 6.13.

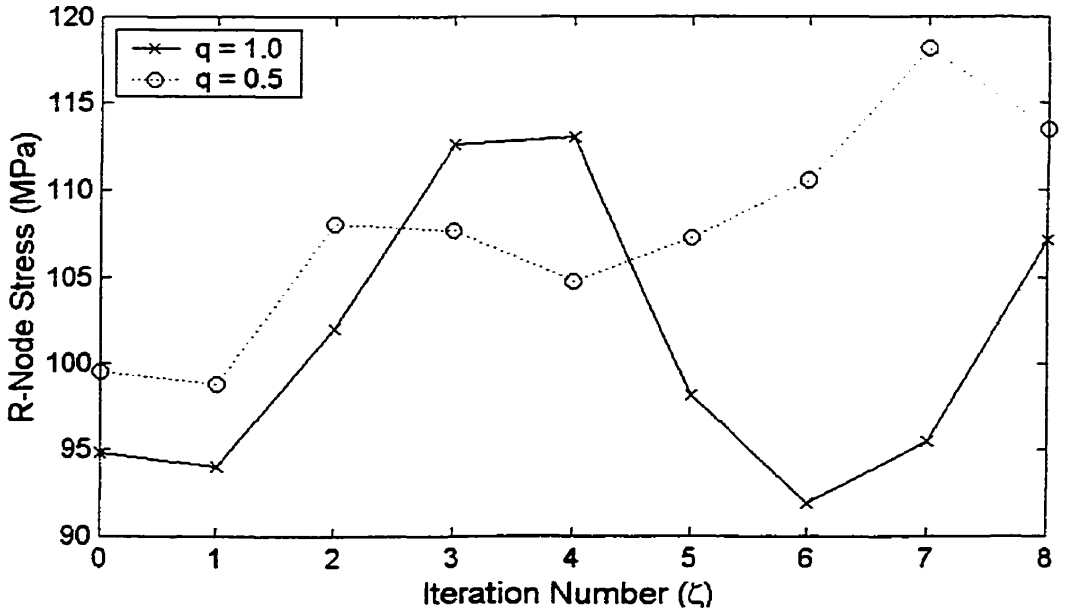

Figure 6.8: Variation of average r-node stresses for increasing ζ and influence of modulus adjustment index q for the arctic icebreaker grillage (model - AIG)

Table 6.6: Variation of maximum r-node stresses and maximum equivalent stresses for increasing ζ for arctic the icebreaker grillage (model - AIG)

Iteration number (ζ)	Maximum r-node stress $\sigma_{r\text{-}node}$ (MPa)		Maximum equivalent stress σ_{MAX} (MPa)	
	$q = 1$	$q = 0.5$	$q = 1$	$q = 0.5$
0	94.80	99.49	233.3	233.0
1	94.00	98.81	227.6	155.8
2	101.99	108.08	**369.8**	115.3
3	112.61	107.70	207.9	107.7
4	113.02	104.72	127.4	104.7

6.2 The m_α Method

Analysis using the m_α method is carried out in a similar manner as the r-node method. Each of the models listed in Chapter 5 were analysed to study the effect of elastic modulus adjustment and the influence of the modulus adjustment index q on the m_α lower bound limit load estimates. Iterative adjustments of the elastic modulus of the elements of a structure are carried out to redistribute and relax peak stresses in the structure to a limit state from which a lower bound limit load can be evaluated. The m_α method calculates a limit load multiplier based on any two consecutive linear elastic analyses. Previous authors suggest that just two linear elastic analysis (one iteration) are required to predict an improved lower bound multiplier (Seshadri and Mangalaramanan, 1997). The results presented in this section suggest that one iteration (or two analyses) may not be sufficient, and three or more iterations are necessary. Eight iterations were carried out on all structures to study their convergence behaviour. In the event that proper convergence behaviour was not achieved, the nominal value of modulus adjustment index ($q = 1$) was reduced. Also, the structures are classified according to the convergence behaviour of the limit load multipliers based on guidelines presented by Seshadri and Mangalaramanan (1997).

6.2.1 Indeterminate Beam (model - IB)

To accurately determine the optimum m_α multiplier, it is necessary that the reference volume be determined. On the basis of two consecutive linear elastic analyses for any given iteration, the variation of the upper bound multipliers can be plotted against the

percent volume of the structure, as illustrated in Figure 6.9. The reference volume (V_R) and reference volume multiplier (m^o_R) can be determined from these curves. The two curves m^o_i and m^o_{ii} each represent the upper bound multiplier for linear elastic analysis one and linear elastic analysis two respectively after the elastic moduli have been adjusted. The reference volume (V_R) and the reference volume upper bound multiplier (m^o_R) are identified as the intersection of the two curves and are locations where the energy dissipation for both analyses is the same. This intersection defines the extent of the sub-region of the structure that encounters the most significant amount of plastic action or where the most energy is dissipated due to plasticity. According to Seshadri and Mangalaramanan (1997), it is also the location where the theorem of nesting surfaces is barely satisfied. This assumption is similar a plastic hinge formation mechanism where the indeterminate beam is considered collapsed when two plastic hinges have formed, even though the whole structure has not encountered plasticity.

Figure 6.10 illustrates the convergence of the upper bound multiplier m^o (Calladine and Druker, 1962 and Boyle, 1982), lower bound multiplier m' (Mura et el., 1963 and 1965) and the m_α multiplier (Seshadri and Mangalaramanan, 1997) toward the exact limiting value with increased iterations. The upper bound multiplier progressively reduces while the lower bound multiplier increases as the stresses within the structure are relaxed. The m_α multiplier lies between the two.

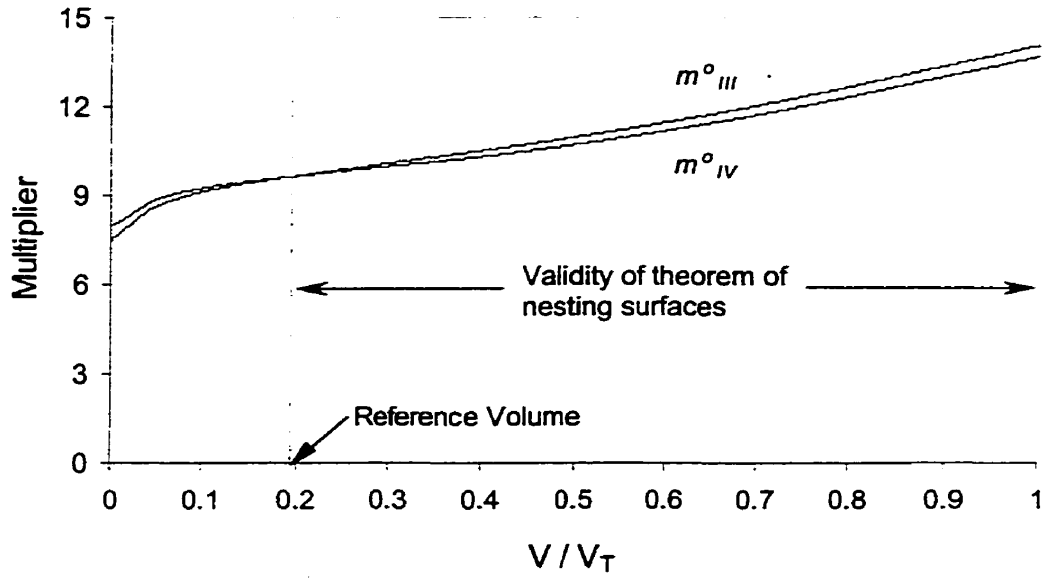

Figure 6.9: Determination of the reference volume multiplier as function of normalised volume V/V_T for $\zeta = 4$; $q = 0.5$ for the indeterminate beam (model - IB) The reference volume and reference volume multiplier m^o is taken at intersection

Calculation of the m_α limit load for the indeterminate beam based on the reference volume multiplier from Figure 6.9 is illustrated as

Structure: Indeterminate beam subject to uniform pressure

Applied Load	P	8.75	N (Distributed over length)
Yield Stress	σ_y	206.85	MPa
Upper Bound Multiplier			
Linear Analysis I	m^o_I	14.04	
Linear Analysis II	m^o_{II}	13.66	
Max Equivalent Stress			
Linear Analysis I	$[(\sigma_e)_M]_I$	27.63	MPa
Linear Analysis II	$[(\sigma_e)_M]_{II}$	25.95	MPa
Classical Limit Load for			
linear analysis II	$(P_{LC})_{II} =$	$P \times \sigma_y / [(\sigma_e)_M]_{II}$	
	=	69.80	KN

Upper Bound Multiplier (Reference Volume) m^o_R = 9.63

Upper Bound Limit load $P_U = m^o_R * P$

= 84.34 kN

Maximum Normalised Stress $\bar{\sigma}^o_M = \frac{\sigma^o_M}{\sigma_Y}$

= 0.1255

Coefficients A, B, C for quadratic equation

$Am_\alpha^2 + Bm_\alpha + C$

$A = (m_i^o)^4(\bar{\sigma}^o_{Mi})^4 + 4(m_i^o)^2(\bar{\sigma}^o_{Mi})^2 - 1$

$B = -8(m_i^o)^3(\bar{\sigma}^o_{Mi})^2$

$C = 4(m_i^o)^3(\bar{\sigma}^o_{Mi})$

A = 6.97
B = -112.47
C = 448.20

Discrm = 152.13

Discrim > 0 – Two Real roots

Multiplier m_α m_α = Max (8.95 , 7.18)

m_α = **8.95**

m_α limit load **Pm_α = m_α * P**

= **78.4** **N**

= **1543** **kPa**

The values of m^o, m', m_α for the first four iterations are listed in Table 6.7. It can be noted that the multiplier for the maximum equivalent stress evaluated as (σ_y / σ_{MAX}) is actually the same as the lower bound multiplier (eg. for q = 1, ζ = 1 the multiplier for maximum equivalent stress is evaluated as 206.85 / 27.61 = 7.49). This basically states that the lower bound multiplier is no better than the same evaluated using the maximum equivalent stress in the structure.

The convergence behaviour of a structure can be classified according to guidelines set forth by Seshadri and Mangalaramanan (1997) in section 3.6.5. The maximum equivalent stress progressively reduces and hence there is a progressive increase in the lower bound multiplier, but the upper bound multiplier does not progressively decrease. Thus, the indeterminate beam is considered a Class II type structure. By reducing the value of the modulus adjustment index q, the numerical instabilities stabilise and the structure exhibits a Class I type behaviour.

The variation of the upper bound multiplier m^o, Mura's lower bound multiplier m' and the resultant m_α multiplier for increased volume is shown in Figure 6.11. The values of limit load multipliers m^o, m' and m_α are the same when based on the single element having the highest energy dissipation or highest stressed element. The limit load evaluated on the basis of these values is the same as the classical lower bound limit load. The reference volume evaluated in Figure 6.9 accounts for approximately 39% of the total volume of the structure and identifies the sub-region where plasticity leading to collapse is concentrated.

It should be noted in Figure 6.11, that the influence of volume (V/V_T), on the m_α multiplier is minimal. This suggests that m_α limit loads are valid for any volume (V/V_T), provided the theorem of nesting surfaces is satisfied. Identifying the sub-region is important if limit loads are to be evaluated on the basis of m^o and m'.

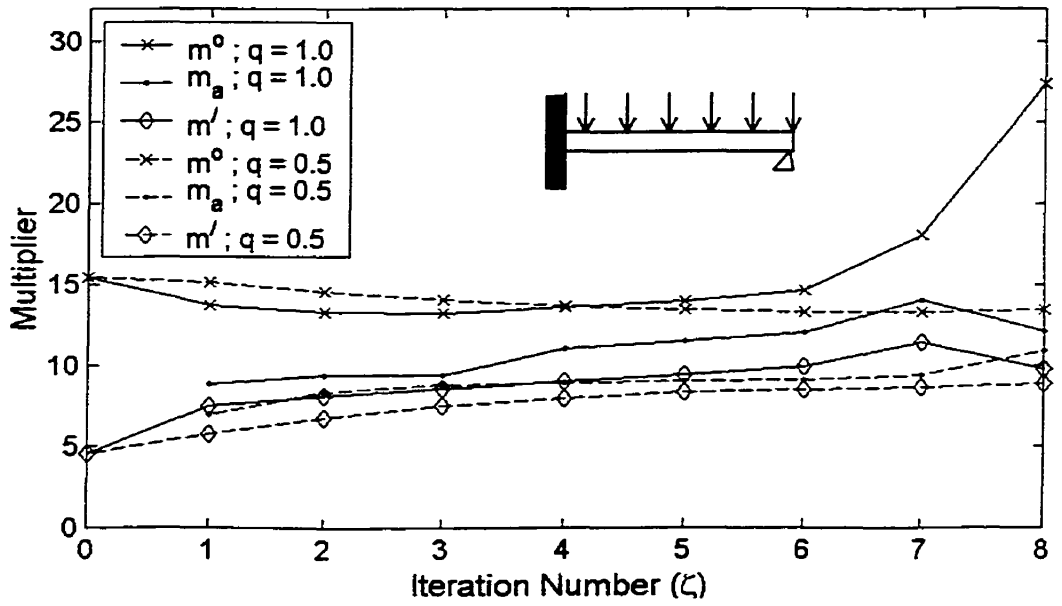

Figure 6.10: Variation of m^o, m', m_α with increasing iteration number ζ and influence of modulus adjustment index q, for the indeterminate beam (model - IB)

Table 6.7: Variation of m^o, m', m_α and σ_{max} for increasing iteration number ζ for the indeterminate beam (model - IB)

Iteration Number (ζ)	$q = 1$				$q = 0.5$			
	m^o	m'	m_α	σ_{MAX}	m^o	m'	m_α	σ_{MAX}
0	15.43	4.60	-	44.99	15.43	4.60	-	44.99
1	13.70	7.49	8.85	27.61	15.16	5.80	6.97	35.68
2	13.28	8.13	9.39	25.43	14.57	6.78	8.34	30.51
3	13.16	8.55	9.35	24.20	14.04	7.49	8.79	27.63
4	**13.60**	9.02	11.0	22.94	13.66	7.97	8.95	25.95

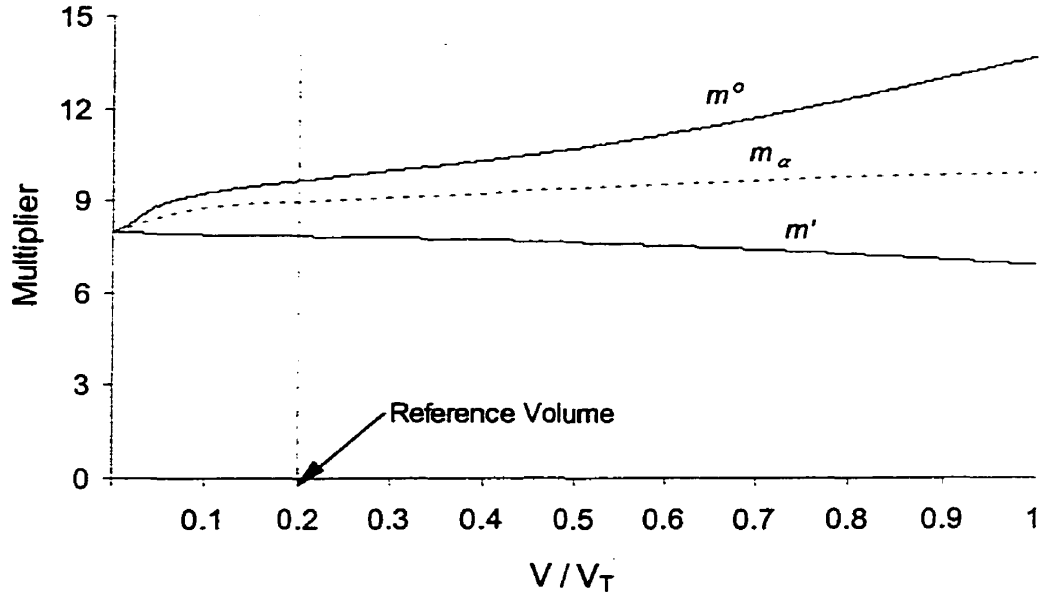

Figure 6.11: Variation of m^o, m', m_α with normalised volume V/V_T for $\zeta = 4$; $q = 0.5$, for the indeterminate beam (model - IB)

6.2.2 Mainframe Stiffeners

The variations of the upper and lower bound multipliers m^0 and m' and the m_α multiplier for increased iterations for the three mainframe stiffeners, flat bar (model - FB), angle (model - L) and tee (model - T) are illustrated in Figure 6.12, Figure 6.13 and Figure 6.14. The values for these parameters for the first four iterations are listed in Table 6.8, Table 6.9 and Table 6.10. The m_α limit loads for these structures are listed in Table 6.13.

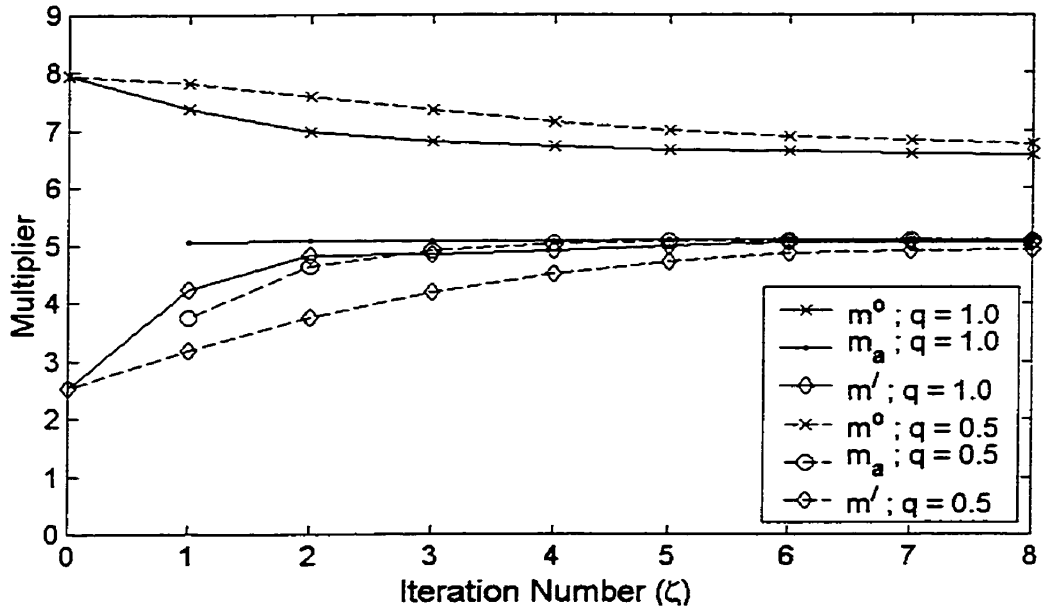

Figure 6.12: Variation of m^o, m', m_α with increasing iteration number ζ and influence of modulus adjustment index q for the flat bar stiffener (model - FB)

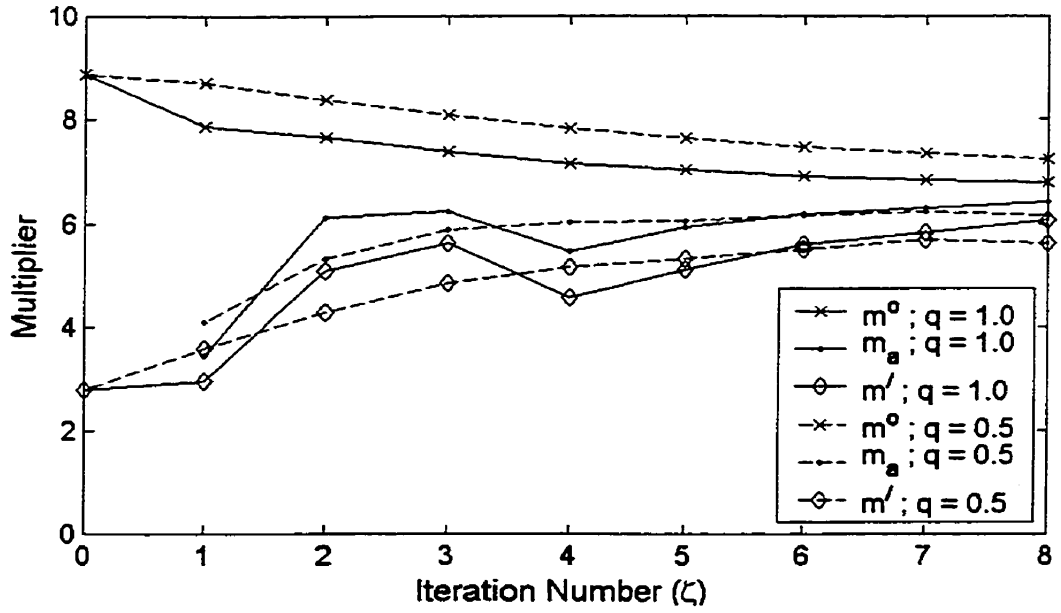

Figure 6.13: Variation of m^o, m', m_α with increasing iteration number ζ and influence of modulus adjustment index q for the angle stiffener (model - L)

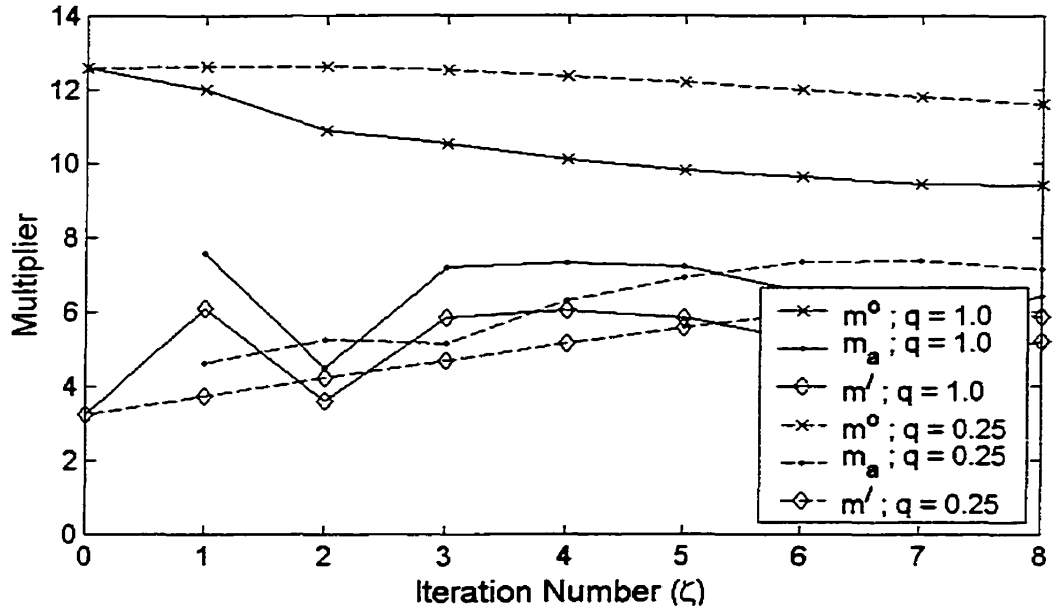

Figure 6.14: Variation of m^o, m', m_α with increasing iteration number ζ and influence of modulus adjustment index q for the tee stiffener (model - T)

Table 6.8: Variation of m^o, m', m_α and σ_{max} for increasing iteration number ζ for the flat bar stiffener (model - FB)

Iteration Number (ζ)	$q = 1$			$q = 0.5$		
	m^o	m'	m_α	m^o	m'	m_α
0	7.95	2.53	-	7.95	2.53	-
1	7.37	4.23	5.05	7.83	3.19	3.75
2	6.97	4.82	5.09	7.59	3.76	4.63
3	6.8	4.84	5.08	7.35	4.20	4.92
4	6.72	4.91	5.09	7.15	4.51	5.03

Table 6.9: Variation of m^o, m', m_α and σ_{max} for increasing iteration number ζ for the angle stiffener (model - L)

Iteration Number (ζ)	$q = 1$			$q = 0.5$		
	m^o	m'	m_α	m^o	m'	m_α
0	8.88	2.78	-	88.88	2.78	-
1	7.88	2.96	3.44	8.72	3.58	4.10
2	7.65	5.09	6.12	8.39	4.29	5.32
3	7.38	5.61	6.23	8.08	4.85	5.88
4	7.15	**4.56**	5.45	7.83	5.16	6.02

Table 6.10: Variation of m^o, m', m_α and σ_{max} for increasing iteration number ζ for the tee stiffener (model - T)

Iter'n No. (ζ)	$q = 1$			$q = 0.5$			$q = 0.25$		
	m^o	m'	m_α	m^o	m'	m_α	m^o	m'	m_α
0	12.58	3.25	-	12.58	3.25	-	12.58	3.25	-
1	12.01	6.10	7.56	12.57	4.34	-	12.63	3.73	4.63 *
2	10.88	**3.62**	4.50 *	12.26	5.37	6.54	12.61	4.22	5.23 *
3	10.54	5.85	7.18	11.83	5.22	6.48	12.52	4.70	5.16
4	10.11	6.03	7.31	11.48	5.05	6.26	12.37	5.16	3.61

* A reference volume was not attainable since the two upper bound multiplier (m^o) curves for two consecutive iterations did not intersect. Values represent maximum attainable m_α.

The results for the flat bar (model – FB) indicate that with increased iterations ζ and a reduced modulus adjustment index number q, proper convergence behaviour is achieved. The upper bound multiplier m^0 decreases and the lower bound multiplier m' increases as the iteration number ζ increases. Thus, based on classification guidelines proposed by Seshadri and Mangalaramanan (1997), the structure is a Class I type structure. The

theorem of nesting surfaces is satisfied, and an m_α multiplier evaluated on the basis of any iteration is valid.

Proper convergence behaviour for increased ζ for the angle stiffener (model – L) was not achieved using the nominal value of the modulus adjustment index number (q = 1). The upper bound multiplier m^0 decreased but the lower bound multiplier m' fluctuated at iteration four. This structure is therefore classified as a Class II type structure at this iteration. Reducing the modulus reduction index number q to 0.5 satisfied the convergence requirements for upper and lower bound multipliers. This structure was therefore transformed into a Class I type structure, thereby satisfying the criteria of the theorem of nesting surfaces, and validated the calculation of m_α multiplier for all such iterations.

Achieving proper convergence behaviour for increased ζ for the tee stiffener (model – T) was somewhat difficult. Using the nominal value of the modulus reduction index number (q = 1), the upper bound multiplier m^0 decreased but the lower bound multiplier m' fluctuated. This structure is therefore classified as a Class II type structure. Reducing q to 0.25 resulted in a continued decrease in the upper bound multiplier m^0 and an increase in the lower bound multiplier m'. This structure was therefore transformed into a Class I type structure.

The variation of the m^0, m' and m_α multipliers, for increasing elemental volume, for the three mainframe stiffeners after four iterations of the elastic modulus is illustrated in

Figure 6.16 (model - FB), Figure 6.18 (model - L) and Figure 6.20 (model - T). Seshadri and Managalaramanan, (1997) have suggested that the m_α multiplier be evaluated on the basis of the upper bound multiplier at the reference volume or reference volume multiplier, $m^o(V_R)$ of the structure. However, it is apparent that the m_α multiplier is valid for any volume, provided the theorem of nesting surfaces is not violated. The influence of volume or V/V_T on the m_α multiplier is minimal for any region provided the theorem of nesting surfaces is satisfied.

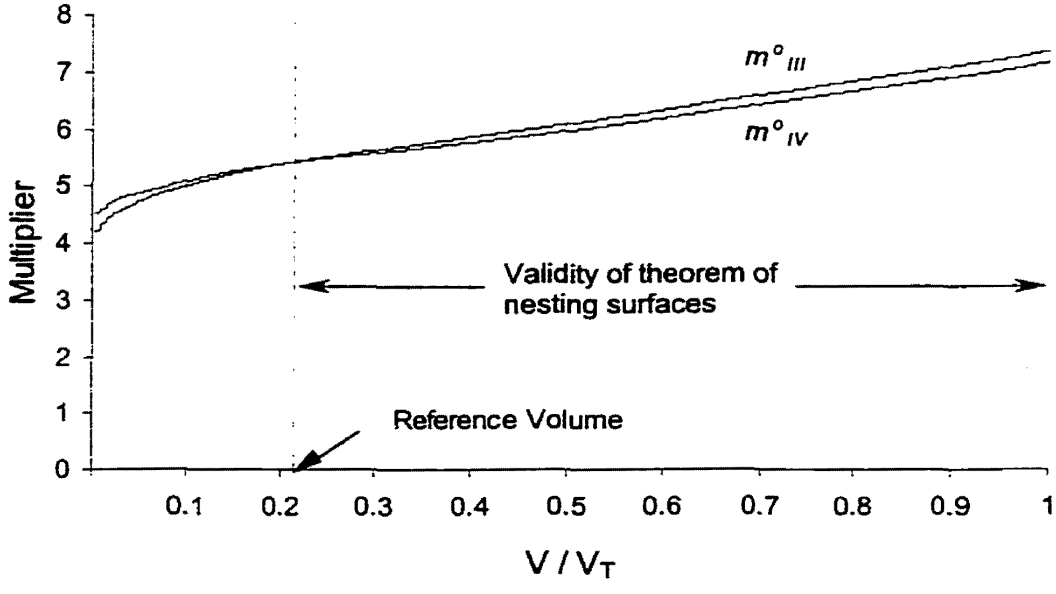

Figure 6.15: Variation of the m^o for two consecutive linear elastic FEA with normalised volume V/V_T for $\zeta = 4$; $q = 0.5$, for the flat bar stiffener (model - FB). Reference volume and reference volume multiplier m^o is taken at intersection.

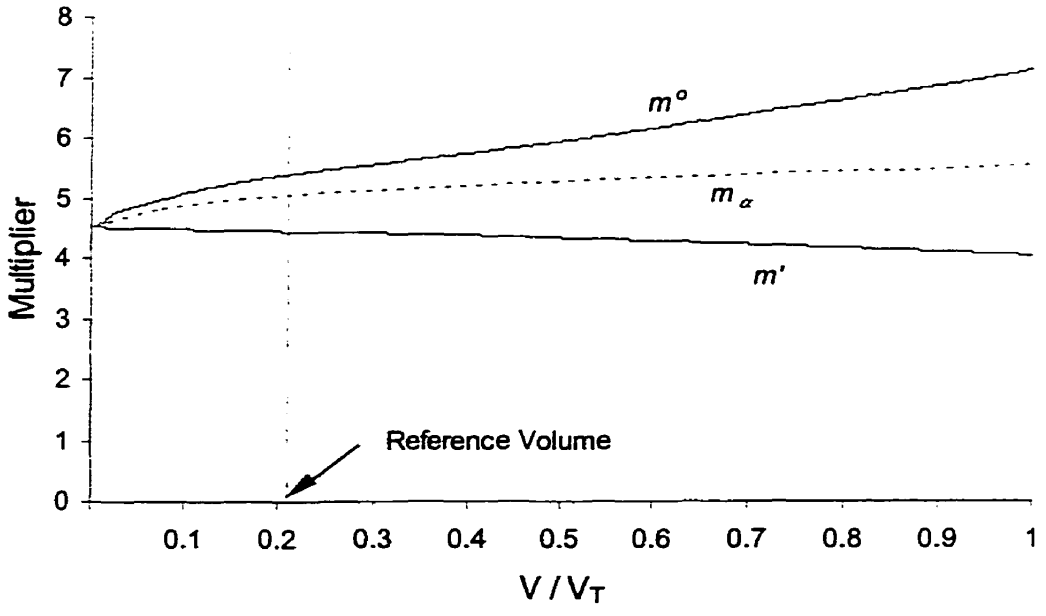

Figure 6.16: Variation of m^0, m' and m_α for normalised volume V/V_T for $\zeta = 4$, $q = 0.5$ for the flat bar stiffener (model - FB)

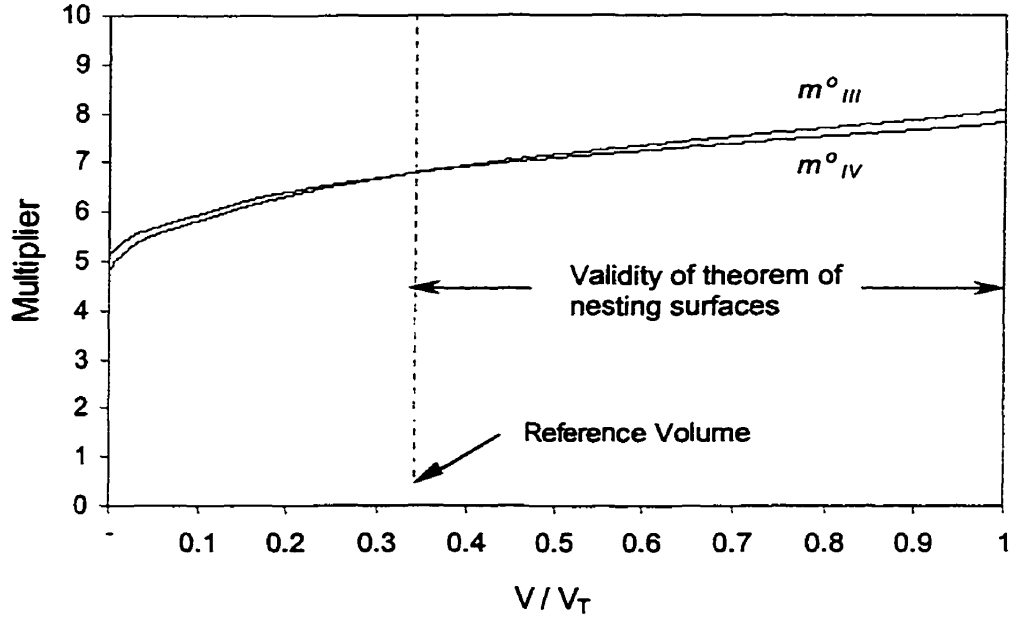

Figure 6.17: Variation of the m^o for two consecutive linear elastic FEA with normalised volume V/V_T for $\zeta = 4$; $q = 0.5$ for the angle stiffener (model - L). Reference volume and reference volume multiplier m^o is taken at intersection.

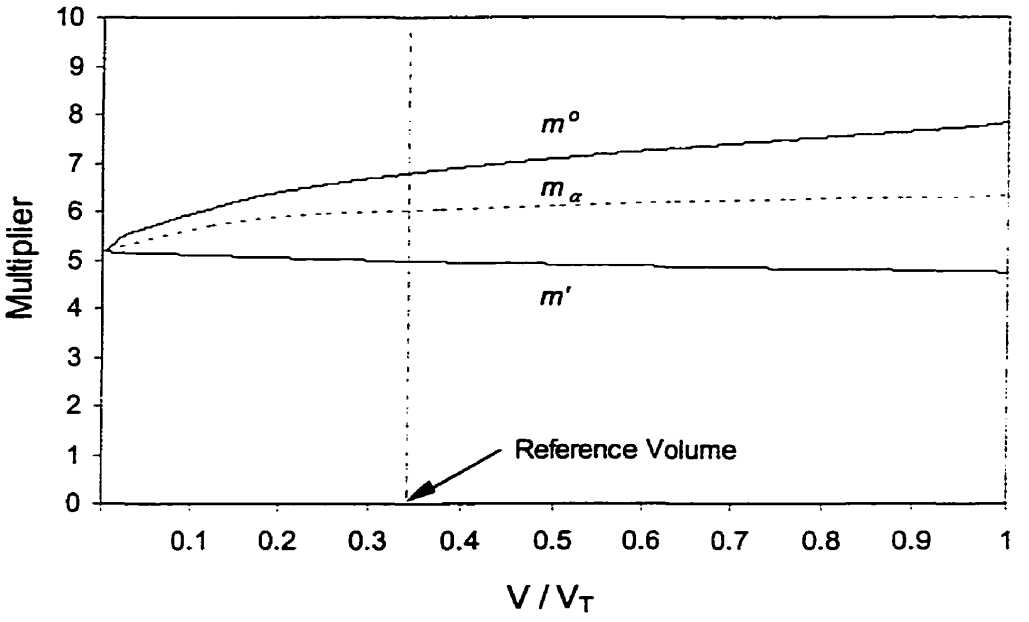

Figure 6.18: Variation of m^0, m' and m_α for normalised volume V/V_T for $\zeta = 4$; q = 0.5 for the angle stiffener (model - L)

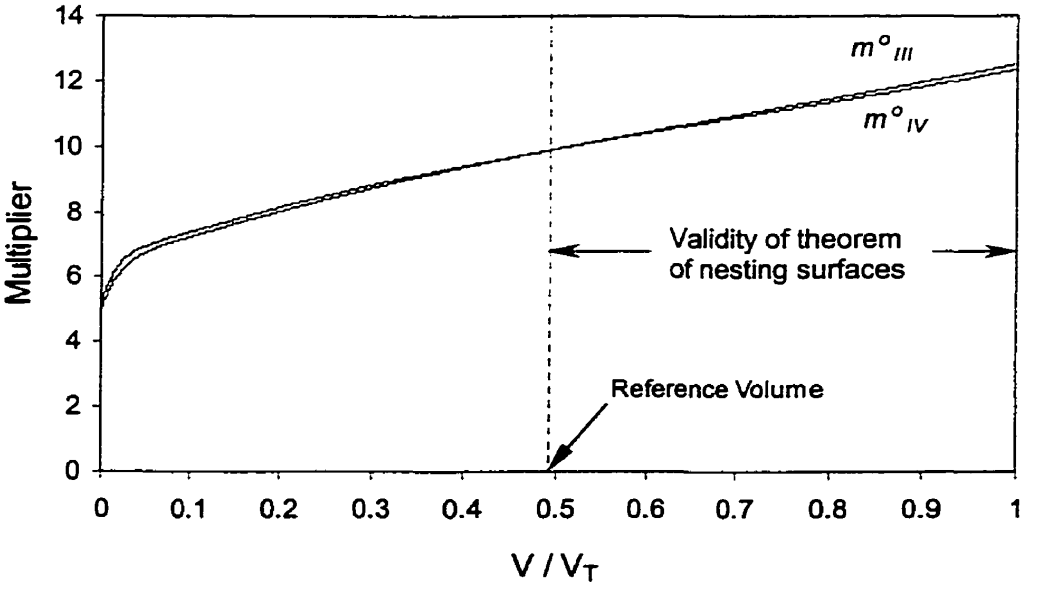

Figure 6.19: Variation of the m^o for two consecutive linear elastic FEA with normalised volume V/V_T for $\zeta = 4$; $q = 0.5$ for the tee stiffener (model - T). Reference volume and reference volume multiplier m^o is taken at intersection.

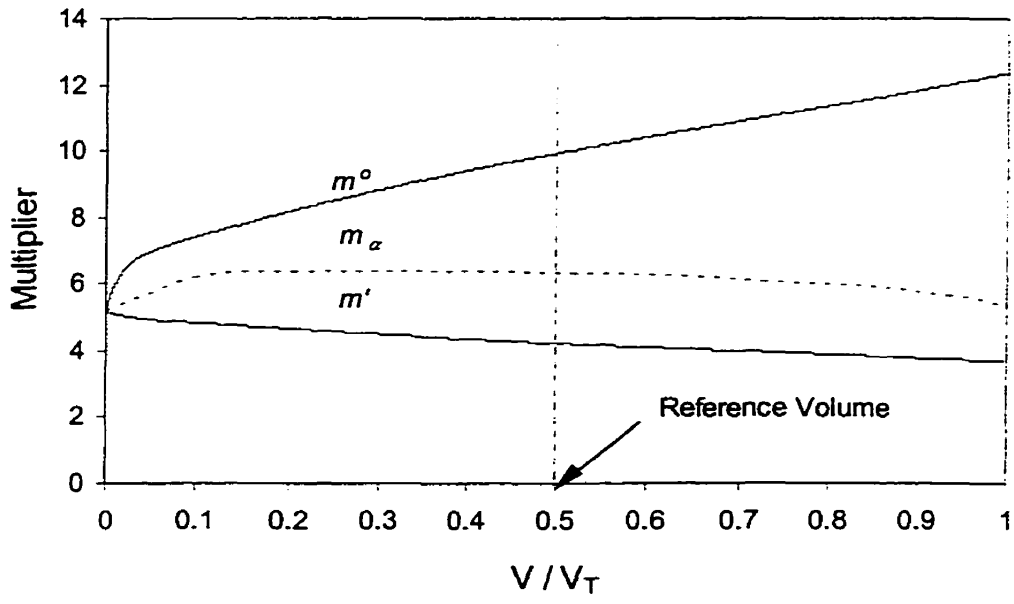

Figure 6.20: Variation of m^0, m' and m_α for normalised volume V/V_T for $\zeta = 4$; q = 0.25 for the tee stiffener (model - T).

6.2.3 Flat Bar Stiffened Panel (model - FBSP)

Variations of the upper and lower bound multipliers m^0 and m' and the m_α multiplier for increased iterations ζ for the flat bar stiffened panel (model – FBSP) are illustrated in Figure 6.21. The values for these parameters for four iterations of the elastic modulus are listed in Table 6.11.

This structure demonstrated a progressive decrease in the upper bound multiplier m^0 and a progressive increase in the lower bound multiplier m'. Based on the classification guidelines proposed by Seshadri and Mangalaramanan (1997), this structure analysis can be classed as a Class I type structure. Reducing the modulus index number ($q = 0.5$) has

no significant effect in this case because the theorem of nesting surfaces is satisfied with the nominal value ($q = 1$). It does however, show that reducing q results in much smoother relaxation process or smooth monotonic convergence behaviour. The variation of m^0, m' and m_α for increased volume V/V_T for the flat bar stiffened panel (model – FBSP) is illustrated in Figure 6.23. Here, the region of plasticity or where energy dissipation due to plasticity is the greatest accounts for approximately 40% of the whole structural volume.

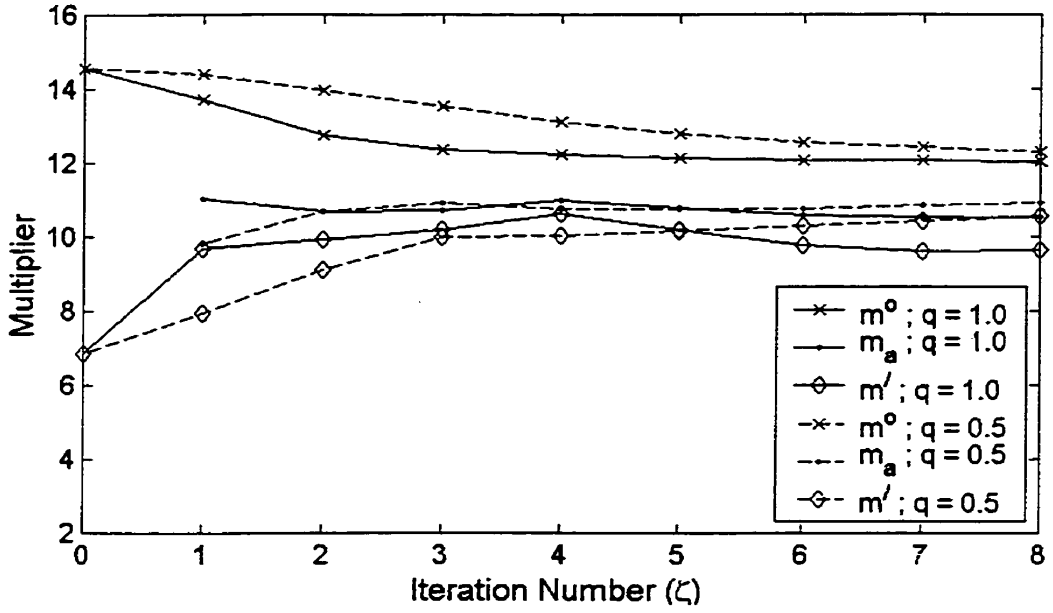

Figure 6.21: Variation of m^o, m', m_α with increasing ζ and influence of modulus adjustment index q for the flat bar stiffened panel (model - FBSP)

Table 6.11: Variation of m^o, m', m_α and σ_{max} for increasing iteration number ζ for the flat bar stiffened panel (model - FBSP)

Iteration Number (ζ)	$q = 1$			$q = 0.5$		
	m^o	m'	m_α	m^o	m'	m_α
0	14.56	6.86	-	14.56	6.86	-
1	13.71	9.68	11.01	14.39	7.94	9.79
2	12.77	9.95	10.68	13.98	9.12	10.68
3	12.36	10.21	**10.73**	13.53	10	10.92
4	12.22	10.62	10.98	13.13	10.02	10.79

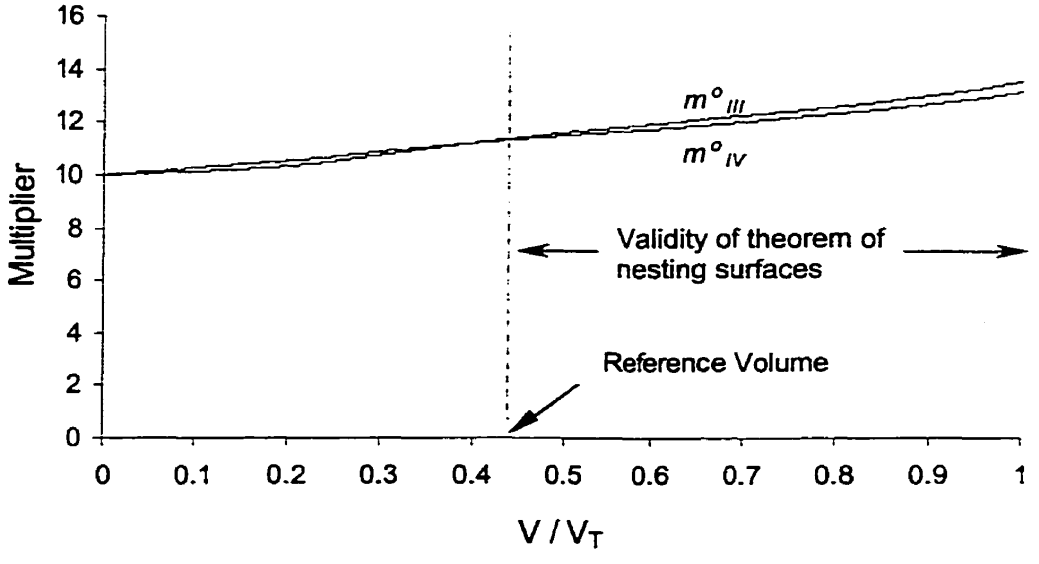

Figure 6.22: Variation of the m^o for two consecutive linear elastic FEA with normalised volume V/V_T for $\zeta = 4$; $q = 0.5$ for the stiffened panel (model - FBSP). Reference volume and reference volume multiplier m^o is taken at intersection.

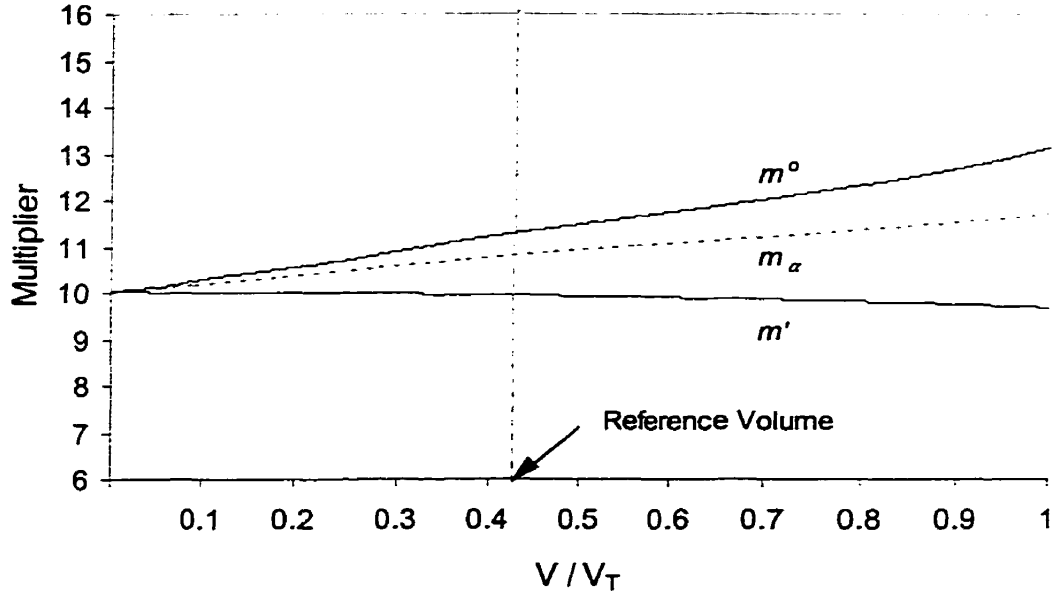

Figure 6.23: Variation of m^o, m' and m_α for normalised volume V/V_T for $\zeta = 4$, $q = 0.5$ for the flat bar stiffened panel (model - FBSP).

6.2.4 Arctic Icebreaker Grillage

Variations of the upper bound multiplier m^o, lower bound multiplier m' and the m_α multiplier for increased iteration number ζ for the arctic icebreaker grillage (model - AIG) are shown in Figure 6.24. The values of these parameters for the first four iterations are given in Table 6.1 2.

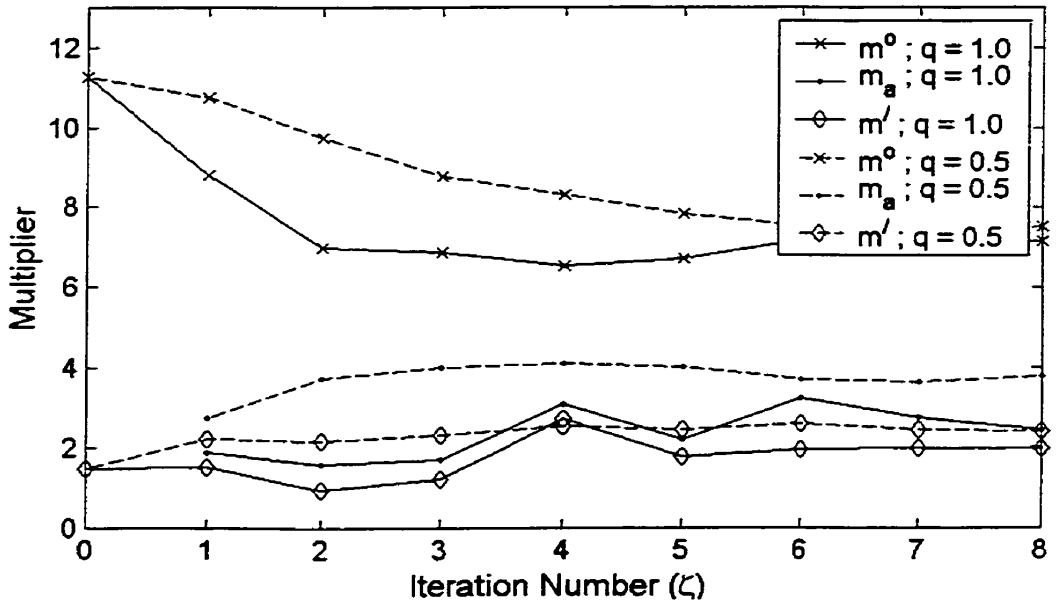

Figure 6.24: Variation of m^o, m', m_α with iteration number ζ and influence of modulus adjustment index q for the arctic icebreaker grillage (model - AIG).

Table 6.12: Variation of m^o, m' and m_α for increasing iteration number ζ for the arctic icebreaker grillage (model - AIG)

Iteration Number (ζ)	$q = 1$			$q = 0.5$		
	m^o	m'	m_α	m^o	m'	m_α
0	11.25	1.48	-	11.25	1.48	-
1	8.79	1.52	1.88 *	10.75	2.21	2.75 *
2	6.96	0.93	1.50 *	9.74	2.16	3.72 *
3	6.84	1.22	1.69 *	8.77	2.31	3.96 *
4	6.51	2.70	3.02	8.31	2.54	4.09 *

* A reference volume was not attainable since the two upper bound multiplier (m^o) curves for two consecutive iterations did not intersect. Values represent maximum attainable m_α.

The use of the nominal modulus modification index number was not satisfactory for this structure, as convergence requirements were not met. The upper bound multiplier m^0 increased after iterations four and five and lower bound multiplier m' fluctuated (see

Figure 6.24). Based on the classification guidelines proposed by Seshadri and Mangalaramanan (1997), this structure is deemed a Class III type structure which does not satisfy the theorem of nesting surfaces. Reducing the modulus index number (q = 0.5) resulted in a continued decrease in m^0 and a general increase in m' except for a slight decrease at iteration two. Reducing q to 0.25 cause the structure to behave as a Class I type structure. Convergence requirements and the theorem of nesting surfaces were satisfied.

The variation of the m^o, m' and m_α multipliers for increased volume is illustrated in Figure 6.26. This figure points out that the energy disspation rates fluctuate throughout the structure, as opposed to the smooth dissapation rates observed with the other models. This may be attributed to the non-uniform element sizes used in meshing the model. Also, the two upper bound multipliers m^o for two linear elastic analyses at iteration four did not intersect thereby not identifying a reference volume. However, as illustrated in Figure 6.26, the m_α multiplier can still be evaluated based on the upper bound multipliers for the whole structure. The limiting m_α multiplier can be taken as the maximum evaluated multiplier for the structure.

It should be noted that evaluation of the m_α multiplier may not be numerically possible for the total volume for complex geometric structures such as the arctic icebreaker grillage. As shown in Figure 6.26, the m_α multiplier can only be evaluated for a structural volume up to 93% (approx.) of the total volume, at which point the quadratic equation used to evaluate m_α calculates imaginary roots.

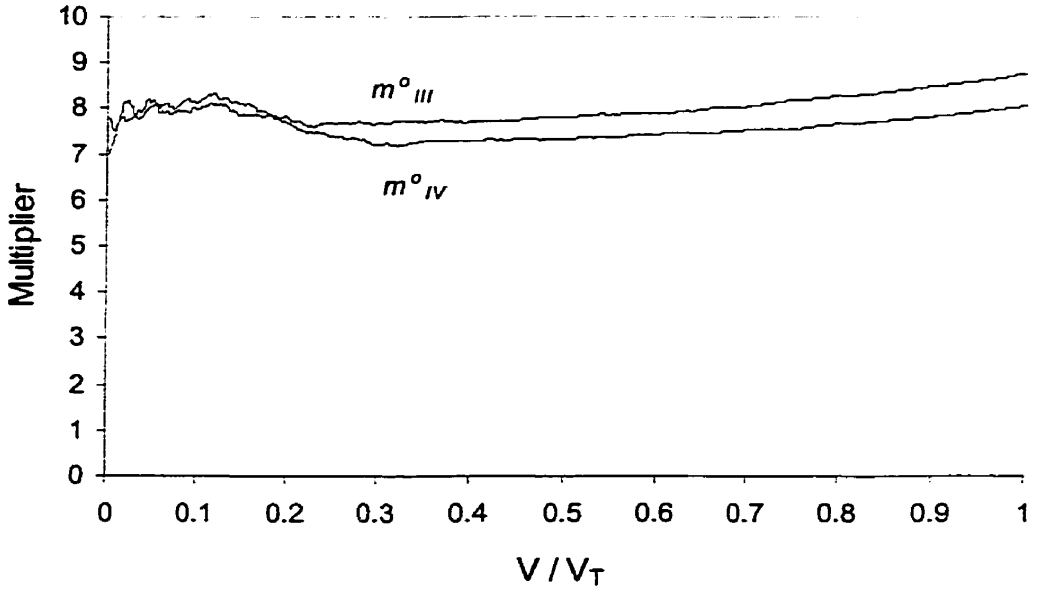

Figure 6.25: Variation of the m^o for two consecutive linear elastic FEA with normalised volume V/V_T for $\zeta = 4$; q = 0.5 for the arctic icebreaker grillage (model - AIG). Reference volume and reference volume multiplier m^o is taken at intersection.

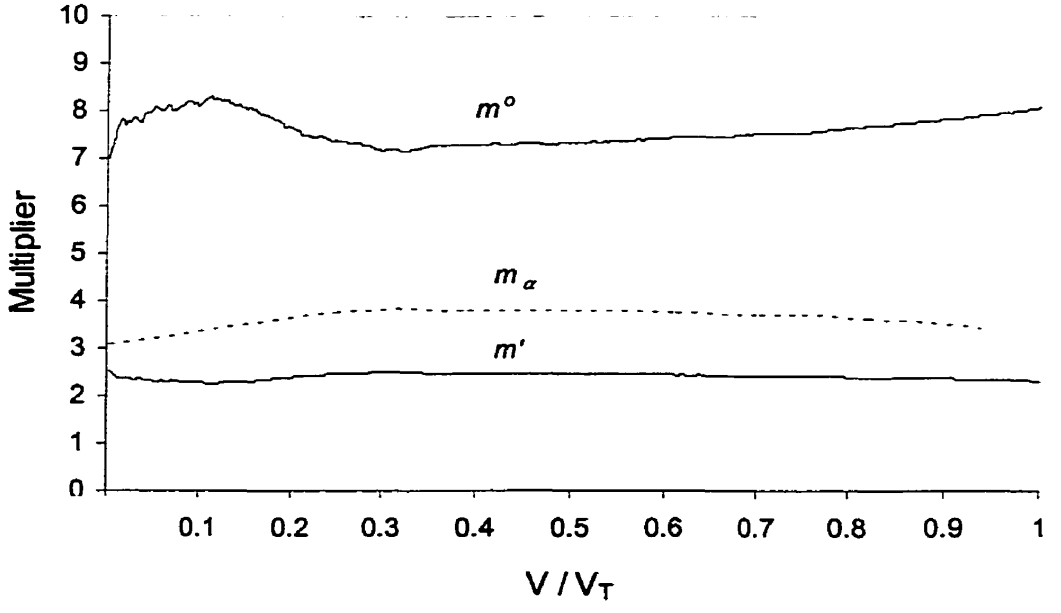

Figure 6.26: Variation of m^0, m' and m_α for normalised volume V/V_T for $\zeta = 4$, q = 0.5 for the arctic icebreaker grillage (model - AIG).

6.3 Limit Loads

The limit loads for the various structures analysed are evaluated on the basis of four linear elastic iterations and a value of the modulus adjustment index q that ensures the stress convergence behaviour matches that of a Class I type structure. The limit loads are plotted as load levels on a load deflection diagram that compares the load deflection results for non-linear analysis and the progressive modulus reduction method of analysis. The limit loads for the various structures are illustrated in Figure 6.27 through to Figure 6.32. The values of the limit loads are recorded in Table 6.13.

The load curves illustrate limit load capacities of the structures for the first yield condition (classical lower bound limit load), second analysis yield condition, non-linear analysis, analytical solution (where available), the robust techniques namely Progressive Modulus Reduction (PMR), r-node, m_α and full scale lab test results where available. The first yield limit load is classical limit load, based on the maximum Von Mises equivalent stresses in the model for the initial analysis with homogeneous elastic modulus throughout the structure. The second analysis yield limit load is also a classical limit load, but is based on the maximum Von Mises equivalent stresses in the second analysis or after the initial homogeneous elastic modulus distribution have been modified or adjusted on the basis of the stress distribution of the first analysis. Modifying the elastic modulus redistributed and relaxed the peak stresses in the structure, causing the stress peaks to level off and reduce. The result is an improved estimate of a lower bound limit load for of the structure.

The analytical estimates of the limit loads were evaluated for the indeterminate beam (model - IB), mainframe stiffeners (model - FB, model - L, model - T) and the flat bar stiffened panel (model - FBSP). The analytical limit load for the indeterminate beam (model - IB) was evaluated as $P = 11.66*Mp/L^2$ (Mendelson, 1968). The mainframe stiffeners (model - FB, model - L, model - T) and the flat bar stiffened panel (model - FBSP) were evaluated using rigid plastic hinge formation theory (Huges, 1988). The analytical curves evaluated using rigid plastic hinge formation theory, indicate the loads and corresponding deflections at which edge hinges form (first change in slope) and the collapse load as the third hinges form (second change in slope = 0). The slope of the elastic portion of the load deflection curves evaluated using rigid plastic hinge formation theory is generally steeper than those evaluated using FEA. This is because the analytical plastic hinge deflections are evaluated at the neutral axis whereas the FEA deflections represent maximum section deflections taken at the point of load application and include deformation in the elements.

The limit load levels for the non-linear and PMR analyses are represented by the asymptotic behaviour in the load deflection curves. This identifies the load at which full plastic hinge collapse occurs. Physically the structures would have an increased load bearing capacity after the structure yields as a result of membrane action. However, numerically this is difficult to model since deformations in the structure at limiting load levels cause numerical instabilities (i.e., presence of negative stiffness terms on the diagonal of the stiffness matrix) that prevent further analysis.

The results demonstrate that robust methods can be use to evaluate limit loads. Also, the load levels are a significant improvement over the traditional classical lower bound limit load estimates for a single linear elastic analysis. In the cases of the indeterminate beam (model – IB) and the flat bar stiffener (model –FB), the robust methods predict load levels up to 100% higher than classical limit loads and are essentially the same as those predicted using full non-linear analysis.

The limit load evaluated on the basis of the second linear elastic analysis after the element moduli have been adjusted is a significant improvement over the classical single linear elastic approach. This improved load level from this second analysis demonstrates the effect of stress relaxation in lowering the peak stress levels in a structure.

6.3.1 Influence of the Flange

The addition of the flange to the stiffening members slightly increases the modelling complexity and appears to increase the difficulty in attaining proper convergence behaviour with the peak r-node stresses and the upper and lower bound multipliers in the m_α methods. Reducing the modulus adjustment index q and hence the rate of relaxation helps alleviate the fluctuation, but results in a higher state of limit stress evaluated for a given iteration. As a result, a lower value of the limit load would be evaluated for such structures. This is illustrated in Figure 6.30 for the tee stiffener where q was reduced to 0.25 to obtain proper convergence characteristics. The limit load evaluated using the r-

node and m_α methods was significantly lower then those evaluated using the PMR method and full non-linear methods.

It is noted in Figure 6.28 that limit loads predicted using full non-linear analysis and robust methods for a flat bar stiffener are higher than those predicted using the analytical method which is based on rigid plastic hinge theory. However, for the angle and tee stiffeners in Figures 6.29 and 6.30 respectively, the non-linear and robust methods predict similar limit loads to the analytical solutions. Since the analytical method and robust methods both account for material non-linearities, it is expected that the predicted limit loads be similar, as illustrated in the angle and tee stiffeners in Figures 6.29 and 6.30. This suggests that the flat bars have more plastic load-bearing capacity than that predicted using rigid plastic hinge theory.

The fact that the limit loads predicted by non-linear and robust methods are no higher than the analytical predictions for flanged members indicates that the influence of the flange is not as effective for plastic behaviour as it is for elastic behaviour. While tees and angles do exhibit increased load bearing capacities for elastic and plastic behaviour, the effect of the flange is optimised for elastic behaviour and reduces for plastic behaviour.

6.3.2 Influence of the Shell Plating

The effect of membrane action is evident in the flat bar stiffened panel (model – FBSP) (Figure 6.31) and the Arctic icebreaker grillage (model – AIG) (Figure 6.32). The limit

load level predicted by the non-linear analysis and full scale lab tests is considerably higher than that predicted using the robust methods. This is becaue the added stiffening that results from geometric nonlinearities were accounted for in non-linear analyses but not in the robust methods used in this thesis. However, the limit load estimates evaluated using the robust methods are still in excess of 50% higher than that predicted using the classical lower bound limit load approach based on a single linear elastic analysis, and predictions are well into plastic load levels. Also, the three robust methods r-node, m_α and PMR predict similar limit load levels for each of the plated structure models.

It should be noted in the results of the arctic icebreaker grillage (model – AIG), Figure 6.32, that the full scale and full non-linear load deflection curves are only plotted for deflections up to 60 mm and do not represent the limit load of the structure. The actual curves extend much further, but results are only plotted up to a level necessary to compare estimates using robust methods. As shown in the load curves, the robust estimates of the load capacity are well within the plastic regions of the structure, but sufficiently conservative for initial design purposes. Bond and Kennedy (1998) discuss the suitability of the non-linear prediction against the full-scale lab test.

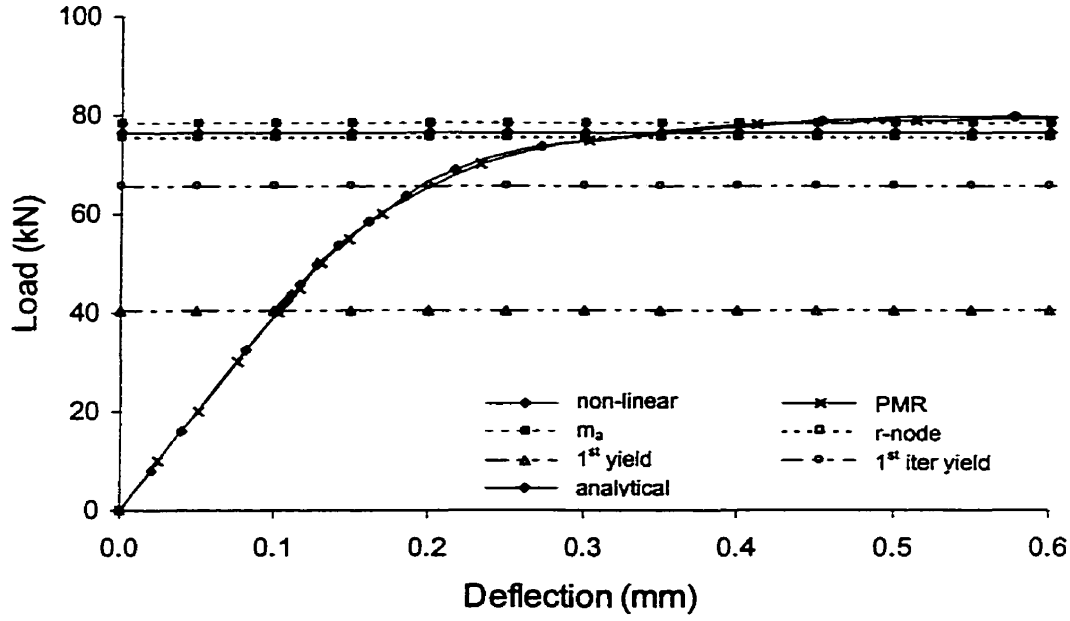

Figure 6.27: Limit load levels for indeterminate beam (model – IB)

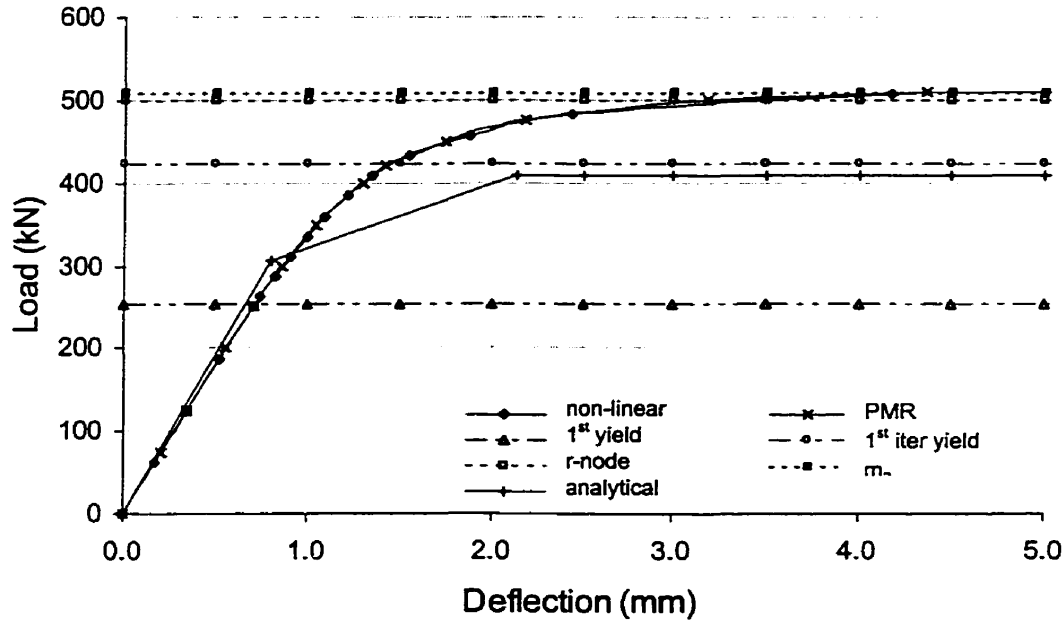

Figure 6.28: Limit load levels for mainframe flat bar stiffener (model – FB)

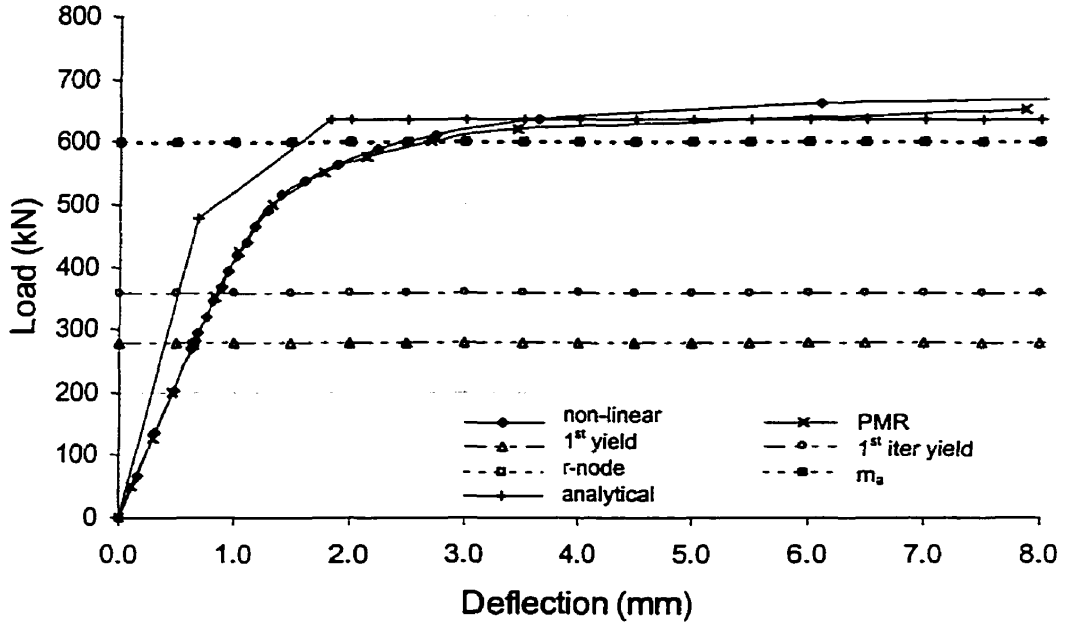

Figure 6.29: Limit load levels for mainframe angle stiffener (model – L)

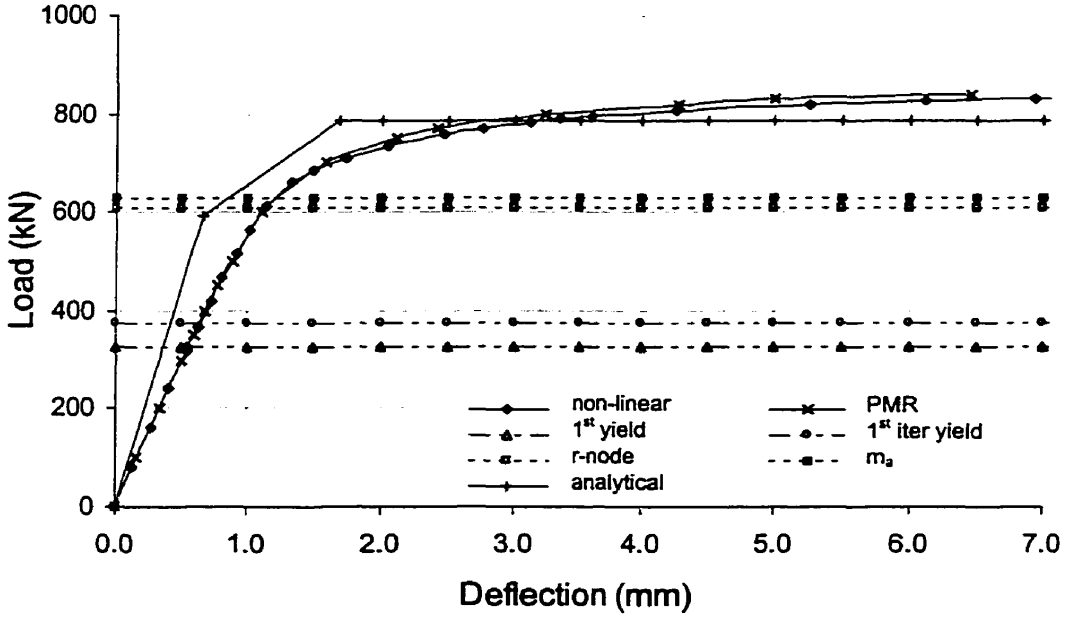

Figure 6.30: Limit load levels for mainframe tee stiffener (model – T)

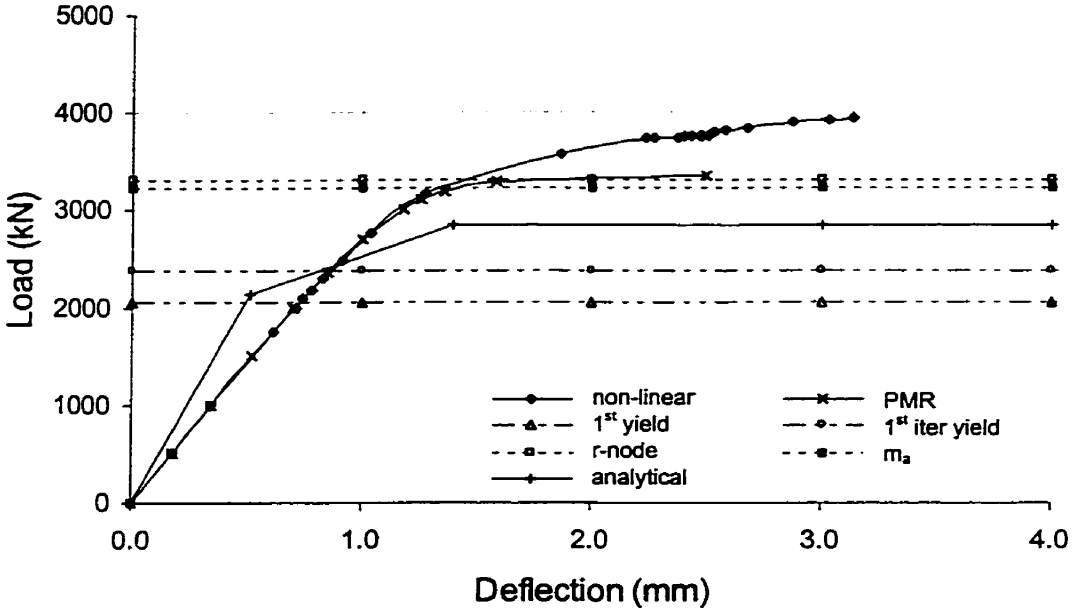

Figure 6.31: Limit load levels for flat bar stiffened panel (model – FBSP)

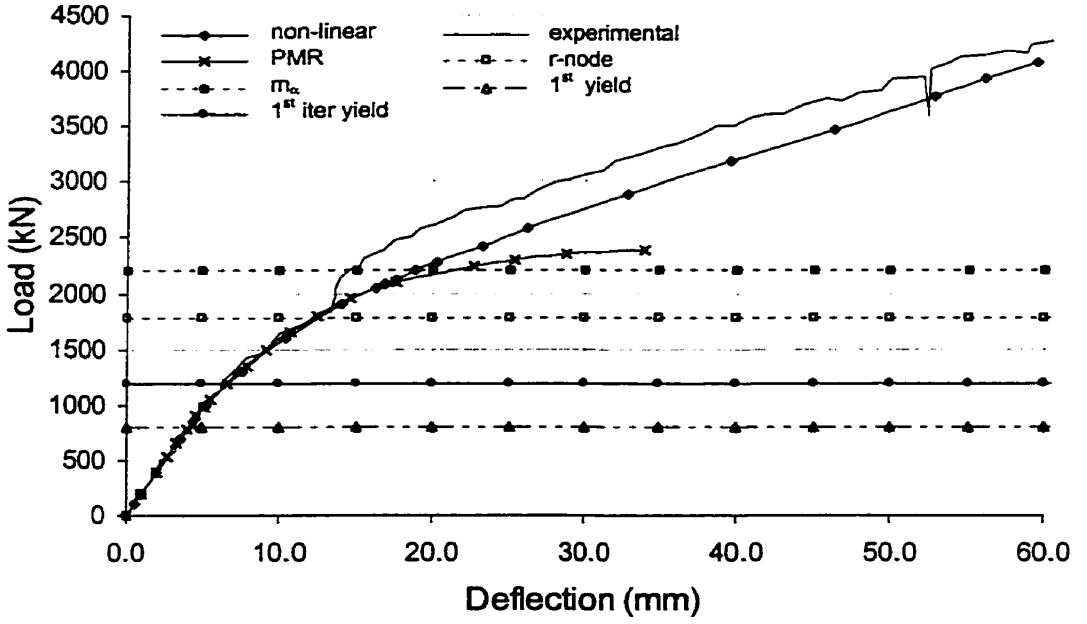

Figure 6.32: Limit load levels for arctic icebreaker grillage (model – AIG)

6.3.3 Limit Load Summary

A summary of the various limit loads for the different structures analysed using robust methods for an iteration number $\zeta = 4$, $q = 0.5$ (unless noted otherwise) are given in Table 6.13. Limit loads evaluated on the basis of robust methods are compared to analytical solutions, full non-linear analysis solutions and full-scale lab results, where available.

Seshadri and Mangalaramanan, (1997) state that limit loads can be evaluated on the basis of two iterations. This is true for structures modelled in two dimensions, but for structural geometry with stiffening in three dimensions (i.e., stiffeners having flanges), three or more iterations may be necessary. This ensures that the stresses in the structure are sufficiently redistributed and relaxed with peak stresses levelled off and that limit load multipliers convergence toward an exact limiting stress level occurs.

The results suggest that lower bound limit loads of structures evaluated using robust techniques offer an attractive alternative to non-linear analysis techniques. Not only are the results for plated structures and stiffening structures sufficiently accurate, there are enormous CPU time savings. For the structures analysed in this thesis, a maximum of four linear elastic analysis iterations were required to obtain sufficiently accurate results, which are completed in only a few minutes. The PMR method requires more CPU time since a sufficient number of analyses must be carried out to define a load deflection curve for the structure. However, depending on the analysis results required, the PMR method may be best suited to predict the expected non-linear response of the structure for the

limit load estimates evaluated using other robust methods, and then used to confirm the limit load estimates.

In addition to CPU time savings, the fact that all robust analysis techniques are carried out based on linear elastic analysis generally ensures that the solutions are stable. Numerical convergence difficulties encountered with full non-linear FEA (i.e., balancing the internal forces with the applied load) are avoided. This alone makes the use of robust techniques attractive.

Table 6.13: Summary of robust limit loads evaluated for the various structures for $\zeta = 4$; $q = 0.5$ (unless otherwise noted)

STRUCTURE	Limit Load (kN)							
	$(P_{LC})_I$ *	$(P_{LC})_{II}$ **	P_{ANAL}	$P_{R\text{-}Node}$	Pm_α	P_{PMR}	P_{NL}	P_{LAB}
Indeterminate Beam **(model – IB)**	40.28	65.63	76.56+	75.69	78.33	-	78.79	-
Flat Bar Stiffener **(model - FB)**	253	423	408++	499	509	508	509	-
Angle Stiffener **(model –L)**	278	358	635++	597	602	650	667	-
Tee Stiffener ^ **(model – T)**	325	373	788++	608	631	840	830	-
Flat Bar Stiffened Panel **(model – FBSP)**	2058	2382	2844++	3316	3236	3300	4237xx	-
Arctic Icebreaker Grillage **(model – AIG)**	799	1196	-	1779 x	2203	2380	2925xx	3275xx

* Von Mises equivalent classical lower bound limit load for 1st linear elastic analysis

** Von Mises equavalent lower bound limit load based on 2nd linear elastic analyis

\+ Analytical limit load proposed by Mendelson, 1968. $P_{ANAL} = 11.66 * Mp/L^2$

++ Analytical limit load proposed by Huges, 1988 (see appendix F)

^ Modulus Softening index $q = 0.25$

x R-node limit load evaluated on the basis of the maximum r-node stress in the structure

xx Values correspond to displacement of structure that corresponds to maximun iterated displacement for the PMR method. Values are for comparison and do not represent the maximum load level for the structure.

Chapter 7

Conclusions

Based on the results of the present thesis, it may be concluded that robust methods of finite element analyses are an attractive alternative to full non-linear analyses for estimating limit loads of structures. The methods are also an improvement over traditional classical lower bound limit load techniques. Each robust method accounts for material non-linearities in the solution process and consequently gives a good estimate of the non-linear design load of the structure.

Although full non-linear analysis give the best representation of structural plasticity, obtaining solutions may be difficult. After hours of runtime, there is no guarantee of a numerical solution. The process may terminate as a result of numerical convergence errors, and require the analysis be restarted with necessary modifications made to the geometry, applied loading conditions, or the predefined convergence criteria. Thus, robust techniques have advantages over the non-linear analysis techniques. The methods are fast and efficient, utilising a minimal amount of CPU time. Also, because these methods are based on a series of linear elastic analysis, convergence difficulties are avoided and the solution process is stable.

The solutions of robust analysis do not reflect the exact non-linear collapse loads of structures, but rather improved limit load estimates of the collapse load, over the classical limit loads evaluated on the basis of uniform strengths and yield criteria.

Methods of robust FEA involve elastic modulus adjustment techniques that redistribute pseudo-elastic stresses. This is to ensure that a structure behaving inelastically will achieve equilibrium with internal and external forces and the stresses everywhere are below yield, thus satisfying the requirements of a statically admissible stress field and hence the evaluation of valid lower bound limit load.

The Progressive Modulus Reduction (PMR) method of robust analysis achieves this by modifying the elastic modulus of the pseudo-elastically stressed elements or elements having stresses that exceed the yield limit, until all the stresses are below the yield limit or static admissibility is achieved. The maximum applied load to which static admissibility can be achieved is the collapse load. PMR, as used in this thesis, is not a direct limit load determination technique as are the other proposed robust methods (r-node, and m_α), but is rather a method that gives the non-linear response of a structure for a given load condition. A limit load can be determined from a generated load deflection plot attained through a process of manually incrementing the load, iterating the elastic modulus until static admissibility is achieved and evaluating the resultant non-linear displacement. This curve forms an asymptote that represents limit load of the structure.

The modulus adjustment technique used in the r-node method adjusts all element moduli on an element by element basis such that the stresses are redistributed about load-controlled locations or redistribution nodes within the structure. With two consecutive linear elastic analyses, the r-nodes can be identified as locations or elements where the stress remains constant. The r-node peaks form at locations where plastic hinges are assumed to form using plasticity theory. In the same way that the progressive formation of plastic hinges lead to collapse of the structure, the r-node peaks can be traced until a collapse mechanism is formed. Where the structural geometry and loading conditions result in the formation of two or more r-node peaks, the r-node stress can be evaluated as the average of these peaks.

It has been stated in the literature that solutions can be obtained with just two linear elastic analyses, although better results can be obtained if four or more iterations of elastic moduli are carried out. Increased iterations redistribute stresses in the structure, thereby further relaxing and levelling off the peak stresses. Limit loads evaluated from these relaxed stress distributions are an improvement over those for previous stress distributions.

Keeping track of r-node locations is trivial for simple structures such as single beam geometry and an r-node stress curve for peak r-node stresses in each section can be plotted. However, for more complex structures such as the arctic icebreaker grillage, this becomes difficult. In such cases, the analyst would need to rely on practical experience to identify r-node locations, extract the locations from the stress results and evaluate an

average value. A more conservative approach is to locate the peak r-node stress in the model.

The r-node method, although more robust then the PMR method, is not a direct method of obtaining limit loads. The exact locations of r-node peaks are difficult to identify within a discretised structure. It appears that the exact locations of r-nodes can only be identified if the elements are infinitely small. Hence, a region of redistribution stress must be identified.

The m_α method, as well as the r-node method, uses a modulus adjustment scheme where each element modulus in the structure is adjusted. The m_α method, on the basis of two consecutive linear elastic analyses, evaluates the energy dissipation in the structure. This is used to evaluate upper bound and lower bound multipliers according to Mura and Lee (1965) and hence the m_α multiplier according to Seshadri and Mangalaramanan (1997). The convergence of the evaluated upper and lower bound multipliers for each iteration must adhere to the conditions set forth in the "theorem of nesting surfaces." The surfaces represented by the multipliers must nest inside the two extreme surfaces represented on one side by elastic assumptions and the other by full plasticity. Hence, the upper bound multiplier m^o must monotonically decrease and the lower bound multiplier m' must monotonically increase toward the exact value of the limit load of the structure. m_α estimates evaluated for such conditions are valid.

Since the m_α multiplier is evaluated on the basis of a mathematical formulation relating upper and lower bound multipliers, the method is more direct then the PMR or r-node methods. However, because the solutions to limit loads are evaluated on the basis of a quadratic equation, satisfactory results are not always achieved. On occasion, the conditions of the structure and applied loading lead to the evaluation of imaginary roots as solutions to the quadratic equation. In such cases a further iteration can result in satisfactory results provided convergence requirements are met for the two consecutive linear elastic analysis.

m_α solutions to problems where the model meshing has variations in the element size are somewhat unstable and difficult to obtain, as was encountered with the arctic icebreaker grillage (model – AIG). However, increased iterations seemed to alleviate the problem.

The modulus adjustment index q, nominally taken to be unity (1), can be reduced to achieve monotonic convergence behaviour in the m_α method. While reducing q does appear to improve convergence behaviour, it essentially reduces the rate of relaxation and hence evaluates a higher state of limit stress for a given iteration. Thus, a lower limit load for the structure is predicted. Also, problems with fluctuation may just be delayed.

Reducing the value of the modulus adjustment index q, did not appear as effective at improving r-node stress relaxation behaviour characteristics with increased iterations. While reducing q reduces the rate of relaxation and hence smoothes the relaxation process by alleviating fluctuation, a progressive relaxation of the r-node stresses could

not be obtained for structures such as the tee stiffener and the Arctic icebreaker grillage. While this may be attributed to the difficulty in locating precise locations of r-nodes using finite mesh density, the influence of q needs to be researched further.

The use of q also suggests that the selection of a relaxation stress is not necessarily arbitrary. Reducing q essentially adjusts the value of the term σ_{arb}/σ_Y to reduce the variation between σ_{arb} and σ_Y and hence the rate of relaxation. It may be the case that the selection of the relaxation stress is not arbitrary but rather should be chosen carefully. Research is necessary to determine if this relaxation stress is a deterministic quantity.

The results of robust methods indicate a significant improvement in the lower bound estimates of limit loads of ship type structures, and the results are conservative when compared to the non-linear FEA results. Also, because the solution process is a stable one, convergence difficulties encountered with full non-linear analysis are avoided. Limit loads can be evaluated in a very timely, cost effective manner, which is particularly attractive at the initial stages of design.

Chapter 8

Recommendations

Authors Seshadri and Mangalaramanan (1997), who previously developed the r-node and m_α techniques suggest that a lower bound limit load can be evaluated based on just two linear elastic iterations. This work, however, suggests that more iterations are necessary first of all to ensure convergence requirements are satisfied and second, to ensure that the peak stresses are sufficiently relaxed.

More research is needed on the influence of the modulus adjustment index q. Seshadri and Mangalaramanan (1997), state that reducing q will stabilise the relaxation process such that monotonic convergence behaviour is exhibited among the upper and lower bound limit multipliers with increased iterations. While this appears effective for the m_α algorithms, it is not as effective with the r-node method. In some cases such as the tee stiffener and the Arctic icebreaker grillage, a monotonic relaxation of the r-node stresses could not be obtained. Also, the selection of q is still arbitrary on the interval $0 < q \leq 1$, and dependent on the complexity of the structure. A deterministic means of selecting q based on model geometry and complexity would be an asset and should be further explored.

It is also noted that the influence of q is simply to minimise the variation between the element stress and the arbitrarily chosen relaxation stress, which essentially reduces the rate of relaxation. It might be the case that judgement is needed in the selection of the relaxation stress (as opposed to choosing an arbitrary value) rather then appropriately selecting q. Further research needs to be carried out to determine if the relaxation stress is a deterministic quantity.

The PMR method used in this thesis is not a direct method of evaluating limit loads such that with just two linear elastic analyses the limit load can be predicted. Rather, it predicts the response of the structure for an applied loading condition. The limit load can be evaluated but only after repeatedly increasing the applied load until static admissibility can no longer be iterated or achieved. However, from the incremental loads a load displacement curve can be plotted. It is suggested that the r-node or m_α method be used to initially predict the lower bound load estimates, which can then be applied to the PMR model to investigate the non-linear response of the structure at the limit load. Achieving static admissibility in the structure at this load level using PMR is a check that the limit load is valid.

A parametric study on meshing density should be carried out to determine the optimum density necessary to yield more stable solutions and to achieve time efficiency with the solution process. Also, the effect of element size variation should be further studied.

Robust methods have great potential because of the added benefits that repeated elastic analysis has over full non-linear analysis. The main advantage is the numerical stability associated with the solution process. The methods should therefore be developed and incorporated into a robust finite element analysis software package. This would be useful to designers and analysts particularly at the initial stages of design. The non-linear behaviour of a structure can be explored with sufficient accuracy in an efficient, robust manner.

References

Adams, P. F., Krentz, H. A., and Kulak, G. L., *Limit States Design in Structural Steel*, Canadian Institute of Steel Construction, Universal Offset Limited, Markham, Ontario, 1979.

Bond, James, American Bureau of Shipping (ABS), Houston, Texas, personal contact, September, 1998.

Bond, J. and Kennedy, S., "Physical Testing and Finite Element Analysis of Icebreaking Ship Structures in the Post Yield Region," *Proceeding of 8th International Offshore and Polar Engineering Conference*, Montreal, Vol. II, May 1998.

Calladine, C. R., *Engineering Plasticity*, Pergamon Press, Oxford, 1969.

Daley, C. G, St. John, J. W., and Seibold F., "Analysis of Extreme Ice Loads Measured on USCGC Polar Sea," *Annual Meeting - The Society of Naval Architects and Marine Engineers*, New York, NJ, November 7-10, 1984.

Dhalla, A. K., "A Simplified Procedure to Classify Stresses for Elevated Temperature Service," *Proceedings of the ASME-PVP Conference*, San Diego, Vol. 120, pp. 177-188, 1987.

Dhalla, A. K., "Verification of an Elastic Procedure to Verify Follow-up," *Design of Elevated Temperature Piping*, Eds. Mallet, R. H., and Mello, R. M., ASME, New York, pp. 81-96, 1984.

Dhalla, A. K., and Jones, G. L., "ASME Code Classification of Pipe Stresses: A Simplified Elastic Procedure," *International Journal of Pressure Vessel and Piping*, Vol. 26, pp. 145-166, 1986.

Duthinh, D., "The Head-on Impact of an Iceberg on a Vertical, Gravity Based Structure," *Speciality Conference on Computer Methods in Offshore Engineering*, Halifax, NS, 1984.

Duthinh, D., Klein, K., Regrettier, J., Guichard A., and Engler, M., "Full Scale Iceberg Impact: A Pilot Experiment in Antarctica," *IAHR Ice Symposium*, Espoo, pp. 890-901, 1990.

Fernando, C. P. D., and Seshadri, R., "Limit Loads of Framed Structures and Arches using the GLOSS R-Node Method," *Transactions of the CSME*, Vol. 17, No. 2, pp. 197-214, 1993.

Fuglem, M., Muggeridge, K., and Jordaan, I., "Design Load Calculations for Iceberg Impacts," *Proceeding of 8th International Offshore and Polar Engineering Conference*, Montreal, pp. 460-466, 24-29 May, 1998.

Guichard, A., Engler, M., Klein, K., and Fauquemberg, P., "Methodology for Full Scale Iceberg Impact Experiments in the Antarctic," *Proceeding of 2nd International Offshore and Polar Engineering Conference*, San Francisco, pp. 718-723, 14-19 June, 1992.

Hieronymi, E., "Ice Impact on Ship Hulls," *12th International Conference on Port and Ocean Engineering under Arctic Conditions*, Hamburg, pp. 307-319, 17-20 August, 1993.

Johnson, R. C., Iceberg Impact Strength, *19th Annual Offshore Technology Conference*, Houston, Texas, pp. 417-423, April, 1987.

Jones, G. L., and Dhalla, A. K., "Classification of Clamp Induced Stresses in Thin-walled Pipe," *Proceedings of the ASME –PVP Conference,* New York, Vol. 81, pp. 1-10, 1981.

Kivimaa, S., "Long-Term Ice Load Measurements with an Ice Load Panel on Board the Cutter M.S. Uisko," *12th International Conference on Port and Ocean Engineering under Arctic Conditions*, Hamburg, pp. 339-347, 17-20 August, 1993.

Kizhatil, R. K., Seshadri, R., "Inelastic Strain Concentration Factors and Low Cycle Fatigue of Pressure Components using GLOSS Analysis," *Proceedings of the ASME-PVP Conference,* San Diego, Vol. 210-2, pp. 149-54, 1991.

Mackenzie, D. and Boyle, J. T., "A Method of Estimating Limit Loads by Iterative Elastic Analysis. I – Simple Examples," *International Journal of Pressure Vessel and Piping*, Vol. 53, pp. 77-95, 1993.

Mangalaramanan, S. P., *Robust Limit Loads using Elastic Modulus Adjustment Techniques*, Ph. D. Thesis, Faculty of Engineering and Applied Science, Memorial University of Newfoundland, St. John's, 1997.

Mangalaramanan, S. P., and Seshadri, R., "Minimum Weight Design of Pressure Components Using R-Nodes," *Transactions of the ASME: Journal of Pressure Vessel Technology*, Vol. 119, pp. 224-231, May 1997.

Marriott, D. L. and Leckie, F. A., "Some Observations on the Deflections of Structures during Creep," *Proceeding of the Institution of Mechanical Engineers,* Vol. 178, Part 3L, pp. 115-125, 1964.

Marriott, D. L., "Evaluation of Deformation or Load Control of Stresses under Inelastic Conditions using Elastic Finite Element Stress Analysis," *Proceedings of the ASME-PVP Conference*, Pittsburgh, Vol. 136, 1988.

Mendelson, A., *Plasticity: Theory and Application*, The Macmillan Company, New York, 1968.

Mura, T., and Lee, S. L., "Application of Variational Principles to Limit Analysis," *Quarterly of Applied Mathematics*, Vol. 21, No. 3, pp. 243-248, 1963.

Mura, T., Rimawi, W. H., and Lee, S. L., "Extended Theorems of Limit Analysis," *Quarterly of Applied Mathematics*, Vol. 23, No. 2, pp. 171-179, 1965.

Prager, W. and Hodge, P. G., *Theory of Perfectly Plastic Solids*, Dover Publications Inc., New York, 1951.

Prager, W., *An Introduction to Plasticity*, Addison-Wesley Publications Co. Inc., Reading, Massachusetts, 1959.

Sanderson, T. J. O., *Ice Mechanics*, Graham and Trotman Limited, London, UK, 1988.

Schulte, C. A., "Predicting Creep Deflections of Plastic Beams," *Proceedings of the ASTM*, Vol. 60, pp. 985-904, 1960.

Seshadri, R. and Fernando C. P. D., "Limit loads of Mechanical Components and Structures Using the GLOSS R-Node Method," *ASME Journal of Pressure Vessel Technology*, Vol. 114, pp. 201-208, May, 1992.

Seshadri, R. and Fernando, C. P. D., "Limit Loads of Mechanical Components and Structures Using the GLOSS R-Node Method," *Transactions of the ASME: Journal of Pressure Vessel Technology*, Vol. 114, pp. 201-208, 1992.

Seshadri, R. and Managalaramanan, S. P., "Lower Bound Limit Loads using Variational Concepts: m_α-method," *International Journal of Pressure Vessels and Piping*, Vol. 71, pp. 93-106, 1997.

Seshadri, R., "The Generalised Local Stress Strain (GLOSS) Analysis – Theory and Applications," *Transactions of the ASME: Journal of Pressure Vessel Technology*, Vol. 113, pp. 219-227, 1991.

Seshadri, R., "Classification of Stress in Pressure Components using the 'GLOSS' Diagram," *Proceedings of the ASME-PVP Conference*, Nashville, Vol. 186, pp. 115-123, 1990.

Seshadri, R., "In Search of Redistribution Nodes," *International Journal of Pressure Vessels and Piping*, Vol. 73, pp. 63-76, 1997.

Seshadri, R., and Kizhatil, R. K., "Inelastic Analyses of Pressure Components using the 'GLOSS' Diagram," *Proceedings of the ASME-PVP Conference*, Nashville, Vol. 186, pp. 105-113, 1990.

Severud, L. K., "Simplified Method Evaluation for Piping Elastic Follow-up," *Proceedings of the 5th International Congress of Pressure Vessel Technology*, ASME, San Francisco, pp. 367-387, 1984.

Appendix A

Extended Theorems of Limit Analysis

The formulation of Mura's lower bound multiplier m' is based on the functional

$$F(v_i, s_{ij}, \sigma_i, R_i, m_i, \mu_i, \phi) = \int_V s_{ij} \tfrac{1}{2}(v_{i,j} + v_{j,i})dV + \int_V s_{ij}\sigma\delta_{i,j}v_{i,j}dV \\ -\int_{S_V} R_i v_i dS - m\left(\int_{S_T} T_i v_i dS - 1\right) - \int_V \mu[f(s_{ij}) + \phi^2]dV \tag{A.1}$$

with the constraint condition $\mu \geq 0$ where v_i is the velocity vector, s_{ij} is the stress deviator, σ, R, m, μ and ϕ are Lagrangian multipliers, T is the surface traction on S_T, V is the velocity of S_V and $S_T + S_V$ equals the total volume of the structure. The yield criterion is given by

$$f(s_{ij}) = \tfrac{1}{2}s_{ij}s_{ij} - k^2 \tag{A.2}$$

Mura and Lee (1963) showed that for a given state of plastic flow, a statically admissible multiplier, or safety factor could be evaluated, such that the function is rendered stationary.

Taking the variation of the functional F gives

$$\begin{aligned}\delta F(v_i, s_{ij}, \sigma_i, R_i, m_i, \mu_i, \phi) = & \int_V \delta s_{ij} \tfrac{1}{2}(v_{i,j} + v_{j,i}) dV + \int_V s_{ij} \tfrac{1}{2}(\delta v_{i,j} + \delta v_{j,i}) dV \\ & + \int_V \delta\sigma \delta_{i,j} v_{i,j} dV - \int_V \sigma \delta_{i,j} \delta v_{i,j} dV - \int_{S_v} \delta R_i v_i dS - \int_{S_v} R_i \delta v_i dS \\ & - \delta m\left(\int_{S_T} T_i v_i dS - 1\right) - m\left(\int_{S_T} T_i \delta v_i dS - 1\right) - \int_V \delta\mu[f(s_{ij}) + \phi^2] dV \\ & - \int_V \mu \frac{\partial f}{\partial s_{ij}} \delta s_{ij} dV - \int_V \mu 2\phi \delta\phi dV\end{aligned} \tag{A.3}$$

Setting the variation to zero and integrating by parts yields the natural boundary conditions given as

$$\tfrac{1}{2}(v_{i,j} + v_{j,i}) = \mu \frac{\partial f}{\partial s_{ij}} \quad \text{in V} \tag{A.4}$$

$$\mu \geq 0 \quad \text{in V} \tag{A.5}$$

$$(s_{ij} + \delta_{ij}\sigma)_{,i} = 0 \quad \text{in V} \tag{A.6}$$

$$(s_{ij} + \delta_{ij}\sigma) n_i = m T_i \quad \text{on } S_T \tag{A.7}$$

$$(s_{ij} + \delta_{ij}\sigma) n_i = R_i \quad \text{on } S_T \tag{A.8}$$

$$f(s_{ij}) + \phi^2 = 0 \quad \text{in V} \tag{A.9}$$

$$\mu\phi = 0 \quad \text{in V} \tag{A.10}$$

$$\delta_{ij} v_{i,j} = 0 \quad \text{in V} \tag{A.11}$$

$$v_i = 0 \quad \text{on } S_V \tag{A.12}$$

$$\int_{S_T} T_i v_i dS = 1 \tag{A.13}$$

The Lagrangian multipliers given here are mean stress (σ), the reaction on S_V (R_i), the safety factor (m), the positive scalar of proportionality (μ) and the yield parameter (ϕ).

It can be noted from the formulation of the natural boundary conditions that when $\phi \neq 0$ and $\mu = 0$, then $f(s_{ij}) < 0$. Also, the $\lim_{\phi \to 0} f(s_{ij}) = 0$. Setting equation (A.13) to unity simply illustrates the positive definite nature of the integral, but determines only the scalar (or size) of an arbitrary velocity vector.

Consider the arbitrary arguments

$$\begin{aligned} v_i^0 &= v_i + \delta v_i \\ s_{ij}^0 &= s_{ij} + \delta s_{ij} \\ \sigma^0 &= \sigma + \delta\sigma \\ m^0 &= m + \delta m \\ \phi^0 &= \phi + \delta\phi \\ \mu^0 &= \mu + \delta\mu \end{aligned} \tag{A.14}$$

where v_i, s_{ij}, σ, ... represent the stationary sets of arguments of (A.1), and δv_i, δs_{ij}, $\delta\sigma$, ... are the variations. Substituting (A.14) into (A.1) regarding the natural boundary conditions (A.4) to (A.13) the functional F can be written as

$$F\left[v_i^0, s_{ij}^0, \sigma^0, R_i^0, m^0, \mu^0, \phi^0\right] = m + \int_V \delta s_{ij} \tfrac{1}{2}(\delta v_{i,j} + \delta v_{j,i}) dV$$
$$+ \int_V \delta\sigma \delta_{i,j} v_{i,j} dV - \int_{S_v} \delta R_i v_i dS - \delta m\left(\int_{S_T} T_i v_i dS - 1\right) \qquad (A.15)$$
$$- \int_V \mu[\tfrac{1}{2} \delta s_{ij} \delta s_{ji} + \phi^2] dV - \int_V \delta\mu[f(s_{ij}) + \phi^2] dV$$

Making use of the boundary conditions (A.6), (A.7) and (A.8), the requirements for a statically admissible stress field is given as

$$(s_{ij}^0 + \delta_{ij}\sigma^0)_{,i} = 0 \quad \text{in V} \qquad (A.16)$$

$$(s_{ij}^0 + \delta_{ij}\sigma^0) n_i = m^0 T_i \quad \text{on } S_T \qquad (A.17)$$

and stipulating that $$(s_{ij}^0 + \delta_{ij}\sigma^0) n_i = R_i^0 \quad \text{on } S_T \qquad (A.18)$$

where R_i^0 represent the reaction of the stress field on S_V, equation (A.15) can be transformed to

$$F = m - \int_V \mu[\tfrac{1}{2} \delta s_{ij} \delta s_{ji} + \phi^2] dV - \int_V \delta\mu[f(s_{ij}) + \phi^2] dV \qquad (A.19)$$

Also, integrating equation (A.1) with the arbitrary arguments $v_i^0, s_{ij}^0, \sigma^0, R_i^0, m^0, \mu^0, \phi^0$ and the constraints (A.6), (A.7) and (A.8) we get

$$F = m^0 - \int_V \mu^0 [f(s_{ij}^0) + (\phi^0)^2] dV \qquad (A.20)$$

The integral mean of the yield can be expressed as

$$\int_V \mu^0 [f(s_{ij}^0) + (\phi^0)^2] dV = 0 \qquad (A.21)$$

where $$\mu^0 \geq 0 \qquad (A.22)$$

Given equation (A.20) and equation (A.21), it is clear that

$$F = m^0 \qquad (A.23)$$

From equations (A.19), (A.20) and (A.21) and also given that $\int_V \mu[\frac{1}{2}\delta\varepsilon_{ij}\delta\varepsilon_{ij} + (\delta\phi)^2$ is always positive definite, we have

$$m^0 \leq m - \int_V \delta\mu [f(s_{ij}^0) + (\phi^0)^2] dV \qquad (A.24)$$

Since $\mu^0 = \mu + \delta\mu$ then the integral mean of yield given in equation (A.21) can be expressed as

$$-\int_V \delta\mu [f(s_{ij}^0) + (\phi^0)^2] dV = \int_V \mu [f(s_{ij}^0) + (\phi^0)^2] dV \qquad (A.25)$$

Therefore equation (A.24) can be rewritten as

$$m^0 \leq m + \int_V \mu [f(s_{ij}^0) + (\phi^0)^2] dV \qquad (A.26)$$

Taking the maximum of the integrand equation (A.26) can be expressed as

$$m^0 \le m + \max\left\{f(s_{ij}^0) + (\phi^0)^2\right\}\int_V \mu dV \qquad (A.27)$$

Because of the nature of equations (A.21) and (A.22), $\max\left\{f(s_{ij}^0 + (\phi^0)^2\right\} \ge 0$.

Given that

$$m = m\int_{S_T} T_i v_i dS = \int_S (s_{ij} + \delta_{ij}\sigma) n_j v_i dS =$$
$$\int_V (s_{ij} + \delta_{ij}\sigma) v_{i,j} dS = \int_V (s_{ij} + \delta_{ij}\sigma) v_{i,j} dV =$$
$$\int_V s_{ij} \tfrac{1}{2}(v_{i,j} + v_{j,i}) dS = \int_V s_{ij} \mu s_{ij} dV = 2k^2 \int_V \mu dV$$

it is evident that

$$\int_V \mu dV = \frac{m}{2k^2} \qquad (A.28)$$

By substituting equation (A.28) back into equation (A.27), the expression for the lower bound multiplier (m') is given as

$$m' = \frac{m^0}{1 + \max\{f(s_{ij}^0) + (\phi^0)^2\}/2k^2} \le m \qquad (A.29)$$

which holds valid for any set of $v_i^0, s_{ij}^0, \sigma^0, m^0, \mu^0, \phi^0$ satisfying

$$(s_{ij}^0 + \delta_{ij}\sigma^0)_{,j} = 0 \quad \text{in V} \qquad (A.30)$$

$$(s_{ij}^0 + \delta_{ij}\sigma^0)n_i = m^0 T_i \quad \text{on } S_T \tag{A.31}$$

$$\int_V \mu^0 [f(s_{ij}^0) + (\phi^0)^2] dV = 0 \tag{A.32}$$

$$\mu^0 \geq 0 \tag{A.33}$$

Using a special form of equation (A.32) and stipulating that $f(s_{ij}^0 + (\phi^0)^2 = 0$, equation (A.29) forms a classical definition of the lower bound. The $\max\{f(s_{ij}^0 + (\phi^0)^2\}$ vanishes and equation (A.29) reduces to

$$m^0 \leq m \tag{A.34}$$

Here, the new lower bound (expressed by m^0) holds for a broader stress field than for the statically admissible stress field using the integral mean of the yield criterion of equation (A.32).

Appendix B

Models and Boundary Conditions

B1 - **Indeterminate Beam**

B2 - **Main Frame Stiffeners**

Flat Bar (FB) Stiffener

Angle (L) Stiffener

Tee (T) Stiffener

B3 - **Flat Bar Stiffened Structural Panel**

Uniformly Distributed Load

B4 - **Arctic Icebreaker Grillage** (*file available opon request*)

B1 – Indeterminate Beam

```
!=============================================================
!INPUT MODEL FOR ANALYSIS OF INDETERMINATE BEAM

/prep7

L=50.8
H=2.54
t=1

YM=206850
YS=206.85
RS=250

r,1,t
r,2,t

xdiv=1
ydiv=10
zdiv=100

!DEFINE MATERIAL PROPERTIES

et,1,shell43
!et,2,solid73

ex,1,YM
ex,2,YM/5
nuxy,1,0.3

tb,bkin,1
tbdata,1,ys,0

type,1
real,1
mat,1

!keypoints
K,1,0,0,0
K,2,0,0,-L
K,3,0,H,-L
K,4,0,H,0

!lines
L,1,2
```

```
LESIZE,1,,,zdiv
L,2,3
LESIZE,2,,,ydiv
L,4,3
LESIZE,3,,,zdiv
L,1,4
LESIZE,4,,,ydiv

!STIFF AREA MESHING
A,1,2,3,4
amesh,all

nummrg,all
fini

! APPLYING BOUNDARY CONDITIONS AND LOADS TO OBTAIN
! A STATIC SOLUTION

/solu
antype,static

!  END CONDTIONS

!End A - Fixed
nsel,s,loc,z,0
d,all,all,0
nsel,all

!End B - Pinned

nsel,s,loc,z,-L
nsel,r,loc,y,0
d,all,uy,0
nsel,all

!FORCE LOAD
force=8.7579/100

nsel,s,loc,y,h
nsel,r,loc,z,-L/100+0.1,-L
f,all,fy,-force
nsel,all

save
solve
fini
```

B2 – Main Frame Stiffeners

```
!=============================================================
!INPUT MODEL FOR ANALYSIS OF FLAT BAR STIFFENER

/prep7

L=1200
H=200
t=15

YM=207000
YS=245
RS=300
q=1

r,1,t
r,2,t

xdiv=1
ydiv=10
zdiv=60

!DEFINE MATERIAL PROPERTIES

et,1,shell43
!et,2,solid73

ex,1,YM
ex,2,YM/5
nuxy,1,0.3

type,1
real,1
mat,1

!keypoints
K,1,0,0,0
K,2,0,0,-L
K,3,0,H,-L
K,4,0,H,0

!lines
```

```
L,1,2
LESIZE,1,,,zdiv
L,2,3
LESIZE,2,,,ydiv
L,4,3
LESIZE,3,,,zdiv
L,1,4
LESIZE,4,,,ydiv

!STIFF AREA MESHING
A,1,2,3,4
amesh,all

nummrg,all

fini

! APPLYING BOUNDARY CONDITIONS AND LOADS TO OBTAIN
! A STATIC SOLUTION

/solu
antype,static

! END CONDTIONS

!End A - Fixed
nsel,s,loc,z,0
d,all,all,0
nsel,all

!End B - Fixed
nsel,s,loc,z,-L
d,all,all,0
nsel,all

!PLATE EDGE RESTRAINT
nsel,s,loc,y,h
d,all,ux,0
nsel,all

!EXCENTRIC FORCE
fdist=200/61
nsel,s,loc,y,0
nsel,r,loc,x,0
f,all,fx,-fdist
nsel,all
```

```
! LOAD APPLIED
force=100*1000/61

nsel,s,loc,y,h
f,all,fy,-force
nsel,all

save
solve
save
fini


!=================================================================
!INPUT MODEL FOR ANALYSIS OF ANGLE STIFFENER


/prep7

L=1200
H=200
t=15
wf=60

YM=207000
YS=245
RS=300
q=1

r,1,t
r,2,t

xdiv=1
xfdiv=3
ydiv=10
zdiv=60

!DEFINE MATERIAL PROPERTIES

et,1,shell43
!et,2,solid73

ex,1,YM
ex,2,YM/5
nuxy,1,0.3
```

```
type,1
real,1
mat,1

!keypoints
K,,1,0,0,0
K,,2,0,0,-L
K,,3,0,H,-L
K,,4,0,H,0
K,,5,wf,0,0
K,,6,wf,0,-L

!lines
L,1,2
LESIZE,1,,,zdiv
L,2,3
LESIZE,2,,,ydiv
L,4,3
LESIZE,3,,,zdiv
L,1,4
LESIZE,4,,,ydiv
L,2,6
LESIZE,5,,,xfdiv
L,5,6
LESIZE,6,,,zdiv
L,1,5
LESIZE,7,,,xfdiv

!STIFF AREA MESHING
A,1,2,3,4
A,1,2,6,5
amesh,all

nummrg,all
fini

! APPLYING BOUNDARY CONDITIONS AND LOADS TO OBTAIN
! A STATIC SOLUTION

/solu
antype,static

! END CONDTIONS

!End A - Fixed
```

```
nsel,s,loc,z,0
d,all,all,0
nsel,all

!End B - Fixed
nsel,s,loc,z,-L
d,all,all,0
nsel,all

!PLATE EDGE RESTRAINT
nsel,s,loc,y,h
d,all,ux,0
nsel,all


! LOAD APPLIED
force=100*1000/61

nsel,s,loc,y,h
f,all,fy,-force
nsel,all

save
solve
save
fini
```

```
!=============================================================
!INPUT MODEL FOR ANALYSIS OF TEE STIFFENER


/prep7

L=1200
H=200
t=15
wf=60

YM=207000
YS=245
RS=300
q=1

r,1,t
```

```
r,2,t

xdiv=1
xfdiv=3
ydiv=10
zdiv=60

!DEFINE MATERIAL PROPERTIES

et,1,shell43
!et,2,solid73

ex,1,YM
ex,2,YM/5
nuxy,1,0.3

type,1
real,1
mat,1

!keypoints
K,1,0,0,0
K,2,0,0,-L
K,3,0,H,-L
K,4,0,H,0
K,5,wf,0,0
K,6,wf,0,-L
K,7,-wf,0,0
K,8,-wf,0,-L

!lines
L,1,2
LESIZE,1,,,zdiv
L,2,3
LESIZE,2,,,ydiv
L,4,3
LESIZE,3,,,zdiv
L,1,4
LESIZE,4,,,ydiv
L,2,6
LESIZE,5,,,xfdiv
L,5,6
LESIZE,6,,,zdiv
L,1,5
LESIZE,7,,,xfdiv
```

```
L,2,8
LESIZE,8,,,xfdiv
L,7,8
LESIZE,9,,,zdiv
L,1,7
LESIZE,10,,,xfdiv

!STIFF AREA MESHING
A,1,2,3,4
A,1,2,6,5
A,1,2,8,7
amesh,all

nummrg,all
fini

! APPLYING BOUNDARY CONDITIONS AND LOADS TO OBTAIN
! A STATIC SOLUTION

/solu
antype,static

! END CONDTIONS

!End A - Fixed
nsel,s,loc,z,0
d,all,all,0
nsel,all

!End B - Fixed
nsel,s,loc,z,-L
d,all,all,0
nsel,all

!PLATE EDGE RESTRAINT
nsel,s,loc,y,h
d,all,ux,0
nsel,all

!EXCENTRIC FORCE
fdist=200/61
nsel,s,loc,y,0
nsel,r,loc,x,0
f,all,fx,-fdist
nsel,all
```

```
! LOAD APPLIED
force=100*1000/61

nsel,s,loc,y,h
f,all,fy,-force
nsel,all

save
solve
save
fini
```

B3 – Flat Bar Stiffened Structural Panel

```
!=================================================================
!INPUT MODEL FOR ANALYSIS OF STIFFENED PANEL

/prep7

L=1200
S=400
B=2*S
H=200
t=15
w=50
nst=3

YM=207000          !Youngs Modulus
YS=245             !Yield Stress
RS=400             !Reference Stress
q=0.5              !Modulus Softening Index

r,1,t          Shell plate thickness = t
r,2,t          Stiffener thickness = t

xdiv=32  !Element size 50 x 50 mm
ydiv=4
zdiv=24

!DEFINE MATERIAL PROPERTIES

et,1,shell43
!et,2,solid73

mp,ex,1,YM
mp,ex,2,YM/5

nuxy,1,0.3
!tb,biso,1,1
!tbdata,1,245,0

!SHELL PLATE

type,1
real,1
mat,1

!keypoints
```

```
K,1,B,0,0
K,2,B,0,-L
K,3,-B,0,-L
K,4,-B,0,0

!lines
L,1,2
LESIZE,1,,,zdiv
L,2,3
LESIZE,2,,,xdiv
L,4,3
LESIZE,3,,,zdiv
L,1,4
LESIZE,4,,,xdiv

!PLATE AREA MESHING
A,1,2,3,4                    !plate
amesh,all

!STIFFENERS

type,1
real,2
mat,1

!STIFF1

*DO,c,1,nst

!keypoints
K,5+4*(c-1),-S+S*(C-1),0,0
K,6+4*(c-1),-S+S*(C-1),0,-L
K,7+4*(c-1),-S+S*(C-1),H,0
K,8+4*(c-1),-S+S*(C-1),H,-L

!lines
L,5+4*(c-1),6+4*(c-1)
LESIZE,5+4*(c-1),,,zdiv
L,6+4*(c-1),8+4*(c-1)
LESIZE,6+4*(c-1),,,ydiv
L,7+4*(c-1),8+4*(c-1)
LESIZE,7+4*(c-1),,,zdiv                    !stiffener 1
L,5+4*(c-1),7+4*(c-1)
LESIZE,8+4*(c-1),,,ydiv

!STIFF AREA MESHING
```

```
A,5+4*(c-1),6+4*(c-1),8+4*(c-1),7+4*(c-1) !stiffener 1
AMESH,c+1

*ENDDO

!ICE PATCH
!type,2
!mat,2
!tb,biso,3,1
!tbdata,1,1E6,0

!block,-w,w,0,-t,-L/2+w,-L/2
!lsel,s,loc,y,-t/2
!lesize,all,,,1

!lsel,s,line,,9,20,1
!lsel,r,loc,x,0
!lesize,all,,,4
!lsel,all

!lsel,s,line,,9,20,1
!lsel,r,loc,z,-L/2+25
!lesize,all,,,2
!lsel,all

!vsel,s,loc,y,-t/2

!vmesh,1

nummrg,all
fini

! APPLYING BOUNDARY CONDITIONS AND LOADS TO OBTAIN
! A STATIC SOLUTION

/solu
antype,static

!BOUNDARY CONDITIONS

!PLATE EDGE RESTRAINT
nsel,s,loc,x,-B
d,all,ux,0
d,all,uy,0
d,all,rotz,0
nsel,all
```

```
nsel,s,loc,x,B
d,all,ux,0
d,all,uy,0
d,all,rotz,0
nsel,all

! END CONDITIONS

!  FIXED END
nsel,s,loc,z,0
d,all,all,0
nsel,all
nsel,s,loc,z,-L
d,all,all,0
nsel,all

save
fini

/solu

! DISTURBING FORCE – to break eccentricity in the stiffeners
fdist=150
nsel,s,loc,y,H
nsel,r,loc,x,S
nsel,r,loc,z,-L/2
f,all,fx,fdist
nsel,all
nsel,s,loc,y,H
nsel,r,loc,x,0,-S
nsel,r,loc,z,-L/2
f,all,fx,-fdist
nsel,all

! APPLIED LOAD
!force=300000/825
force=300*1000/125
!force=300000/49

!Uniformly Distributed Surface Load
!nsel,s,loc,y,0

!Rectangular Strip Load
nsel,s,loc,z,-L/2+1*L/zdiv+1,-L/2-3*L/zdiv-1
nsel,r,loc,y,0
nsel,r,loc,x,-s-3*(2*B/xdiv)-1,s+5*(2*B/xdiv)+1
```

```
!Square Patch load
!nsel,s,loc,z,-L/2+3*L/zdiv+1,-L/2-3*L/zdiv-1
!nsel,r,loc,y,0
!nsel,r,loc,x,-2*(2*B/xdiv)-1,4*(2*B/xdiv)+1

f,all,fy,force
nsel,all

save
solve
finish
```

Appendix C

Nonlinear Analysis Run File

RUN FILE FOR A FULL NONLINEAR ANALYSIS OF A STRUCTURAL PANEL

```
!IMPORT MODEL OF STIFF
/inp,nlmodel   (flat bar stiffened panel Appendix B3)

save
fini


!APPLYING LOADS TO OBTAIN A SOLUTION

/solu

antype,static
nlgeom,on
sstif,on
!autots,on
neqit,30
nropt,auto
cnvtol,F,,0.01,,1        !contol,lab,value,toler,norm,minref
cnvtol,M,,0.01,,1        !cnvtol,lab,SSRC(or Minref),0.001(0.1%),2(SSRC),1
ncnv,0
pred,on,,on
outres,basic,all

!BOUNDARY CONDITIONS

! SYYMETRY
!nsel,s,loc,z,-L/2
!d,all,uz,0
!nsel,all

!PLATE EDGE RESTRAINT
nsel,s,loc,x,-B
d,all,ux,0
d,all,uy,0
d,all,rotz,0
nsel,all
nsel,s,loc,x,B
d,all,ux,0
d,all,uy,0
d,all,rotz,0
nsel,all
```

```
! END CONDITIONS

end_con=1

!  FIXED END
*if,end_con,eq,1,then

nsel,s,loc,z,0
d,all,all,0
nsel,all
nsel,s,loc,z,-L
d,all,all,0
nsel,all

*endif

save
fini

/solu

! DISTURBING FORCE
fdist=150
nsel,s,loc,y,H
nsel,r,loc,x,S
nsel,r,loc,z,-L/2
f,all,fx,fdist
nsel,all
nsel,s,loc,y,H
nsel,r,loc,x,0,-S
nsel,r,loc,z,-L/2
f,all,fx,-fdist
nsel,all


! LOAD APPLIED

!fmax=5500*1000/825
!fy=2000*1000/825
fmax=2500*1000/125
fy=507*1000/125
pressure=100000/36

!Uniformly Distributed Surface load
!nsel,s,loc,y,0
```

```
!Rectangular Strip Ice Load
nsel,s,loc,z,-L/2+1*L/zdiv+1,-L/2-3*L/zdiv-1
nsel,r,loc,y,0
nsel,r,loc,x,-s-3*(2*B/xdiv)-1,s+5*(2*B/xdiv)+1

f,all,fy,fy
nsel,all

time,fy          !Load up to approx Yield
nsubst,4

save
solve
save

!Uniformly Distributed Surface load
!nsel,s,loc,y,0

!Rectangular Strip Ice Load
nsel,s,loc,z,-L/2+1*L/zdiv+1,-L/2-3*L/zdiv-1
nsel,r,loc,y,0
nsel,r,loc,x,-s-3*(2*B/xdiv)-1,s+5*(2*B/xdiv)+1

f,all,fy,fmax
nsel,all

time,fmax              !analysis up to max load capacity
!nsubst,100
deltim,100,10,500
autots,on

save
solve
save
finish
```

Appendix D

Robust Analysis Run Files

D1 - Progressive Modulus Reduction

D1-1 - Modulus Reduction file for PMR

D2 - m_α Method and R-Node Method

D2-1 - Modulus Reduction file for m_α and r-node

D1 – Progressive Modulus Reduction

```
! PROGRESSIVE MODULUS REDUCTION (PMR) ALGORITHM AS A ROBUST
!TECHNIQUE FOR PREDICTING A  LOWER BOUND LIMIT LOAD

!IMPORTING MODEL FOR STATIC ANLAYSIS
/inp,pmrmodel        !Models and B.C.'s from Input files given in appendix A
/inp,pmrbc
save
fini

!STRESS RESULTS FOR THE FIRST STATIC ANALYSIS

/post1
set,1,1
etab,seqv,s,eqv
etab,epteqv,epto,eqv
/output,stress1
pretab,seqv,epteqv
/out

!DEFINE CRITERIAN TO ITERATE STIFF REDUCTION UNTIL
!ALL ELEMENTS WITH STRESSES > YIELD ARE RELAXED

*SET,mni,3
*SET,mnii,3

*DO,z,1,50

/post1
set,1,1
etab,seqv,s,eqv

!DETERMINE THE MAXIMUM ELEMENT STRESS

*GET,k,elem,0,count

stmax=0

*DO,t,1,k
        *GET,st,elem,t,etab,seqv
        *IF,st,GT,stmax,THEN
                stmax=st
        *ENDIF
*ENDDO
```

```
*CFOPEN,max
*VWRITE,z,stmax
(10x,f5.1,3x,f15.3)
*CFCLOS

!TERMINATE STIFFNESS REDUCTION IF ALL STRESS
!ARE BELOW YIELD STRESS

*IF,stmax,LT,ys,EXIT

!PERFORM STIFFNESS REDUCTION

/inp,pmrstiffredii      !Stiffness reduction algorithm. creates files 'exval' and 'exmod '

/prep7
mp,ex,1,ym
mp,ex,2,ym/5
/inp,exval              !Inputs new stiffness values for modified elements
/inp,exmod

/soln
save
solve

*ENDDO

fini

/post1
resume
set,1,1
etab,seqv,s,eqv
etab,ept,epto,eqv
/output,stress2
pretab,seqv,ept
/out
/output,disp
prnsol,uy
/out

fini
```

```
!=========================================================================
D1-1  !STIFFNESS REDUCTION ALGORITHM TO MODIFY THE ELASTIC
      !MODULUS OF SELECTED ELEMENTS

/post1

!resume,file,db

!*DIM,DUM1,ARRAY,1
!*DIM,DUM2,ARRAY,1
!*DIM,DUM3,ARRAY,1
!*DIM,DUM4,ARRAY,1

SET,1,1
ETABLE,seqv,s,eqv

MN=mni

*CFOPEN,exval
*GET,C,ELEM,0,COUNT

*DO,I,1,C
      *GET,steq,ELEM,I,ETAB,seqv
      *GET,matno,ELEM,I,ATTR,mat
      *GET,mtex,EX,matno,TEMP,0
      *IF,steq,GE,rs,THEN
            ered=mtex*(rs/steq)**q
            *CFWRITE,mp,ex,mn,ered
            MN=MN+1
            mni=mni+1
      *ENDIF
*ENDDO
*CFCLOSE

MN=mnii

*CFOPEN,exmod
*DO,L,1,C
      *GET,steq,ELEM,L,ETAB,seqv
      *IF,steq,GT,rs,THEN
            *CFWRITE,emodif,L,mat,MN
            MN=MN+1
            mnii=mnii+1
      *ENDIF
*ENDDO
*CFCLOSE
```

D2 – R-Node and M-alpha

```
!ALGORITHM TO IMPLEMENT THE R-NODE & M-ALPHA ROBUST METHODS
!FOR DETERMINING THE LOWER BOUND LIMIT LOAD OF A STRUCTURE

*DIM,strs1,ARRAY,2500
*DIM,strs2,ARRAY,2500
*DIM,strsavg,ARRAY,2500
*DIM,diff,ARRAY,2500
*DIM,perc,ARRAY,2500

*SET,mni,3
*SET,mnii,3

!IMPORTING MODEL FOR ANALYSIS
/inp,rnmodel
/inp,rnbc
save
fini

!DO LOOP TO PERFORM 'IT' ITERATIONS OF MODULUS ADJUSTMENT

IT=3
*DO,a,1,IT

!STRESS RESULTS FOR THE FIRST STATIC ANALYSIS

/post1
resume
set,1,1
etab,vol,volu
etab,seqv,s,eqv
etab,epteqv,epto,eqv

/output,stress1
pretab,seqv,epteqv
/out

! STORE STRESS IN AN ARRAY STRS1(T)

!UNSORTED ENERGY RESULTS FOR LINEAR ELASTIC ANALYSIS I
!ARE STORED IN FILE energy1

*GET,k,elem,0,count

*CFOPEN,energy1          !storing stress and vol for Ma
```

```
*DO,t,1,k
        *GET,st,elem,t,etab,seqv
        *GET,vol1,elem,t,volu
        strs1(t)=st                    !storing first run stresses in array
*VWRITE,t,vol1,st
(2x,f10.1,5x,f15.3,5x,f15.3)

*ENDDO
*CFCLOSE

!PERFORM STIFFNESS MODIFICATION

/inp,rnstiffmod        !Stiffness reduction algorithm. creates files 'exval' and 'exmod '

/prep7
mp,ex,1,ym
mp,ex,2,ym/5
/inp,exval             !Inputs new stiffness values for modified elements
/inp,exmod

/soln
save
solve
fini

*ENDDO                 !End of Iteration loop

/post1
resume
set,1,1
etab,vol,volu
etab,seqv,s,eqv
etab,ept,epto,eqv
/output,stress2
pretab,seqv,ept
/out
!/output,disp
!prnsol,uy
!/out

!UNSORTED ENERGY RESULTS FOR LINEAR ELASTIC ANALYSIS II
!ARE STORED IN FILE energy2

! STORE STRESS IN AN ARRAY STRS2(T)

*GET,k,elem,0,count
```

```
*CFOPEN,energy2              !storing stress and vol for Ma
*DO,t,1,k
        *GET,st,elem,t,etab,seqv
        *GET,vol2,elem,t,volu
        strs2(t)=st                    !storing first run stresses in array
*VWRITE,t,vol2,st
(2x,f10.1,5x,f15.3,5x,f15.3)

*ENDDO
*CFCLOSE

!*********************************************
!R-NODE SELECTION CRITERION

*GET,k,elem,0,count

*CFOPEN,rnode

*DO,t,1,k
        diff(t)=SQRT((strs1(t)-strs2(t))**2)
        strsavg(t)=(strs1(t)+strs2(t))/2
        perc(t)=diff(t)/strsavg(t)

        !*IF,strs1(t),GT,strs2(t),THEN
                !diff=strs1(t)-strs2(t)

        !*ELSEIF,strs1(t),LT,strs2(t),THEN
                !diff=strs2(t)-strs1(t)
        !*ENDIF

        *IF,perc(t),LT,0.1,THEN
                *CFWRITE,elem,t,strsavg(t),perc(t)
                !(5x,f5.1,3x,f10.3,3x,f10.3)
        *ENDIF
*ENDDO
*CFCLOSE

*CFOPEN,stress

*DO,t,1,k
*CFWRITE,e,t,strs1(t),strs2(t)
*ENDDO

*CFCLOSE
fini
```

```
!=============================================================
D2-1  !STIFFNESS REDUCTION ALGORITHM TO MODIFY THE ELASTIC
      !MODULUS OF SELECTED ELEMENTS

/post1

!*DIM,DUM1,ARRAY,1
!*DIM,DUM2,ARRAY,1
!*DIM,DUM3,ARRAY,1
!*DIM,DUM4,ARRAY,1

SET,1,1
ETABLE,seqv,s,eqv

MN=mni

*CFOPEN,exval
*GET,C,ELEM,0,COUNT

*DO,i,1,C
      *GET,steq,ELEM,i,ETAB,seqv
      *GET,matno,ELEM,i,ATTR,mat
      *GET,exold,EX,matno,TEMP,0
            exnew=exold*(rs/steq)**q
            *CFWRITE,mp,ex,MN,exnew
            MN=MN+1
            mni=mni+1
*ENDDO
*CFCLOSE

MN=mnii

*CFOPEN,exmod
*DO,L,1,C
      *CFWRITE,emodif,L,mat,MN
      MN=MN+1
      mnii=mnii+1
*ENDDO
*CFCLOSE
```